Impacts of Global Change and Soil Properties on Phosphorus Transformation and Plant Responses in Alpine Grassland Ecosystem on the Northeastern Tibetan Plateau

Dissertation

der Mathematisch-Naturwissenschaftlichen Fakultät

der Eberhard Karls Universität Tübingen

zur Erlangung des Grades eines

Doktors der Naturwissenschaften

(Dr. rer. nat.)

vorgelegt von

Zuonan Cao, M.Sc

aus Qinghai (Xining), China

Tübingen

2023

Gedruckt mit Genehmigung der Mathematisch-Naturwissenschaftlichen Fakultät der Eberhard Karls Universität Tübingen.

Tag der mündlichen Qualifikation:	19.12.2023
Dekan:	Prof. Dr. Thilo Stehle
1. Berichterstatter:	Prof. Dr. Thomas Scholten
2. Berichterstatter:	Dr. Peter Kühn
3. Berichterstatterin:	Prof. Dr. Yvonne Oelmann

Table of contents

Acknowledgments

This work would not have been possible without the help of many people. Foremost, I would like to express my sincere gratitude to my supervisors, Professor Dr. Thomas Scholten and Dr. Peter Kühn, for offering me the opportunity to spend the time of my PhD after the Master's study in this wonderful little town, Tübingen, for their invaluable guidance, unwavering support, and insightful feedback throughout the entire process of this doctoral research. Their expertise and dedication have been instrumental in shaping the direction of my work. Special thanks to Professor Dr. Jin-sheng He and Dr. Zhen-huan Guan from Lanzhou University, who supported the fieldwork in Haibei Station and the collaboration of the manuscripts. This cooperation will be of unique value in the future as well. I would also like to extend my thanks to Professor Dr. Yvonne Oelmann for reviewing this dissertation. coincidentally, she led my first master's course at UT eight years ago.

I extend my appreciation to my colleagues and fellow researchers for their camaraderie and stimulating discussions, encouragement, and guidance in the laboratory, which have been a source of motivation and inspiration for this study. They are Wen Shao, Dr. Steffen Seitz, Sabine Flaiz, Margaretha Baur, Rita Mögenburg, Dr. Ruhollah Taghizadeh, Dr. Tobias Rentschler, Dr. Corinna Gall, Dr. Zhengshan Song, Nicolas Riveras Munoz and others. Furthermore, I am also deeply thankful to my friends and seniors in Tübingen, including the former members of the association of Chinese students and scholars. They are Dr. Yue Zhang, Dr. Jialin Zhou, Yuchen Liu, Chenhui Chang, Ruijin He, Linmei Chen, Dr. Kai Liu, Professor Dr. Achim Mittag, Danwei Zhu-Mittag, Master Haojun Zhuo, Mrs. Vries-Wehrhahn and others (There are so many other that I should thank, with a long list). It is an honor to meet them all in Tübingen.

Special thanks to my girlfriend, Shanting Hu, for encouraging and sharing happiness and sorrow; it was the last stage of meeting and new beginnings in this beautiful town. Lastly, I am grateful to my family for their unconditional love and unwavering belief in my study. Their encouragement has been the cornerstone of my academic journey.

This research would not have been possible without the collective support and contributions of all those mentioned above. Time flies; I remember the winter when I first got off the train in 2015, the concert in the auditorium in 2017, the pandemic from 2020, and the sunrise in WHO in 2022. So much has changed, but I am still willing to be the connector of our group.

“Berg und Tal kommen nicht zusammen, wohl aber die Menschen.”

List of Figures

Figure 8: Simplified framework of changes in plant phosphorus (P)-acquisition strategies in response to nitrogen (N) addition under different soil P levels. Blue dashed boxes indicate the dominant P effects, grey dashed boxes indicate the dominant N effects, and black thin dashed boxes indicate changes in functional groups. Small arrows represent an increase (red arrows) and a decrease (blue arrows) in the variables with N addition. Abbreviations: AMF = arbuscular mycorrhizal fungi.

Figure 9: General trends of the stocks of P pools in soil with increasing N addition rates in fencing (left) and grazing (right) conditions. The arrows show the main pathways for the increased net accumulation and transformation of organic P in alpine grassland soils.

Figure 10: Proportions of total organic P (Po) in the total P (sum of all Hedley P fractions) on nitrogen addition rates and grazing at 0-10 cm soil depths. The significance of the treatments is shown with P values, where G is the grazing effect, N addition is the N effect, and G*N addition means the coupling effect of grazing and N addition. Grazing effect $P < 0.001$; grazing and N effect, $P = 0.005$. Values are expressed as mean ± 95% confidence intervals. The solid dots indicate the treatment of non-grazing (fencing), and the hollow circle indicates grazing treatment, respectively.

Figure 11: Phosphorus pools in 0–10 cm of soil, including labile, moderate, and stable pools under unwarmed control (CK) and year-round warming using an open-top chamber (W) along three elevational gradients.

Figure 12: Principal component analysis (PCA) shows the relationship between soil P fractions and soil properties at different altitudes. SOC: soil organic carbon; total N: total nitrogen. Total sample point (n = 107).

Figure 13: Pearson correlation analysis of soil P fractions with selected soil properties for all soil samples. Note: Values in the graph represent correlation coefficients (r), while gradient colors represent the Pearson correlation coefficient (r) range from –1 to 1. Red denotes a positive correlation, while blue denotes a negative correlation.

Asterisks denote the extent of the significance level: *** indicates $P \leq 0.001$, ** indicates $P \leq 0.01$, and * indicates $P \leq 0.05$. Total sample point ($n = 107$).

Figure 14: Relationship between different P pools (a and b, respectively), P fraction (c) and total Po (d) with SOC content.

Figure 15: Redundancy analysis (RDA) ordination graph for the relationship between soil P pools and soil properties along elevational gradients (altitude) and slopes (sunny, middle and shadow).

List of Tables

Abbreviations

ACP (APase)	Acid phosphatase
ALP	Alkaline phosphate
AMF	Arbuscular mycorrhizal fungi
FT-NIRS	Fourier transform near-infrared spectra
$HCl_{conc.}$	Concentrated HCl
MBP	Microbial biomass P
MIR	Mid-infrared spectra
OTC	Open-top chambers
PCA	Principal component analysis
Pi	Inorganic phosphorus
PLFA	Phospholipid fatty acid
PLSR	Partial least-squares regression
Po	Organic phosphorus
RDA	Redundancy analysis
RPIQ	performance-to-interquartile range
SOC	Soil organic carbon
SOM	Soil organic matter

List of Publications and personal contribution

Accepted manuscripts.

(1) Cao Z., Kühn P., He J-S., Bauhus J., Guan Z-H., Scholten T. (2022): Calibration of Near-Infrared Spectra for Phosphorus Fractions in Grassland Soils on the Tibetan Plateau. *Agronomy*; 12(4):783.

doi: 10.3390/agronomy12040783

(2) Guan, Z.-H., **Cao, Z.,** Li, X. G., Scholten, T., Kühn, P., Lin, W., Yu, R.-P., & He, J.-S. (2023). Soil phosphorus availability mediates the effects of nitrogen addition on community- and species-level phosphorus-acquisition strategies in alpine grasslands. *Science of the Total Environment*, 906, 167630.

doi: 10.1016/j.scitotenv.2023.167630

(3) Guan, Z.-H., **Cao, Z.,** Li, X. G., Kühn, P., Hu, G., Scholten, T., Zhu, J., He, J.-S. (2023): Effects of winter grazing and N addition on soil phosphorus fractions in an alpine grassland on the Qinghai-Tibet Plateau. *Agriculture, Ecosystems & Environment*, 357, 108700.

doi: 10.1016/j.agee.2023.108700

Share in publication

No.	Accepted for publication	Number of authors	Position of the canditate in the list of authors	Scientific ideas of canditate	Data generation by canditate	Analysis and interpretation by candidate	Paper writing candidate
(1)	Yes	6	1	60	90	80	80
(2)	Yes	8	2	40	40	40	40
(3)	Yes	8	2	40	40	40	40

Abstract

The grassland ecosystems on the Tibetan Plateau have undergone significant changes in recent decades, driven primarily by global factors such as temperature and precipitation changes, nitrogen (N) deposition and regional effects. The shift in richness and distribution of many species towards higher elevations on the Tibetan Plateau is well documented. Yet, there needs to be more plant and soil data from alpine grassland elevation gradients. The effect of soil properties and nutrient supply on vegetation patterns at high altitudes and how the "grass-line" will respond to global warming remain largely unknown. As demonstrated for tree lines in the Himalayas, nutrient limitations may be crucial for vegetation growth and distribution at high elevations. Soil nutrient supply of N, phosphorus (P), calcium (Ca), and magnesium (Mg) becomes more limited with increasing elevation, and this nutrient decline spatially coincides with abrupt changes in vegetation composition and growth parameters. Furthermore, it needs to be clarified how N enrichment and land use changes (i.e., overgrazing) influence soil P transformation from organic to inorganic forms, especially in young soils at the beginning of their formation on the plateau.

To gain a better understanding of the effects of global changes and soil properties on soil P transformation and plant P uptake, as well as the limit factors of plant distribution at high elevations, we analyzed the previous research from a long-term nutrient addition (N and P) experiment and the open-top chambers (OTC) experiment along the elevation gradients, and then collected random soil samples at three altitudes and three geomorphic positions, with three depth increments, from the Haibei grassland in northeastern Tibetan Plateau. Soil properties, such as soil texture, bulk density, soil organic carbon (SOC), and P fractions, were analyzed at the experimental sites. We investigated plant and microbial P pools, the P acquisition strategies, and the biomass. This thesis aimed to determine (1) the influence of N and P input on soil P transformation and soil properties in the alpine grassland, simulating the effects of N deposition and grazing on the productivity and stability of the ecosystem; (2) the

influence of simulated warming with the OTC experiment along the elevational gradients on the soil P fractions and transformation; and (3) the changes of soil P fraction and soil properties along the elevational gradient and slops with an attempt to answer the question from the soil perspective: Which factor limits the distribution of plants shifting to higher altitudes?

The results indicated that N input altered the plant P requirements when soil available P was deficient, particularly under global N deposition in Tibetan alpine grassland. While both N and P additions changed the plant root traits at the soil-plant interface, changes in P-acquisition strategies among different treatments were more influential in driving the community structure and composition. Importantly, soil properties varied among samples from various sites but were consistent with the results of the nutrient addition experiment: the pH remained stable at 0 to10 cm depth of soil, and P addition alone significantly impacted plant growth in the area, indicating the shifting from N to P limitation when N input increases. In addition, P limitation was not the primary factor driving grasses toward higher elevation, as soil available P content did not change with elevation. However, soil properties and other nutrients might be responsible. This study suggests that specific combinations of soil properties could limit plant growth on the northeastern plateau more than warming, thereby controlling biodiversity and biomass production in high mountain grassland ecosystems. The acceptable content of Ca and Mg in the soil was sufficient to buffer the impact of N deposition from soil acidification on the grassland ecosystem. Furthermore, organic P pools were strongly and positively correlated with SOC and total N, highlighting the essential role of soil organic matter in maintaining the soil P reserves. Further research is needed to understand the effect of precipitation changes on soil P transformation in grassland ecosystems in the northeastern Tibetan Plateau. Additionally, other technologies such as ^{31}P- nuclear magnetic resonance and high-throughput sequencing should be employed to explore the response of compound composition of soil P forms and microorganisms related to P transformation and uptake. In all, this thesis enables quantification of the contribution of the different factors to the effective soil nutrients. It provides a reference for

predicting the impact of global changes on the stability and productivity of alpine grassland ecosystems.

Zusammenfassung

Die Graslandökosysteme auf dem Tibetischen Plateau haben sich in den letzten Jahrzehnten erheblich verändert, die hauptsächlich durch globale Faktoren wie Temperatur- und Niederschlagsveränderungen, Stickstoff (N) - Deposition und regionale Effekte angetrieben wurden. Der Wechsel in der Artenvielfalt und Verteilung vieler Arten in höhere Lagen auf dem Tibetischen Plateau ist gut dokumentiert, es bedarf jedoch mehr Pflanzen- und Bodendaten von alpinen Graslandhöhenlagen. Die Auswirkungen der Bodeneigenschaften und der Nährstoffversorgung auf die Vegetationsmuster in großen Höhen und die Reaktion der "Grasgrenze" auf die globale Erwärmung sind noch weitgehend unbekannt. Wie bei den Baumgrenzen im Himalaya gezeigt wurde, können Nährstoffbeschränkungen für das Wachstum und die Verbreitung der Vegetation in großen Höhen entscheidend sein. Die Nährstoffversorgung des Bodens mit N, Phosphor (P), Kalzium (Ca) und Magnesium (Mg) wird mit zunehmender Höhe immer begrenzter, und dieser Nährstoffrückgang fällt räumlich mit abrupten Veränderungen der Vegetationszusammensetzung und der Wachstumsparameter zusammen. Darüber hinaus muss geklärt werden, wie die N-Anreicherung und die veränderte Landnutzung (z. B. Überweidung) die Transformation von Boden-P von organischen in anorganische Formen beeinflussen, insbesondere in jungen Böden, die sich zu Beginn ihrer Entstehung auf dem Plateau befinden.

Um ein besseres Verständnis der Auswirkungen globaler Veränderungen und der Bodeneigenschaften auf die Transformation von Boden-P und die P-Aufnahme durch die Pflanzen sowie der Grenzfaktoren für die Pflanzenverbreitung in hohen Lagen zu erlangen, haben wir frühere Forschungsergebnisse aus einem Langzeitexperiment zur Nährstoffzugabe (N und P) und einem Experiment mit Open-Top Chambers (OTC) entlang der Höhengradienten analysiert und anschließend zufällige Bodenproben in drei Höhenlagen und drei geomorphologischen Positionen mit drei Tiefenstufen auf dem Haibei-Grasland im Nordosten des Tibetischen Plateaus gesammelt. An den Versuchsstandorten wurden Bodeneigenschaften wie Bodentextur, Schüttdichte,

organischer Kohlenstoff im Boden (SOC) und P-Fraktionen analysiert, und wir untersuchten die pflanzlichen und mikrobiellen P-Pools und die P-Aufnahmestrategien sowie die Biomasse. Ziel dieser Arbeit war es, (1) den Einfluss des N- und P-Eintrags auf die P-Transformation im Boden und die Bodeneigenschaften in alpinen Grasländern zu bestimmen, indem die Auswirkungen der N-Deposition und der Beweidung auf die Produktivität und Stabilität des Ökosystems simuliert wurden; (2) den Einfluss der simulierten Erwärmung mit dem OTC-Experiment entlang der Höhengradienten auf die P-Fraktionen und die Transformation im Boden zu bestimmen; und (3) die Veränderungen der P-Fraktion im Boden und der Bodeneigenschaften entlang des Höhengradienten und der Hänge zu untersuchen, um die Frage aus der Perspektive des Bodens zu beantworten: Welcher Faktor begrenzt die Verbreitung von Pflanzen, die sich in höhere Lagen verlagern?

Die Ergebnisse deuten darauf hin, dass die N-Eingabe den P-Bedarf der Pflanzen veränderte, wenn der verfügbare P im Boden mangelhaft war, insbesondere bei globaler N-Deposition im tibetischen alpinen Grasland. Während sowohl N- als auch P-Zusätze die Wurzeleigenschaften der Pflanzen an der Boden-Pflanzen-Schnittstelle veränderten, waren die Änderungen in den P-Aufnahmestrategien bei verschiedenen Behandlungen einflussreicher bei der Steuerung der Gemeinschaftsstruktur und -zusammensetzung. Wichtig ist, dass die Bodeneigenschaften zwischen den Proben der verschiedenen Standorte unterschieden, aber mit den Ergebnissen des Experiments zur Nährstoffzugabe übereinstimmten: Der pH-Wert blieb in 0 bis 10 cm Bodentiefe stabil, und die P-Zugabe allein wirkte sich signifikant auf das Pflanzenwachstum in dem Gebiet aus, was darauf hindeutet, dass sich der Übergang von der N- zur P-Limitierung vollzieht, wenn der N-Eingabe zunimmt. Darüber hinaus war die P-Limitierung nicht der primäre Faktor, der Gräser in höhere Höhen trieb, da der verfügbare P-Gehalt im Boden mit der Höhe nicht verändert wurde. Allerdings könnten Bodeneigenschaften und andere Nährstoffe dafür verantwortlich sein. Diese Studie deutet darauf hin, dass bestimmte Kombinationen von Bodeneigenschaften das Pflanzenwachstum auf dem nordöstlichen Plateau stärker einschränken könnten als die Erwärmung, wodurch die

Biodiversität und die Biomasseproduktion in Ökosystem mit hohen Berggraslanden kontrollieren. Der akzeptable Ca- und Mg-Gehalt des Bodens reichte aus, um die Auswirkungen der N-Deposition aus der Bodenversauerung auf das Grasland-Ökosystem abzupuffern. Darüber hinaus waren die organischen P-Pools stark und positiv mit dem SOC und dem Gesamt-N korreliert, was die wesentliche Rolle der organischen Bodensubstanz bei der Erhaltung der P-Reserven im Boden unterstreicht. Weitere Forschungsarbeiten sind erforderlich, um den Effekt von Veränderungen der Niederschläge auf die P-Transformation im Graslandökosystem im nordöstlichen tibetischen Plateau zu verstehen. Zusätzlich sollten andere Technologien wie die ^{31}P-Kernresonanz und die Hochdurchsatzsequenzierung eingesetzt werden, um die Reaktion der Zusammensetzung der P-Formen im Boden und der Mikroorganismen im Zusammenhang mit der P-Transformation und -Aufnahme zu untersuchen. Insgesamt ermöglicht diese Arbeit eine Quantifizierung des Beitrags der verschiedenen Faktoren zu den effektiven Bodennährstoffen und bietet eine Referenz für die Vorhersage der Auswirkungen globaler Veränderungen auf die Stabilität und Produktivität alpiner Graslandökosysteme.

1. Introduction

Terrestrial ecosystems worldwide are facing significant impacts from global change, with some being more vulnerable than others, such as the alpine ecosystems on the Tibetan Plateau (Qinghai-Tibet Plateau), known as the "Third Pole," characterized by lower temperatures and uneven precipitation due to the extreme environmental conditions resulting from the intense and rapid tectonic uplift, are one of the most important areas particularly susceptible to global change. These changes include climate warming, anthropogenic disturbances (e.g., overgrazing and over-fertilization), and N deposition (Qiu, 2008; Baumann et al., 2009; Yao et al., 2012; Shen et al., 2013; Liu et al., 2013; Shi et al., 2017; Ganjurjav et al., 2020). The alpine grassland on the Tibetan Plateau is notorious for its large scale (occupying 53% total area of the plateau) and provides important services for millions of people as the main pasture in China (Klein et al., 2007; Zhang et al., 2007; Hou et al., 2021) and is influenced by alterations of precipitation and temperature and substantial decreases in the soil available nutrient stocks, such as soil organic carbon (SOC) and phosphorus (P) regarding plant species composition and biomass production (Qiu, 2008; Liu et al., 2018; Tian et al., 2019). Among these factors influenced by global change, soil P is critical in regulating ecosystem processes and maintaining soil quality, particularly in alpine grassland and other areas with poor soils and nutrient deficiencies (Zhou et al., 2021). Soil P cycling and dynamic, i.e., transformation between soil P pool and plant P pool, and its availability are increasingly affected by increased N deposition and climate warming, leading to potential nutrient limitation (i.e., from N to P limitation), which in turn constrains the stability and productivity of alpine grassland ecosystems (Müller et al., 2017; Zhao & Zeng, 2019; Mou et al., 2020; Margalef et al., 2021), making soil P availability a key factor in the stability and productivity of grassland ecosystems. On the other hand, many species showed their distributions by climate-driven shifts toward higher elevation (Chen et al., 2011; Müller et al., 2017; Mamantov et al., 2021); in the Tibetan Plateau, however, the elevational variations of the plants and microbe

community on alpine grassland are rare (Liu et al., 2018; Li et al., 2022) and it is largely unknown how the grass line will respond to global warming and whether P in soils plays a major role.

P exists in various forms in grassland soils, including organic P (Po), inorganic P (Pi) and phosphate, and the transformation and cycling are driven by biotic (phosphatase mobilization, organic acid secretion, etc.) and abiotic processes (sorption/desorption, precipitation/dissolution), which are given in Figure 1 (Zhou et al., 2021; Margalef et al., 2021; Tian et al., 2023), The major mechanisms that decrease soil P availability in terrestrial ecosystems are the adsorption and immobilization of P in active mineral surfaces [aluminum (Al), iron (Fe), calcium (Ca), clays], organic molecules, and the biomass of microbes (Condron & Tiessen, 2004; Wu et al., 2013; Li et al., 2022).

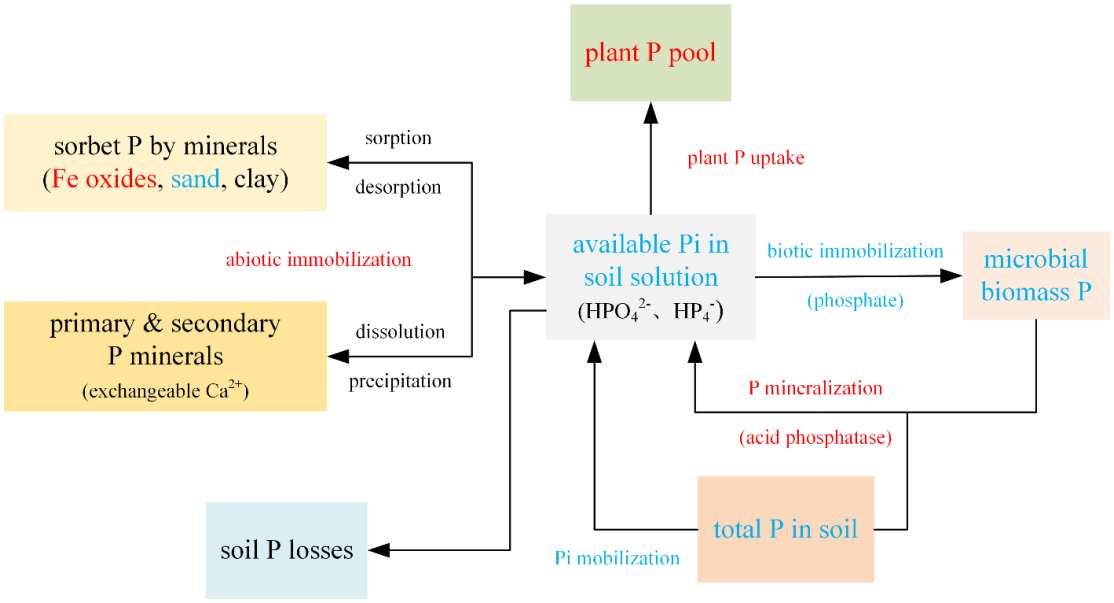

Fig. 1. Schematic illustration of soil phosphorus pool cycle and phosphorus transformation processes, including the abiotic and biotic processes. Red, blue, and black texts indicate the effect of warming increased, decreased, and unchanged indicators, respectively, in the referenced studies; the effects of nitrogen deposition are not labeled because of the inconsistent impacts.

Due to the cold climate of the Tibetan Plateau, the slow rate of soil formation and weathering of mineral rocks, and the relatively low anthropogenic interference, the

input of soil P in the short term is mainly obtained through the decomposition of above-ground plant residues and limited mineralization of organic matter (Baumann et al., 2009; He et al., 2021), resulting in a soluble Pi content that can be directly absorbed and used by plants and microorganisms that is generally less than 1% of the total soil P, and the fractions which are difficult to be used the account for more than 50% (Zhou et al., 2021; Azene et al., 2022; Cao et al., 2022), and this pool needs to be replenished repeatedly to meet the needs of the plant (Niederberger et al., 2019). The P cycling and transformation between different P pools include the mineralization of Po, the mobilization of Pi and the sorption of P by soil minerals (Fig. 1). An understanding of soil P dynamics as affected by biotic and abiotic factors requires first an assessment of different P forms present in the soil. Sequential P fractionation methods have been commonly used to determine inorganic, organic, and microbial P pools. Based on chemical bonds between P and soil compounds (soil minerals and organic molecules), soil P is divided into operationally defined inorganic and organic P fractions. One of the more typical and well-accepted methods is the Tiessen & Moir (2007) modified Hedley continuous extraction method for soil P analyses (Hedley et al., 1987, Table 1); this was a reasonable classification method for fractionating P and has been widely used (Spain et al., 2018). However, few studies have been conducted on transforming different soil P pools in alpine grassland ecosystems and the effects of biotic (microorganisms and plants) and abiotic (soil properties) factors.

Global Change on the Tibetan Plateau

Climatically, the Tibetan Plateau is an abnormal heat source in the middle troposphere, which brings a major component of the Asian monsoonal system, and the large-scale climate model described causes precipitation to decrease from southeast to northwest (Wu et al., 2014; Liu et al., 2020). However, this may differ due to local mountain ranges, elevation differences, and extreme relief positions. Rapid increases in annual mean air temperatures have been observed on the Tibetan Plateau, which is an increasing temperature up to 0.37 ℃ per decade, approximately 2.5 times the global

rate (Blue Book on Climate Change in China, 2022). It has become much warmer since 2000 (Chen et al., 2015), and overall, 60–90% of the precipitation occurs during the summer months (Turner & Annamalai, 2012). Meanwhile, N deposition on the Tibetan Plateau has been increasing with large fluctuations and significant spatial heterogeneity, although it is lower than the national average (Liu et al., 2015).

Table 1. Experimental procedure for the modified Hedley fractionation steps and assignment of P fractions to soil P pools.

P Pools	**P fractions**	**Extraction Procedure**	**Properties and Bonding Forms of Pi and Po in the Fractions**
Labile P	Resin-P	Anion-exchange resin 0.5 mol L^{-1} HCl	Soluble Pi, marginal Po; biologically most available P form; adsorbed on the surface of crystalline compounds.
	$NaHCO_3$-Pi $NaHCO_3$-Po	0.5 mol L^{-1} $NaHCO_3$	Highly labile P; plant-available Pi, associated with Fe and Al oxides; Po is easily mineralized.
Moderate P	NaOH-Pi NaOH-Po	0.1 mol L^{-1} NaOH	Moderately labile P; Pi associated with Fe and Al-oxides;
	HCl-Pi	1.0 mol L^{-1} HCl	Po is involved in slow transformation processes.
Stable P	$HCl_{conc.}$-Pi $HCl_{conc.}$-Po	12 mol L^{-1} HCl	Very stable Pi; covers P associated with Ca; Po in very stable pools, eventually also derived from particulate organic matter.
	Residual-P	0.5 mol L^{-1} H_2SO_4	Highly resistant and occluded P forms; Physicochemical protected

Pi: inorganic phosphorus; Po: organic phosphorus (Tiessen & Moir, 2007; Pätzold et al., 2013; Niederberger et al., 2015; Hou et al., 2018)

On the Tibetan Plateau, two of the world's largest alpine ecosystems predominate:

the alpine steppe ecosystems of the arid south-western Tibetan Plateau which covers about 800,000 km^2, and the *Kobresia pygmaea* pastures of the more humid eastern Tibetan Plateau, which extend across 450,000 km^2 (Miehe et al., 2019). Both ecosystems are under pressure from a set of abiotic factors that limit the net primary production, including the low mean annual temperature, the short vegetative period, low oxygen levels, high ultraviolet radiation, and nutrient deficiency in the soil (Callaway et al., 2002; Miehe et al., 2008, 2019; Sun et al., 2018; Han et al., 2019). Global change (i.e., warming and N deposition) and consequent nutrient limitation can alter plant biomass production and plant community composition (Elser et al., 2007; Shen et al., 2022; Speißer et al., 2022). Climate warming is most distinct in the northeastern Tibetan Plateau, implying increasing air and surface temperatures as well as duration and depth of thawing (Cuo et al., 2013; Barry & Hall-McKim, 2018). The main ecological consequences of these changes are a disturbed vegetation cover of the surface and a depletion of nutrient-rich top-soils (Baumann et al., 2009, 2014) coupled with an increase in greenhouse gas emissions, mainly CO_2 (Bosch et al., 2017). However, CO_2 elevation, warming, and increased precipitation with apparent spatial heterogeneity increased plant community biomass, and the effects were additive rather than interactive (Zong et al., 2013; Kuang & Jiao, 2016). Climate warming enhances vegetation activity by extending the growing season's length and intensifying maximum productivity rates. In turn, increased vegetation productivity reduces albedo, which causes positive feedback on temperature (Shen et al., 2015). In addition, the latest study shows that warming increased plant productivity in the meadow but decreased productivity in the steppe, and the composition of plant species in response to the changes stabilized the production (Ganjurjav et al., 2016; Liu et al., 2018). Those changes in soil hydrology and associated soil moisture lead to essentially changed preconditions for soil development, including the decomposition of soil organic matter (SOM), nutrient supply and weathering processes (Jobbágy & Jackson, 2000; Baumann et al., 2014; Lehmann & Kleber, 2015; Nannipieri et al., 2017). Thus, the soil is the crucial link between global change and ecosystem functioning, influencing plants,

hydrology, carbon sequestration, and greenhouse gas emissions (Lal, 2004; IPCC, 2019). However, there is little focus on the role of soil P in these processes.

Global change and soil phosphorus transformation

Increases in mean temperature induced by global change can have significant impacts on soil enzyme activity and microbial properties, which in turn affect the transport and transformation of soil P in ecosystems (Fig. 1). Previous research has suggested that warming can increase the total P content of the soil in terrestrial ecosystems while reducing plant-available P in soils (Geng et al., 2017; Mei et al., 2019). This may be due to warming enhancing P adsorption on mineral surfaces, reducing soil Po pools by stimulating the mineralization of Po (Rui et al., 2012) and mobilization of soil P by simultaneously increasing the phosphate content while decreasing the proportion of orthophosphate in soil (Zhou et al., 2021). These effects can lead to increased difficulty in soil Po mineralization and decreased soil available P content (Fig. 1, Tian et al., 2023). On a global scale, warming has been found to increase soil phosphatase activity significantly (Sardans et al., 2006; Tian et al., 2023) or to have no effect (Margalef et al., 2021), which may be attributed to the fact that warming affects different soil matrices in terms of organic matter decomposition and microbial activity. Additionally, climate warming interacts with other environmental factors in toil P transformation. Increased temperature and precipitation can increase the solubility of Pi in soils and stimulate the release of P from SOM (Ren et al., 2018), while increased temperature and fertilizer application can reduce phosphatase activity because fertilizer application affects the decomposition of organic matter (Wu et al., 2020). Overall, warming accelerates the mineralization of Po and affects the mobilization of Pi by altering soil moisture conditions, enhancing microbial activity, and increasing plant demand for P.

However, the effect of N deposition on P transformation in grassland ecosystems is not consistently understood compared to the impact of increased temperature. Anthropogenic simulated N deposition (N addition) has mainly influenced P effectiveness in the long term by changing soil pH, which is related to the underlying

soil properties in the study area (Wang et al., 2016). The effect of N addition on total and effective soil P content has been shown to increase (Tian et al., 2021), decrease (Gong et al., 2015), or have no effect (Liu et al., 2017; Cao et al., 2022), indicating that N addition may increase soil microbial load and plant aboveground biomass, leading to more P being returned to the soil through residues, or it may produce abiotic stresses that stimulate increased plant root secretion while accelerating P uptake and consumption, leading to P limitation (Chai & Schachtman, 2021). The reasons for this variation include differences in the duration and amount of N addition experiments, as the turnover of insoluble Pi and Po in the soil usually takes months or even years, and moderate amounts of N promote plant growth and development and enhance microbial activity. In contrast, excess N causes soil acidification and reduces microbial activity. Variations in soil properties such as pH, texture, and water content may also affect the results. Furthermore, N deposition may increase the amount and activity of soil microorganisms, increasing microbial demand for P and reducing the available P in the soil (Vitousek et al., 2013). Changes in enzyme activity related to soil P transformation are also associated with the duration and accumulation of N addition (Zuccarini et al., 2021). N addition can significantly increase acid phosphatase (Zhang et al., 2013) and decrease or increase alkaline phosphatase activity (Zhang et al., 2019), while phosphodiesterase activity showed a trend of increasing and then decreasing with increasing N addition (Zhang et al., 2019). The effect of N deposition on soil P transformation varies significantly under different environmental factors, and both N deposition and warming are long-term processes. Therefore, it is necessary to conduct short-term and long-term field experiments that consider different grassland ecosystems' characteristics and mechanisms of soil P response to long-term global changes.

Plants and phosphorus

Plants require P for essential physiological and biochemical processes such as photosynthesis, energy transfer, and nucleic acid synthesis (Vance et al., 2003).

However, P is often limited in soil, and its availability can restrict plant growth and productivity (Elser et al., 2007; Vitousek et al., 2010). To overcome P limitation, plants have evolved various strategies to enhance their P uptake, including changes in root architecture, symbiosis with mycorrhizal fungi, and exudation of organic acids and phosphatases (Shen et al., 2011; Wen et al., 2019). Phosphatases, including phosphate monoesterase and phosphodiesterase, play a crucial role in the mineralization of Po, making it available for plant uptake (Turner et al., 2005; Huang et al., 2017). These enzymes are primarily secreted by soil microorganisms and plant roots. In addition, organic acids and protons released by plant roots and microorganisms are involved in the mobilization of Pi, promoting the conversion of insoluble P into available forms that can be used by plants and microorganisms (Hidaka & Kitayama, 2011; Shen et al., 2011). Root-associated microorganisms also play a critical role in P acquisition by plants. These microorganisms use similar mechanisms to increase P availability, such as enzymes and organic acids and solubilizing Pi through acidification (Shulse et al., 2019). Furthermore, plants have evolved diverse root architectures and morphologies that increase their ability to explore the soil for P, including longer roots, greater root density, and the production of root hairs and proteinoid roots (Niu et al., 2013; Jiang et al., 2019; Kirchgesser et al., 2023). Symbiosis with mycorrhizal fungi is another crucial strategy plants use to improve their P uptake. Mycorrhizal fungi form a mutualistic relationship with plants, providing them with P in exchange for plant-derived carbon (Averill et al., 2019). However, it is unclear how plants adjust their P uptake strategies in response to N deposition in the presence of different soil P contents, making it difficult to predict vegetation dynamics under these conditions.

Soil properties and phosphorus availability

The availability of P in soil depends on various factors, such as soil pH, organic matter content, and other nutrients. Many soil properties like texture, structure, and soil pH can affect the availability of soil P (Carson & Ozores-Hampton, 2013; Liu et al., 2022). For instance, soil texture and clay mineralogy are relevant to the abiotic immobilization

of Pi; in particular, clay minerals with a higher specific surface area may form stable chemical bonds with P by Ca^{2+} and magnesium Mg^{2+} (Bünemann, 2015; Spohn, 2020). Soil pH also plays a critical role in the availability of P, as Fe oxyhydroxides have a strong sorption site for Pi, and this capacity increases with decreasing soil pH (Boily et al., 2001; Gregory, 2005; Fig. 1).

The Tibetan Plateau is a unique environment that various geological, geomorphological, and climatic processes have shaped. The soil formation on the plateau is primarily influenced by geomorphological, cryogenic, erosive, and aeolian sedimentation processes (Baumann et al., 2014). Aeolian sediments are dominant, resulting in young soils showing polygenetic formation and strong degradation features (Stauch et al., 2012). The eastern part of the plateau is particularly vulnerable to intense precipitation during the summer months, combined with the dry winter monsoon and sparse vegetation, resulting in aeolian erosion and re-deposition (Dong et al., 2014). The resulting soil substrates have varying properties and characteristics that affect nutrient availability and plant growth. Nevertheless, it is unclear which abiotic factors primarily affect soil P transformation under warming and N deposition conditions on the Tibetan Plateau.

2. Objectives

Objective

This thesis investigated soil P fraction and transformation in alpine grassland ecosystems. In this context, the effects of nutrient enrichment (simulated N deposition), grazing, warming, soil properties, and geomorphology on soil P fractions and transformation and the plant responses on P uptake were investigated. Additionally, a promising approach with Fourier transform near-infrared spectra (FT-NIRS) and mid-infrared spectra (MIR) was used to measure soil P fraction as proxies with reasonable accuracy in forest soil P analysis as a less expensive and time-saving technique (Gruselle & Bauhus, 2010; Niederberger et al., 2015). As the complexity of the factors and mechanisms influencing soil P transformation and the wide range of sampling sets, the thesis focused on the following objectives to investigate:

1. the impacts of nitrogen and phosphorus additions in phosphorus transformation and soil properties compared with the FT-NIRS technique (manuscript 1);
2. the influences of nitrogen deposition on soil phosphorus fractions and plant P uptake (manuscript 2)
3. the impact of nitrogen deposition and grazing in phosphorus transformation (manuscript 3)
4. the responses of soil phosphorus transformation to OTC warming along elevational gradients (manuscript in preparation)
5. the variation in phosphorus fractions along elevational gradients and slopes (manuscript in preparation)

3. Materials and methods

3.1 Experimental site

The experimental site is located at the Haibei National Field Research Station of Alpine Grassland Ecosystem (37°37’ N, 101°19’ E, 3250 m above sea level), run by the Chinese Academy of Science in the northeastern Qinghai-Tibetan Plateau. The station is inside a flat valley with mountains surrounding it. To the north lies the mountain of Leng-long-Ling, averaging 4600 m, covered in snow throughout the year. The mountain of Daban lies in the south, with an average of 4000 m. The region has a continental monsoon climate in summer, and high pressure from Siberia in winter, with a mean annual temperature of –1.7 °C, ranging from an average monthly temperature of –14.8 °C in January to a high of 9.8 °C in July and an average annual rainfall of 489.0 mm, with over 80% occurring from May to September (Liu et al., 2018). During the summer, frost, ice, and snow can still occur. It has long, dry, cold and short, wet warm seasons. The base clay-loam-textured soil around the station is classified as **Mat-Cryic Cambisol** (Chinese Soil Taxonomy Research Group, 1995), corresponding to **Gelic Cambisol** (WRB, 2015), which is relatively newly developed, shallow and rich in soil organic matter content. The plant community at the site is dominated by *Kobresia humilis*, *Stipa aliena*, *Elymus nutans*, and *Festuca ovina*. The nutrient addition experiment site is located near the station, and the warming and altitude gradient experiment sites are on the northeast side of the station at a distance of 10 km.

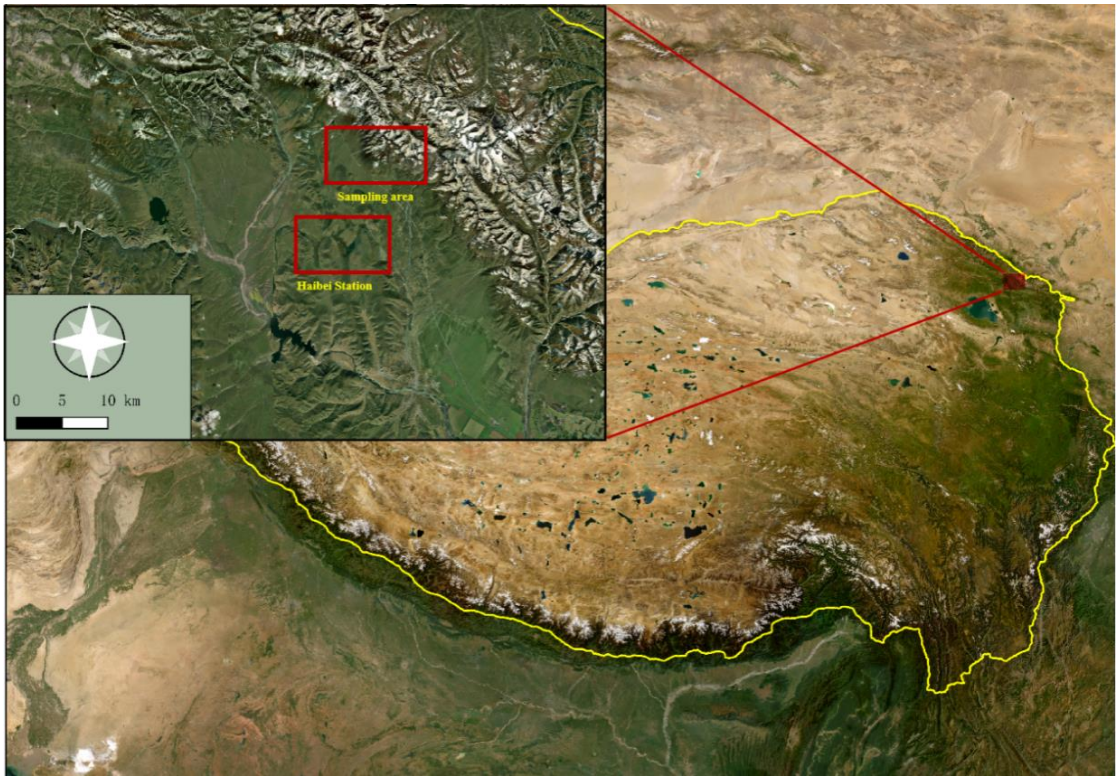

Fig. 2 Field sampling area in alpine grassland ecosystem on the northeastern Tibetan Plateau (Zhang et al., 2021).

3.2 Experimental design

3.2.1 Nutrient addition experiment

The long-term field experiment (initiated in 2011 to 2018) is based on a fully randomized two-factor (P and N fertilization) design with six replications. Each plot is 6 m × 6 m in size. A 2 m buffer strip separated the blocks, and a 1 m buffer strip separated the plots within each block to minimize interference from neighbouring plots. The fertilizers (triple superphosphate supplied at 50 kg P ha^{-1} yr^{-1} and urea supplied at 25, 50, and 100 kg N ha^{-1} yr^{-1}) were distributed by hand to the soil surface after sunset in early June, July, and August during the growing season of each year (Ren et al., 2016), consisting of varying P and N addition levels (control, P, NP, N25, N50 and N100, Fig. 3b).

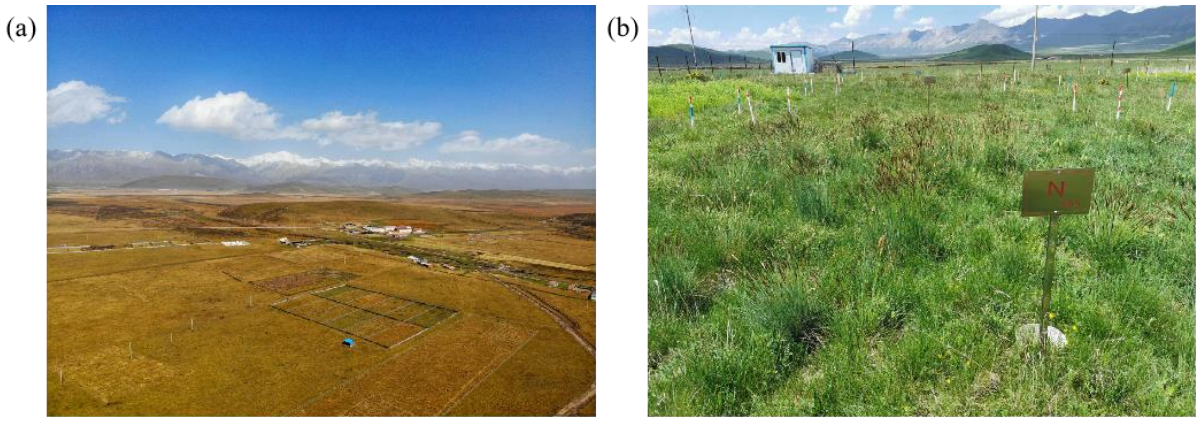

Fig. 3. Drone view of the Haibei Station (a) and NP addition experiment plots (b) the station.

3.2.2 Warming experiment

In order to simulate global warming, from 1997 to 2011, the open-top chambers (OTC) were set up at three altitude gradients near the Haibei station (3200 m, 3600 m, 3900 m asl.) on the Leng-long-Ling Mountain, in which the temperature was expected 2 °C higher than the outside (Fig. 4). The experiment design of this study is the same as Klein et al. (2004) and Chen et al. (2016), which contained more detail on the experimental design and characteristics of the site.

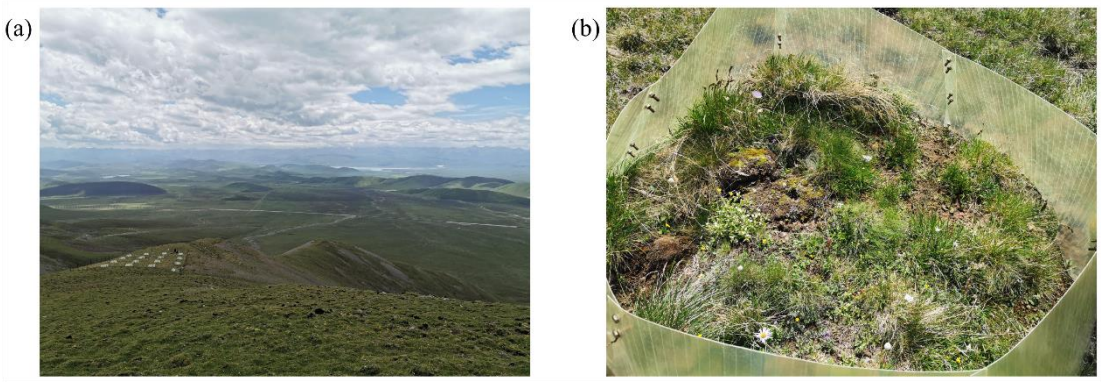

Fig. 4. OTC experiment site at 3900 m (July. 2019): a) view of the site from above; b) inside the warming device.

3.2.3 Altitude gradient sampling

Random sampling was carried out at three elevations along the gradient of the OTC sites, with points near the plots. An additional point was at a higher elevation, above the upper limit of plant growth, where some moss existed (Fig. 5). Each sample site included three slopes, ridgeline, northwest (Yin, shadow) and southeast (Yang, sunny) slopes (Middle), according to the orientation of the geomorphology. In addition, two ridges to the southeast were selected as replicates. The altitudes were 3200 m, 3600 m, 3900 m and 4200 m.

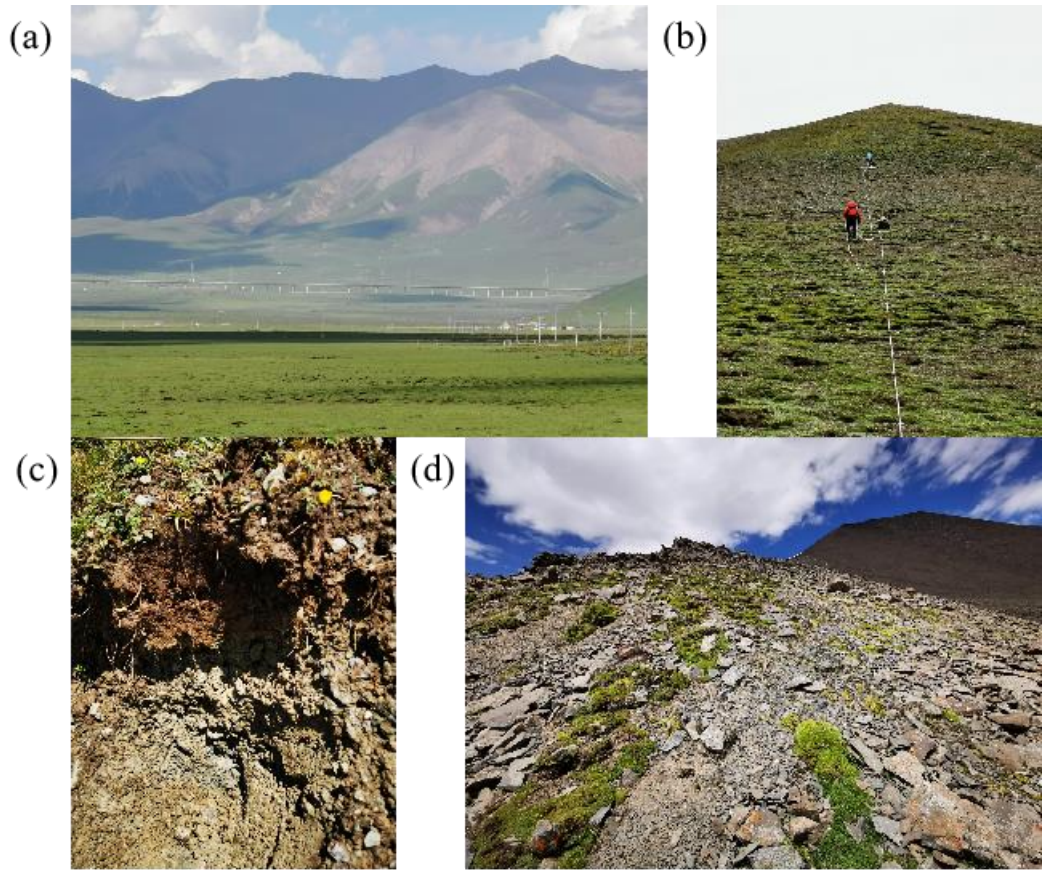

Fig. 5. The grouping shows: a) a distant view of the altitude gradient sampling (where OTC site also located); b) the climbing process; c) the upper soil profile and 4) the distribution of vegetation above the grass-line.

3.3 Soil and plant sampling

Sampling was conducted in August 2018 for the nutrient addition experiment and in July 2019 for altitude gradient experiments. A 0.5 m × 0.5 m sampling area was set at each point. Soils were sampled from 0–10 cm depth (topsoil, covering the A horizon) and in a second depth increment from 10–20 and 20–30 cm depth (subsoil). Five soil samples were randomly taken per plot and depth from each replicate using a soil corer with a diameter of 5 cm and combined into one mixed sample. In random sampling, each soil sample collected two cutting ring samples as soil cores to determine soil bulk density and other indicators. All soil samples were packed in polyethylene bags and stored in an ice box before being shipped to the laboratory. Subsequently, soils were sieved (< 2 mm) and all visible roots, residues, and stones were removed.

Vegetation communities in the nutrient addition experiment were surveyed in mid-August 2018 at the peak of the growing season. Each plot was surveyed three times for species richness, ranging from 1 m^2. Plants were harvested from a randomly chosen 0.5 m × 0.5 m quadrat within each plot. Shoots were cut, and litter was collected at the base with scissors and sorted to measure aboveground biomass. Plants in OTC and altitude gradient experiments were surveyed in July 2019 and harvested from a randomly chosen 0.3 × 0.3 m quadrat within each plot.

3.4 Samples analyses

Hand-held sensors measured soil temperature and moisture with three repetitions of each soil layer and plot. The soil core in the cutting ring was dried in the oven overnight at 105 °C to determine soil bulk density (100 cm^3 intact core). Soil textures, as soil particle size distributions, were measured using the laser diffraction method (Sedigraph III particle size analyzer, Micromeritics, Aachen, Germany). Other soil samples were air-dried and sieved to a fine fraction (<2 mm). The amounts of total SOC, total N were tested by the elemental analyzer (Vario EL III, Elementar, Hanau, Germany); approximately 40 mg of ground sample material was weighed into tin foil and analyzed

using an oxidative heat burn at 1150 °C in an atmosphere of helium. Soil pH was determined with a 1 M KCl solution (soil-to-solution ratio 1: 2.5) by pH meter (pH 340, WTW GmbH, Weinheim, Germany) using a Sentix 81 electrode.

An amount of 0.5 g from each sample was weighed into a 50 mL centrifuge tube for extraction. The fractionation steps are given in Table 1. For the regular Hedley fractions, the amount of organically bound P in the 1 M HCl extracts was considered negligible and not analyzed, and the concentrated HCl ($HCl_{conc.}$) fraction was applied (Alt et al., 2011; Pätzold et al., 2013; Niederberger et al., 2015). All Pi fractions were determined by continuous flow analysis (CFA, SEAL Auto Analyzer AA3, SEAL Analytical GmbH, Norderstedt, Germany). Total $NaHCO_3$-P and NaOH-P were determined by inductively coupled plasma–optical emission spectrometry (ICP–OES, Optima 5300 DV, PerkinElmer, Waltham, MA, USA). Among the extracted Pi fraction, resin-Pi and $NaHCO_3$-Pi are considered as labile Pi, NaOH-Pi as moderate Pi, and $HCl_{conc.}$-P with residual P as stable P (Hou et al., 2018). The major elements (Ca, Mg, Al, Fe), as well as the trace elements of samples, were measured by the wavelength dispersive X-ray fluorescence spectrometer (XRF, S2 Picofox, Bruker AXS GmbH, Karlsruhe, Germany).

All the plant and microbial properties, including the plant biomass, P contents, microbial biomass phosphorus (MBP), soil acid phosphatases (ACP), colonization rate by arbuscular mycorrhizal fungi (AMF) in rhizosheath, etc., were analyzed at partner Lanzhou University and associated laboratories and are detailed in the manuscript 2 and 3 (based on the nutrient addition experiments). It is worth noting, however, that plant samples of altitude gradient sets were lost due to uncontrollable factors in the laboratory and could not be resampled due to the pandemic and related control measures in the following two years, which unfortunately could not be analyzed.

3.5 Statistical analysis

To evaluate differences in P fractions between the treatments and soil depth increments, one-way ANOVA and independent-sample t-tests were used in JASP statistical software (University of Amsterdam, Amsterdam, Netherlands). Differences were considered significant at $P < 0.05$. Correlations between P fractions and other environmental factors were examined using Pearson's correlation coefficients with heat maps; correlations between soil physicochemical indicators and P fractions were analyzed using principal component analysis (PCA) and redundancy analysis (RDA) using Origin v.2021 and Canoco v.5 (Microcomputer Power, Ithaca, New York, USA) software. Especially, the calibration of FT-NIRS models of P fractions was processed by the spectroscopic software OPUS/QUANT (v.7.5, Bruker Optik GmbH, Ettlingen, Germany, 2014), the partial least-squares regression (PLSR) models were used and detailed in manuscript 1. All other statistical analyses in manuscripts were conducted using SPSS v.25.0, Origin v.2021 and Excel 2019.

4. Results and discussion

4.1 Impact of nitrogen and phosphorus additions in phosphorus dynamics and soil properties

This study was conducted in order to investigate the influence of N and P input on soil P transformation (i.e., from Po to Pi form) and soil properties in the alpine grassland simulating the effects of N deposition on the productivity and stability of the ecosystem, which has been divided into three sections: 1) effect of N and P addition on the Hedley P fractions (**manuscript 1**); 2) effect of N addition on plant P acquisition strategy with varying P availability in the soil (**manuscript 2**); and 3) effect of N addition and grazing on soil P transformation (**manuscript 3**).

Manuscript 1

The bioavailability and dynamics of soil P can be significantly affected by nutrient inputs and climatic conditions by influencing chemical, biological and biochemical processes. Manuscript 1 aimed to investigate the effects of N and P inputs on soil P availability and transformation under alpine grassland soils, combined with a tentative analysis of P fraction in alpine grassland soil using near-infrared spectroscopy (FT-NIRS). Therefore, modified Hedley P fractions were extracted from 191 samples from the nutrient addition experimental site at four depth increments (0–10 cm, 10–20 cm, 20–40 cm, and 40–70 cm), including N and P additions. Among the extracted Pi fraction, resin-Pi and $NaHCO_3$-Pi (i.e., Pi adsorbed on soil surfaces) are considered as labile Pi, NaOH-Pi (i.e., Pi associated with aluminum and iron oxides or carbonates) as moderate Pi, and $HCl_{conc.}$-P (i.e., Pi bound to Ca) residual P as stable P fraction (Tiessen & Moir, 2007; Niederberger et al., 2015; Hou et al., 2018). The results of the P extraction were compared with the NIRS model using PLSR in the laboratory.

We found that the available P (i.e., labile Pi and Po) accounted for 11% of the total P in the tested soil, which is always considered as labile P that can be directly absorbed and

used by plants was significantly increased by P addition, but not with the N addition (Fig. 6). Intriguingly, the contribution of Po to total Hedley-P was greater in treatments without P addition. In the study, the $HCl_{conc.}$-P fraction was the dominant Pi fraction among all fractions, suggesting that Ca-bound Pi was the main Pi fraction in alpine grassland soil. In contrast, the content of NaOH-Po fraction dominated the Po fractions and only increased significantly with the addition of NP combination, indicating that Fe and Al -bound Po. In addition, the P addition could promote the mineralization of the labile Po pools and the accumulation (mobilization) of labile and moderate Pi pools (Fig. 6; Liao et al., 2021).

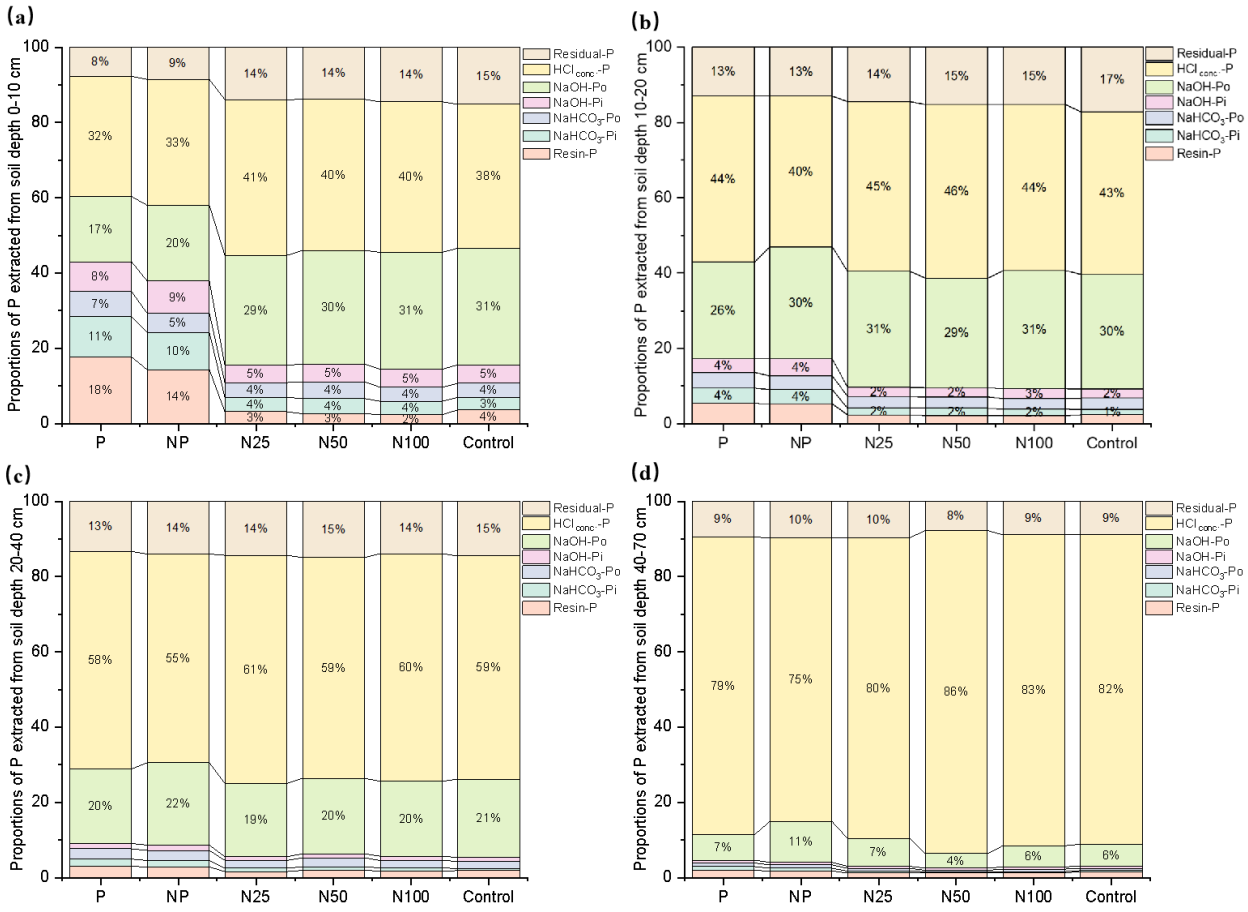

Fig. 6. Proportions of P-extracted Hedley fractions from soil depth increments: (a) 0–10 cm; (b) 10–20 cm; (c) 20–40 cm; and (d) 40–70 cm.

The relative availability of soil N and P in alpine grasslands is a major determinant in regulating plant nutrient uptake and controlling plant metabolic and growth rate (Zhang

et al., 2018). N addition could lower the soil pH and enhance the dissolution of recalcitrant Ca-bound Pi into moderately occluded Pi and available P fractions (Liu et al., 2019). In this study, however, the stable pH after N and P input indicated another possibility of affecting the P fractions by promoting the secretion of microbial extracellular phosphatase, which enhances the mineralization of Po, thereby increasing the leaching of available P (Figs. 6 and 7 in manuscript 2), highlighting the P-limit after N input and the composition of the plant species must be considered to estimate plant access to soil P (Pätzhold et al., 2013). Most of the P was present in stable forms (up to 65%, Fig. 6), which can be attributed to the formation of the relatively young soil of the Tibetan Plateau (Baumann et al., 2019).

On the other hand, the fractionation data was correlated with the corresponding NIRS soil spectra; the coefficient of determination (R^2) of the NIRS calibrations for predicting the fractions of P in P was between 0.12 and 0.90; the ratio of the (standard error of) prediction to the standard deviation (RPD) was between 1.07 and 3.21; the performance-to-interquartile range (RPIQ) ratio ranged between 0.3 and 4.3; and the model prediction quality was higher for Po than Pi fractions, and decreased with N and P addition (Table 2). The calibration models of individual P fractions achieved relatively satisfactory results for some, but not all, individual P fractions. It is obvious that nutrient amendments increased the data redundancy (higher heterogeneity) significantly, resulting in reduced accuracy. Overall, the accuracy and reproducibility of the results from the Hedley fractionation method are critically important to the quality of the predictions of the NIRS models (Niederberger et al., 2015). The labile P pools performed poorly, while moderate and stable pools were better, which was hypothesized that organic acid might slowly displace Pi because many naturally occurring acids, such as citric acid and oxalic acid, compete with phosphates for sorption sites (Richter et al., 2006). In addition, the model showed little variance in performance with Pi and Po fractions, indicating that both P forms are bound to primary soil properties detected directly by NIRS. According to present knowledge, P or phosphate are not excited through NIR light waves to reflect in a particular part of the

NIR spectrum. Hence, the recognizable excitation of P depends on organic or mineral compounds. If the model is improved, NIRS can help to evaluate the data obtained with the Hedley method, which means that the model based on the large sample numbers could be more precise. In summary, this manuscript indicates that using NIRS to predict more stable P pools, coupled with Hedley fractionation focused on the labile P pool, could be a promising approach for soils in the alpine grasslands of the Tibetan Plateau.

Table 2. Quality parameters for NIRS model calibration in the cross-validation process for all Hedley fractions with different treatments.

P Pools		**Labile P**			**Moderate P**		**Stable P**	
P fractions and treatments		Resin-P	$NaHCO_3$-Pi	$NaHCO_3$-Po	NaOH-Pi	NaOH-Po	$HCl_{conc.}$-P	Residual-P
Control	R^2	0.52	0.82	0.67	0.86	0.95	0.79	0.67
	RPD	1.44	2.33	1.73	1.99	4.43	2.24	1.74
	Bias	0.137	0.023	0.344	0.605	0.517	8.15	−0.417
	RMSECV	4.09	3.21	4.47	3.97	12.9	39.7	10.9
	RPIQ	1.5	3.1	2.1	3.4	5.9	2.7	1.9
P	R^2	0.08	0.42	0.43	0.53	0.86	0.06	0.66
	RPD	1.04	1.32	1.33	1.46	2.74	0.99	1.71
	Bias	−2.3	−0.164	0.096	0.0252	−3.94	8.15	−0.268
	RMSECV	74.9	34.6	20.2	23	21.5	70.5	8.36
	RPIQ	0.9	1.3	1.1	1.5	3.5	0.7	2.0
NP	R^2	0.59	0.62	0.37	0.74	0.75	0.40	0.26
	RPD	1.57	1.63	1.26	1.97	2.04	1.29	1.17
	Bias	0.33	0.397	0.528	0.414	0.865	−0.989	−0.668
	RMSECV	35.7	23.5	16	16.6	30.4	57.8	13.7
	RPIQ	2.1	2.5	1.6	2.9	3.0	1.0	1.4

	R^2	0.48	0.81	0.54	0.87	0.91	0.70	0.80
	RPD	1.39	2.28	1.48	2.75	3.35	1.83	2.22
N25	Bias	−0.045	−0.15	0.3	−0.347	−4.45	1.49	−0.179
	RMSECV	4.43	4	6.3	3.9	18.8	43.9	6.83
	RPIQ	1.2	2.1	1.9	3.3	3.8	1.5	2.4
	R^2	0.02	0.65	0.57	0.77	0.91	0.82	0.69
	RPD	0.92	1.69	1.53	2.1	3.35	2.36	1.8
N50	Bias	0.422	0.209	0.294	0.893	2.02	5.24	0.241
	RMSECV	6.1	5.2	6.35	4.87	17.9	38.7	9.58
	RPIQ	0.6	1.7	1.4	2.1	3.7	2.6	2.2
	R^2	0.10	0.76	0.70	0.80	0.90	0.71	0.72
	RPD	1.06	2.03	1.82	2.26	3.25	1.85	1.88
N100	Bias	0.424	0.0426	0.15	0.203	−1.23	−0.862	0.723
	RMSECV	4.21	3.93	4.26	4.54	18.7	45.9	8.44
	RPIQ	1.3	2.8	2.3	3.0	4.0	2.1	2.3

R^2: coefficient of determination; RPD: ratio of (standard error of) prediction to the standard deviation; RMSECV: root mean squared error of cross-validation; RPIQ: ratio of performance to the inter-quartile range.

Manuscript 2

Based on the nutrient addition experiment and Hedley P fractionations, manuscript 2 focused on the plant P uptake and acquisition strategies (i.e., modifying root morphology, exudate composition, or degree of symbiosis with arbuscular mycorrhizal fungi) in various soil P availability supply at the background of N deposition in the alpine grassland. In this study, the field experiment combined with a glasshouse experiment with four treatments (N addition, P addition, combined N and P addition and control) was conducted to investigate both the community and species levels of the strategies. Here, the responses on the species levels have low relevance to the thesis, thus, are not shown or discussed.

The results showed that neither N nor P addition changed the soil pH; N addition increased soil N availability (NH_4^+ and NO_3^- contents) but decreased available P (sum of resin-Pi and $NaHCO_3$-Pi and Po contents). P addition decreased the total N content but increased P availability. Combined N and P additions significantly increased SOC content compared to the control but did not alter total N content (Table 3). The mean plant shoot biomass was 64% higher in plots with N addition than those without, regardless of soil P availability (Table 4). Furthermore, N addition significantly decreased the root/shoot biomass ratio, and there was a greater increase in the shoot N/P ratio in N-added plots without P addition than in plots with P addition. Shoot P uptake, root P storage, and plant P pool size showed a greater increase with N and P addition than with N addition alone (Table 4). Meanwhile, N addition decreased root biomass at low soil P availability but increased when P was added and enhanced the secretion of acid phosphatase (APase, or ACP) and release of carboxylates in the rhizosheath, which differed from the high P condition (Fig. 7). An increase in colonization by AMF in plots without P application, but high soil P availability significantly inhibited colonization was observed (Fig. 7). These findings provide novel insights into how the plant P acquisition strategies are adapted with N addition (Fig. 8),

which is also a tentative breakthrough in the studies usually based on soil P availability (Wen et al., 2019; Lambers, 2022).

Table 3. Effects of nitrogen (N) and phosphorus (P) addition on soil properties.

Variable	Control	N addition	P addition	N + P	*P* values, two-way ANOVA		
					N	P	N × P
pH	7.37±0.12	7.61±0.05	7.52±0.14	7.34±0.14	0.859	0.596	0.069
SOC ($g\ kg^{-1}$)	60.5±1.3	51.7±3.5	52.4±2.0	74.6±4.0	0.038	0.025	<0.001
Total N ($g\ kg^{-1}$)	8.18±0.50	8.63±0.36	7.57±0.17	8.36±0.39	0.120	0.261	0.655
NO_3^- ($mg\ kg^{-1}$)	2±0.1	18±3	2±1	9±1	<0.001	0.004	0.001
NH_4^+ ($mg\ kg^{-1}$)	6±1	12±3	5±1	5±2	0.058	0.022	0.065
Total P ($g\ kg^{-1}$)	0.70±0.03	0.70±0.02	1.26±0.09	1.16±0.05	0.364	<0.001	0.319
Available P ($mg\ kg^{-1}$)	64.5±3.2	50.6±4.7	407.3±20.7	273.6±11.5	<0.001	<0.001	<0.001

pH, soil organic carbon (SOC), total nitrogen (total N), soil nitrate and ammonium (NO_3^- and NH_4^+), total phosphorus (total P), and available P concentrations were recorded in 2018. Data are presented as the mean (± SE) of six replicates.

The low P availability in soil requires plants to alter their root morphology to promote the rate of nutrient exchange in rhizosheath through partitioning of root biomass, inhibition of primary root growth, promotion of lateral root growth, and promotion of

root hairs of total length (Lambers, 2006, 2022). However, the changes in root morphology observed in this study were not consistent with the expected but reflected the optimization of C costs and not an effective strategy in alpine ecosystems (Jackson et al., 2008; Ven et al., 2019), which is because the kinetic mechanism of available P uptake by the root system plays only a minor role in the acquisition of P (Lambers, 2022). Carboxylates, which are important constituents of root exudates, especially under N-induced P limitation, could mobilize both Pi and Po (He et al., 2020; Prescott et al., 2020; He et al., 2021), consistent with the findings that N addition enhanced the release of carboxylates under conditions of low P availability (Fig. 7b). In addition, N-induced P limitation promoted AMF colonization rate, suggesting that the symbiosis is driven by P availability, which was similar to those observed at low soil P levels and could be the optimal strategy for plants to acquire P under conditions of P limitation (Ven et al., 2019).

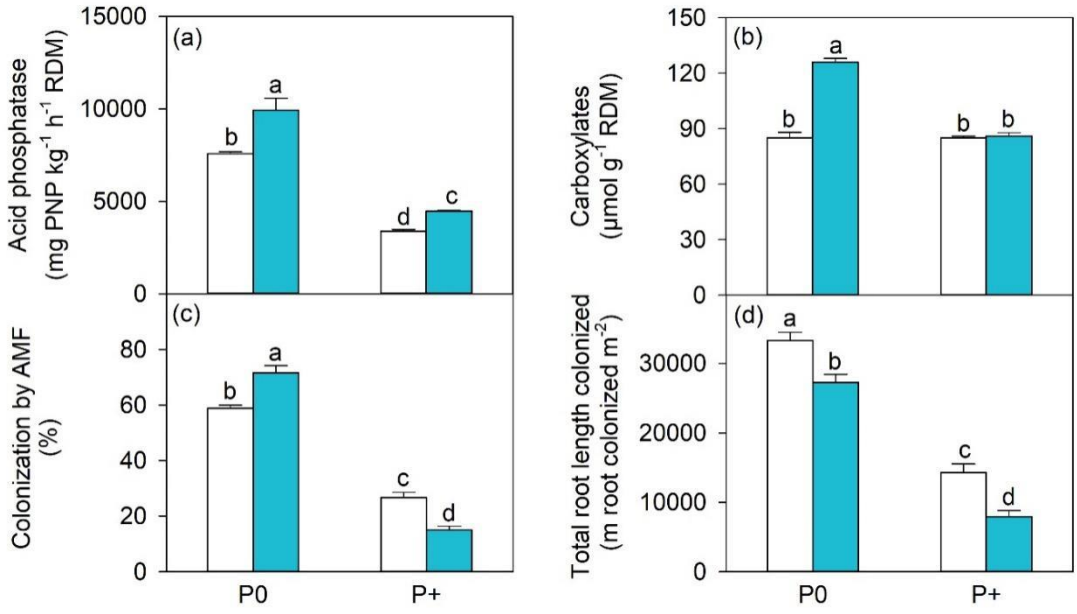

Fig. 7. Rhizosheath exudate (acid phosphatase [APase] and carboxylates), colonisation rate by arbuscular mycorrhizal fungi (AMF), and AMF phospholipid fatty acid (PLFA) concentration under different N and P levels in the field experiment. (**a**) APase, (**b**) carboxylates, (**c**) colonisation rate by AMF, and (**d**) total root length colonised by AMF. All indexes (except APase) were influenced by the significant interaction between N and P addition ($P < 0.05$, Table S4). Lowercase letters indicate that means vary among fertiliser treatments ($P < 0.05$). Data are presented as the mean (+ SE) of six replicates. P0: without P addition; P+: with P addition; N0: without N addition; N+: with N addition.

Table 4. Effects of nitrogen (N) and phosphorus (P) addition on plant variables.

Variable	Control	N addition	P addition	N + P	*P* values, two-way ANOVA		
					N	P	N × P
Shoot biomass ($g\ m^{-2}$)	298±34	472±42	320±25	543±67	<0.001	0.308	0.597
Total biomass ($g\ m^{-2}$)	1776±39	1726±32	1857±52	2182±65	0.010	<0.001	0.001
Root/shoot biomass ratio	5.23±0.48	2.83±0.42	4.95±0.43	3.22±0.34	<0.001	0.894	0.438
Shoot P concentration ($mg\ g^{-1}$)	1.21±0.04	1.12±0.07	3.93±0.15	3.58±0.20	0.101	<0.001	0.325
Shoot N concentration ($mg\ g^{-1}$)	16.8±0.64	23.3±0.71	16.0±0.18	17.9±0.48	<0.001	<0.001	<0.001
Shoot N/P ratio	13.9±0.32	21.3±1.35	4.08±0.14	5.10±0.37	＜0.001	<0.001	<0.001
Root P concentration ($mg\ g^{-1}$)	0.86±0.02	1.06 ± 0.04	0.91±0.01	2.20±0.05	<0.001	0.001	0.160
Shoot P uptake ($mg\ m^{-2}$)	362±48	517±42	1262±114	1945±277	0.013	<0.001	0.100
Root P storage ($mg\ m^{-2}$)	1277±31	1325±59	1391±29	3597±43	<0.001	<0.001	<0.001
Total plant P pool ($mg\ m^{-2}$)	1639±45	1842±57	2653±118	5542±274	<0.001	<0.001	<0.001

Plant shoot biomass, total biomass, root/shoot biomass ratio, shoot P and N concentrations, shoot N/P ratio, root P concentration, shoot P uptake, root P storage and total plant P pool were recorded in 2018. Data are presented as the mean (± SE) of six replicates.

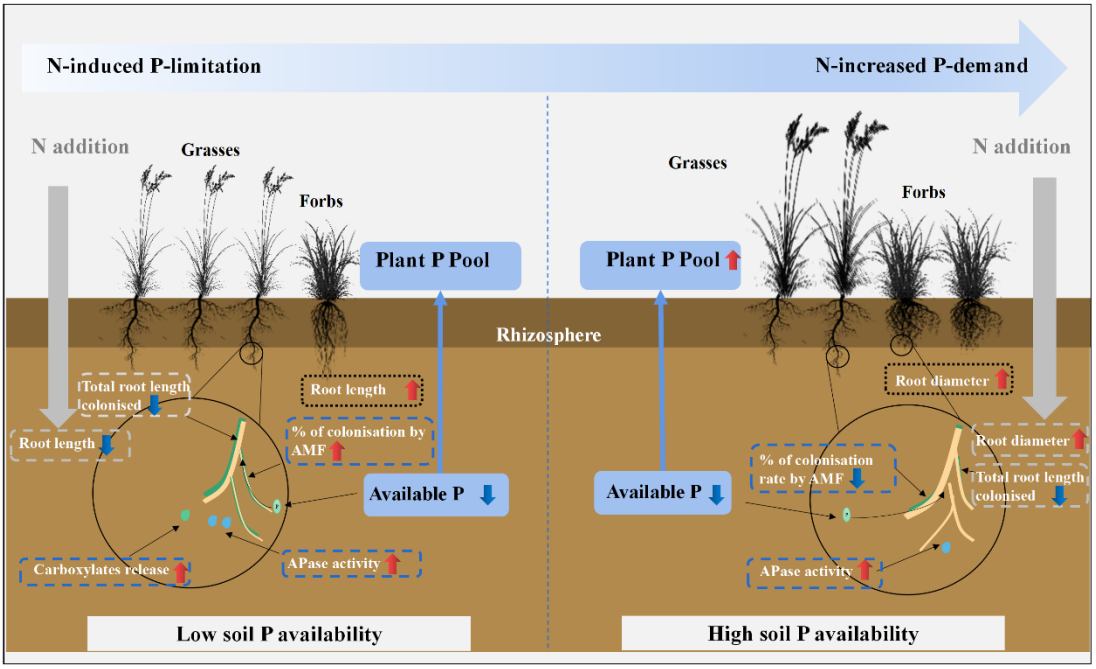

Fig. 8. Simplified framework of changes in plant phosphorus (P)-acquisition strategies in response to nitrogen (N) addition under different soil P levels. Blue dashed boxes indicate the dominant P effects, grey dashed boxes indicate the dominant N effects, and black thin dashed boxes indicate changes in functional groups. Small arrows represent an increase (red arrows) and a decrease (blue arrows) in the variables with N addition. Abbreviations: AMF = arbuscular mycorrhizal fungi.

As opposed to enhanced carboxylate release under N-induced P limitation, in order to inhibit the release of carboxylates under conditions with sufficient P (Fig. 7). The results also showed that N addition enhanced APase activity in the rhizosheath at both high and low P availability, which agree with results of He et al. (2020) and Schleuss et al. (2020), who indicated that under P-limited condition, plants use additional N to produce phosphatases to mineralize soil Po. Moreover, the AMF biomass (given as phospholipid fatty acid, PLFA) decreased with N and P additions, suggesting that plants have reduced photosynthetic C supply to the AMF under sufficient nutrient levels (Grman, 2012). We thus inferred that under sufficient P supply, the plant could use gradual N accumulation as an effective strategy without consuming photosynthetic products.

N-induced P limitation could enhance AMF colonization and carboxylate release but

inhibit root expansion, suggesting that N supply has a greater effect on root morphology than P limitation. With high P availability in soil, N input could increase root diameter and APase activity but not carboxylate release or colonization by AMF. This suggests that plants can compensate for the increased P demand by increasing the root–soil interface and Po mineralization. In summary, this study suggests that the shift in plant P acquisition strategies caused by N input (i.e., N deposition) depends on the soil P availability and highlights the importance of considering soil nutrient availability and species differences in predicting nutrient limitation and plant community adaptation in alpine grasslands in the context of increased N input.

Manuscript 3

In the background of global change, in addition to nitrogen deposition and warming, the Tibetan Plateau is also increasingly affected by land use change, a prominent example being grazing. Grazing practices, including winter and annual grazing, have distinct impacts on soil microbes and their functions (Yang et al., 2019), plant species composition and diversity (Wei et al., 2022), and soil nutrient cycles through litter decomposition (Yang et al., 2019) on the Tibetan Plateau. Manuscript 3 aimed to investigate the effects of N addition and grazing on P transformation based on the nutrient addition experiment and modified Hedley P fractionations in this area. The results showed that increasing the N input rate without grazing led to a greater P storage in plant shoots and litter but a decrease in the microbial P pool (Fig. 9). The Po content and its proportion in the soil total P increased with N addition at a soil depth of 10 cm (Fig. 10). However, the labile Pi and moderate Pi pools were not mobilized by N addition (same results in Fig. 6), despite plants intensifying their P-acquisition strategies, including rhizosheath acid phosphatase activity and carboxylate release, and symbiosis with AMF (as the given results in Fig. 7). In contrast, soil Po content and its contribution to total P decreased with increasing N addition with grazing treatment (Fig. 10). Moreover, grazing effect decreased soil Po pools and root P pool, despite showing more aggressive P-acquisition strategies (Fig. 9). Additionally, soils in alpine grasslands that are rich in basic cations (Ca^{2+}, Mg^{2+}) can limit P mobilization by stabilizing soil pH (Tian & Niu, 2015). In this study, although the highest N addition rate decreased soil exchangeable Ca^{2+} and Mg^{2+} contents by 23.4% and 29.8%, respectively (Table 5), they are still high enough to maintain soil pH stability until these cations are depleted in our experimental fields (Bowman et al., 2008). This is due to the short development time of soils on the plateau (Baumann et al., 2009).

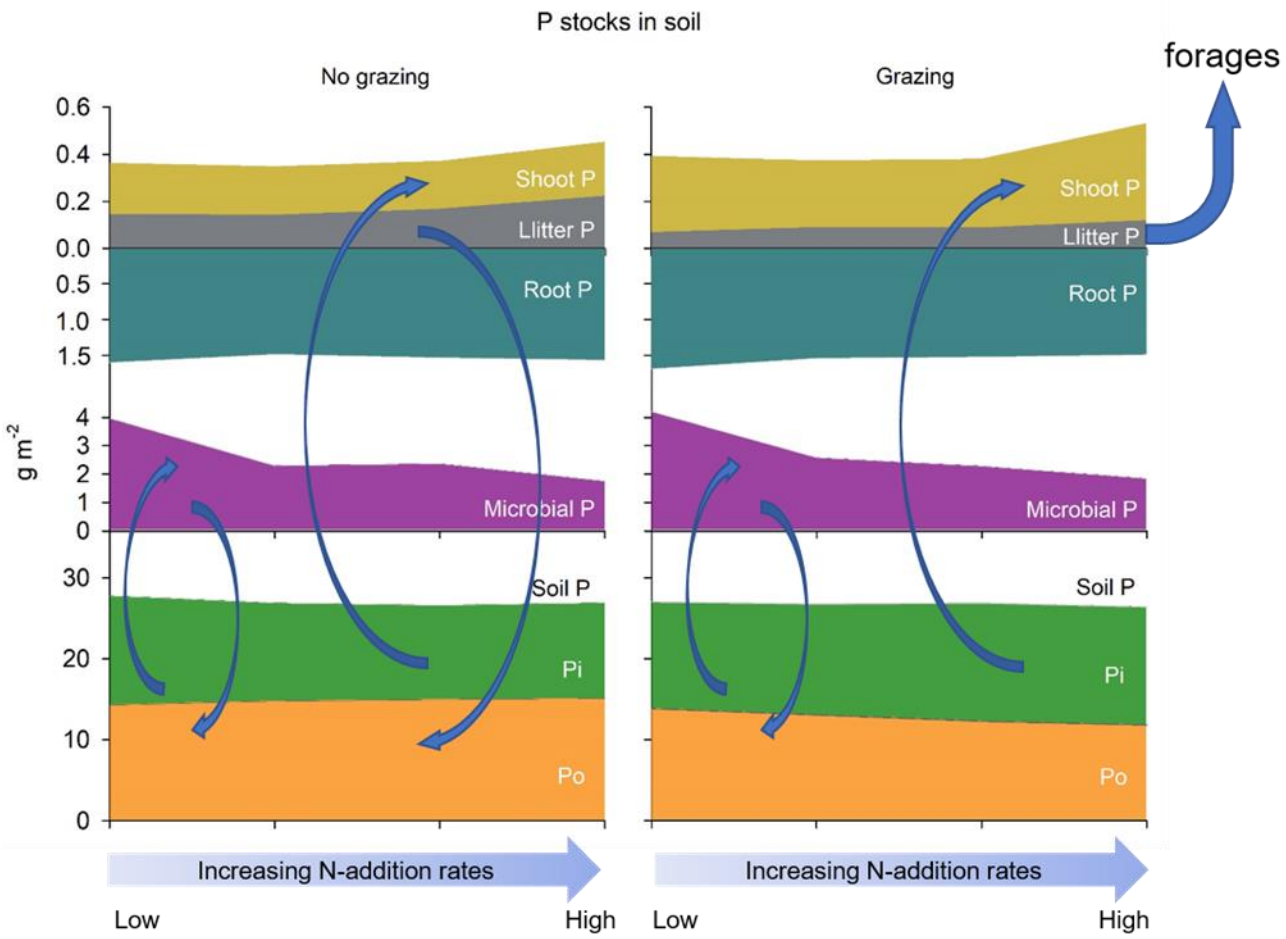

Fig. 9. General trends of the stocks of P pools in soil with increasing N addition rates in fencing (left) and grazing (right) conditions. The arrows show the main pathways for the increased net accumulation and transformation of organic P in alpine grassland soils.

It is also noteworthy that winter grazing interfered with Po accumulation by reducing litter in the field, which decreased litter P stocks, but on the other hand, trampling by grazing animals results in less litter and shallow seed deposition, which promotes the germination and growth of plants the following year (Hao et al., 2018). The cold climate of the alpine grasslands on the Tibetan Plateau and the slow decomposition of the litter prevent the normal germination and photosynthesis of the grasses, and grazing during winter promotes normal plant growth by removing leaf litter as forages (Wei et al., 2022). Moreover, it has been observed that cattle and sheep rarely defecate at grazing sites, leading to a reduction in the litter P pool and impeded plant P return (Fig. 9).

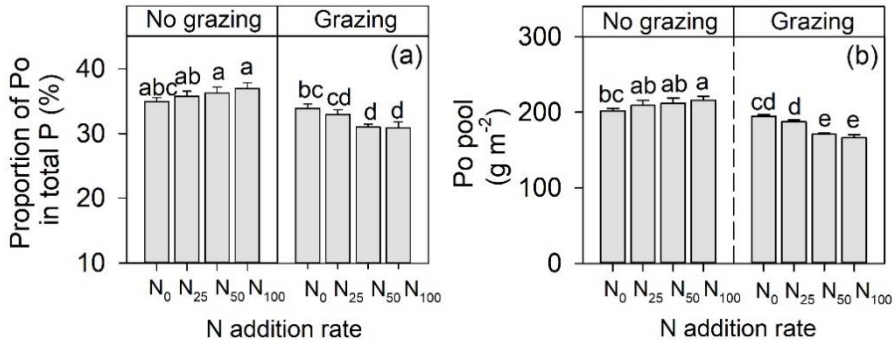

Fig. 10. Plots of the (a) proportions of total organic P (Po, sum of $NaHCO_3$- and NaOH-Po) in the total P and (b) Po pool versus the nitrogen addition rates and grazing in the 0–10 cm soil depths interval. The different lowercase letters indicate that the means are different at $p < 0.05$. The values are expressed as the mean ± 95% confidence intervals.

In summary, this study suggests that N addition increases P conversion from inorganic to organic pools without grazing. Winter grazing increases plant uptake of Pi but inhibits Po accumulation. Plants are the critical factors for the P transformation in alpine grassland soils, and continued N input to grazed areas increases the risk of P loss in the form of Po.

Table 5. Effects of nitrogen (N) addition rate and grazing (G) on soil properties in 0–10 cm depth.

Treatment		pH	SOC (g kg^{-1})	TN (g kg^{-1})	MBC (mg kg^{-1})	MBN (mg kg^{-1})	NH_4^+_N (mg kg^{-1})	NO_3^-_N (mg kg^{-1})	EX. Mg^{2+} (mg g^{-1})	EX. Ca^{2+} (mg g^{-1})	Soil bulk density (g cm^{-3})
NG	Ctrl	7.47±0.08	61.9±5.21	8.80±0.26	1366±3.24	257±4.04	0.63±0.04	2.01±0.42	0.58±0.02	16.82±0.80	0.71±0.02
	N_{25}	7.40±0.10	61.4±4.92	8.44±0.19	1172±35.8	253±11.7	0.80±0.15	5.16±1.87	0.53±0.03	14.36±1.22	0.71±0.02
	N_{50}	7.46±0.10	66.1±1.36	8.65±0.54	998±12.3	227±1.34	0.97±0.20	2.63±0.52	0.47±0.02	13.46±0.24	0.71±0.02
	N_{100}	7.53±0.14	67.2±0.95	8.74±0.48	925±3.94	172±3.22	0.80±0.15	2.88±0.86	0.41±0.03	12.03±0.28	0.70±0.03
G	Ctrl	7.37±0.12	67.4±0.87	8.18±0.50	1361±8.66	263±8.98	0.67±0.04	1.16±0.14	0.58±0.04	16.15±0.61	0.71±0.01
	N_{25}	7.35±0.05	66.6±0.42	9.01±0.87	1109±83.0	214±4.44	0.74±0.05	4.04±0.94	0.56±0.04	13.80±0.83	0.70±0.04
	N_{50}	7.42±0.02	65.9±0.99	8.26±0.47	1106±22.7	228±17.3	0.79±0.06	3.14±0.39	0.45±0.03	15.10±0.86	0.72±0.03
	N_{100}	7.61±0.05	66.4±1.35	8.63±0.36	939±27.2	168±4.63	0.73±0.04	3.20±0.37	0.36±0.04	11.40±0.89	0.71±0.01

pH, soil organic carbon (SOC), total nitrogen (TN), microbial biomass carbon (MBC), microbial biomass nitrogen (MBN), soil nitrate and ammonium (NO_3^-_N and NH_4^+_N), soil exchangeable Mg^{2+} and Ca^{2+} and soil bulk density were recorded. Ctrl indicates the treatment with no N addition, and N addition indicates the treatment with N fertilizer with three levels; G: treatment with grazing; NG: treatment with non-grazing, fencing. Data are presented as the mean (± SE) of six replicates.

4.2 Responses of soil phosphorus fractions to OTC warming along elevational gradients

This study focused on the influence of simulated warming with the open-top chamber (OTC) along the elevational gradients on the soil P fractions and transformation. The OTC increased the average soil temperature at 5 cm depth by 1.03 °C and decreased the average soil moisture by 1.1%, compared with unwarmed treatment (CK; Chen et al., 2016). Based on the current data, warming did not impact soil total P concentration in the upper 0–20 cm depth of all elevational positions (Table 6).

Numerous studies have suggested that warming increases total P in terrestrial ecosystems but reduces plant-available P in soils (Geng et al., 2017; Mei et al., 2019) or has no effects (Cao et al., 2022). This may be due to warming intensifying P adsorption on mineral surfaces, reducing soil Po pool by stimulating the mineralization of Po (Rui et al., 2012), and mobilizing soil Pi, which enhances plant demand (Lie et al., 2022) and uptake (Gong et al., 2015; Zhou et al., 2021). In our study, mineral weathering and plant biomass loss likely had a minimal impact on soil P loss due to the low warming intensity in the field. The results demonstrated that OTC warming exerted little effect on soil available P, with an increase in the content of labile P fraction (Table 6; Fig. 11), which was likely due to the enhanced soil phosphatase activities being beneficial to the mineralization of Po into labile Pi (Yang et al., 2021). Furthermore, the mineralization of Po has been considered the main process controlling the availability of P due to low rates of weathering of P-containing primary minerals in alpine ecosystems (Rui et al., 2012). Additionally, the roots of plants tend to release more organic acids under higher temperatures (Jia et al., 2015), promoting the transformation of moderate and stable P fractions into labile P fractions through chelation with metal cations (Tian et al., 2021) or facilitating the desorption of Pi by competing with phosphate for adsorption sites on soil particle surfaces (Yu et al., 2023). To investigate these views, more studies and data on the plant P pools and root release are needed.

Table 6. Summary of ANOVA results on the effects of warming on different P pools at three OTC positions, showing soil depth at a) 0–10 cm, b) 10–20 cm and c) 20–30 cm.

a) 0–10 cm

Variable	3200 m			3700 m			3900 m		
	df	*F*	*P*	df	*F*	*P*	df	*F*	*P*
Labile P	1	2.05	0.2	1	1.23	0.31	1	4.11	0.09
Moderate P	1	0.44	0.53	1	9.26	<0.05	1	0.30	0.60
Stable P	1	<0.001	1.00	1	1.46	0.27	1	0.89	0.38
Total P	1	0.73	0.43	1	1.09	0.34	1	1.30	0.30

b) 10–20 cm

Variable	3200 m			3700 m			3900 m		
	df	*F*	*P*	df	*F*	*P*	df	*F*	*P*
Labile P	1	16.22	<0.05	1	0.16	0.70	1	3.81	0.10
Moderate P	1	1.16	0.32	1	0.05	0.83	1	0.03	0.86
Stable P	1	0.02	0.89	1	0.31	0.60	1	0.04	0.84
Total P	1	2.89	0.14	1	0.02	0.89	1	0.10	0.76

c) 20–30 cm

Variable	3200 m			3700 m			3900 m		
	df	*F*	*P*	df	*F*	*P*	df	*F*	*P*
Labile P	1	10.00	0.02	1	1.68	0.24	1	0.66	0.45
Moderate P	1	3.22	0.11	1	0.16	0.70	1	0.02	0.89
Stable P	1	1.10	0.33	1	0.68	0.44	1	1.01	0.35
Total P	1	8.62	<0.05	1	0.15	0.71	1	0.58	0.48

df = degrees of freedom, $F = F$ statistic, $P = P$ value, significant differences at $P < 0.05$.

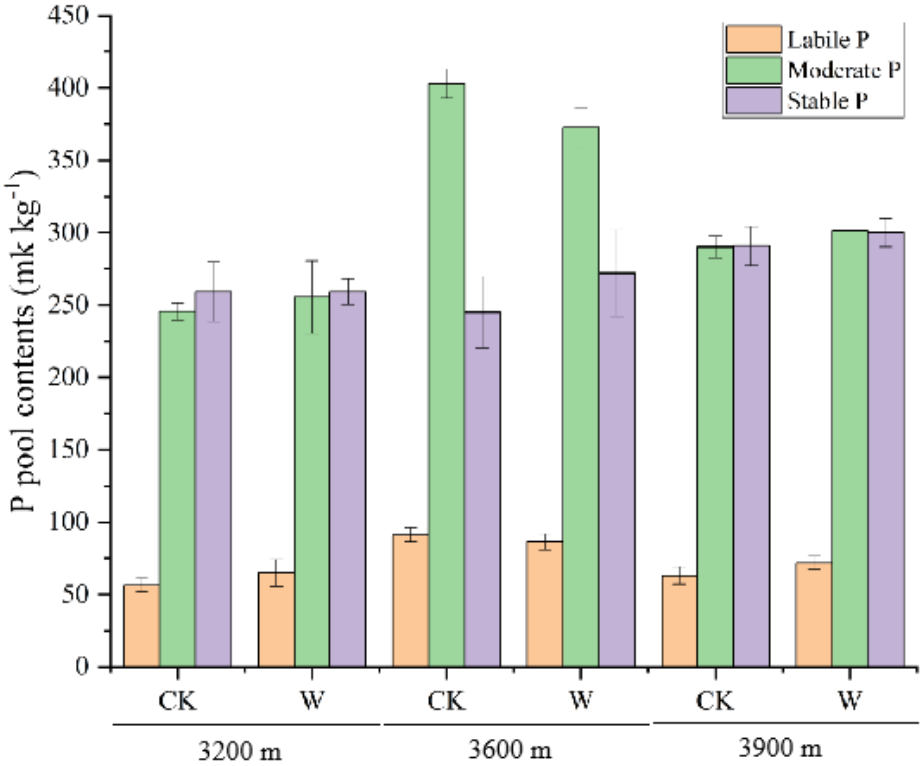

Fig. 11. Phosphorus pools in 0–10 cm of soil, including labile, moderate and stable pools under unwarmed control (CK) and year-round warming using open-top chamber (W) along three elevational gradients.

Table 7. Concentrations (mg kg^{-1}) and proportions (%) of inorganic P (Pi) and organic P (Po) based on the Hedley fractions in 0–10 cm of soil under unwarmed control (CK) and year-round warming using open-top chamber (W) along three elevational gradients.

Treatment		Total Pi (mg kg^{-1})	Total Po (mg kg^{-1})	Proportions of Pi (%)	Proportions of Po (%)
3200 m	CK	308.70±28.05	252.60±7.86	54.91±2.57	45.08±2.57
	Warming	314.78±15.32	265.00±31.09	54.40±2.54	45.61±2.56
3700 m	CK	299.32±30.97	439.98±14.07	40.41±2.10	59.58±2.10
	Warming	322.48±33.46	408.68±22.12	44.05±2.46	55.96±2.45
3900 m	CK	337.95±16.20	306.33±12.01	52.45±1.51	47.56±1.52
	Warming	352.50±15.77	320.70±44.84	52.49±3.78	47.52±3.77

Warming has been found to increase the phosphate content in the soil, but it also decreases the proportion of or thophosphate, which can make soil Po mineralization more difficult and reduce effective soil P content (Tian et al., 2023). However, the results of a 3-year field warming experiment indicated that soil Po concentration decreased at a depth of 0–10 cm (Rui et al., 2012), which is inconsistent with the current findings (Table 7). In addition, no significant impact of warming on SOC content was found (Guan et al., 2018), suggesting that soil Po could be a more sensitive indicator of warming than SOC in alpine grasslands. At a global scale, warming was found to increase soil phosphatase activity significantly (Tian et al., 2023) or to have no effect (Zhang et al., 2017; Margalef et al., 2021). These different findings may be related to the fact that warming affects SOM decomposition and microbial activity in different soil matrices and reduces soil water availability. Climate warming also interacts with other environmental factors in soil P transformation, such as increased precipitation and fertilizer application, which can increase the solubility of Pi in soil and stimulate the release of P from SOM or reduce phosphatase activity due to SOM decomposition (Ren et al., 2018; Li et al., 2018). Further analysis is required in the OTC experiment to investigate whether warming could impact Po's mineralization and affect Pi's activation by altering soil moisture conditions, enhancing microbial activity, and increasing plant demand for P. This may depend on combining other environmental factors with the soil parent material.

4.3 Variation in phosphorus fractions along elevational gradients and slops

This section focused on the changes of soil P pools, soil properties along the elevational gradient and slops with an attempt to answer the question from the perspective of soil: What limits the "grass-line," i.e., the distribution of plants to higher altitudes?

The role of soil properties in accumulating and modifying soil P fractions is well established (Yan et al., 2018; Spohn, 2020). This study revealed strong correlations between certain soil properties and soil P fractions, which also differed significantly along the altitude gradient (Table 8 and Fig. 12), where first two axes explained 58.3% of data variance. For instance, the concentration of total Po pool and NaOH-Po fraction correlated strongly with SOC (r =0.77 and 0.75, $p < 0.001$) and total N (r = 0.76 and 0.74, $p < 0.001$; Fig. 13), are crucial for maintaining soil P reserves. Other study has suggested that SOM stability can limit P loss by binding sites in soil colloids (Antelo et al., 2010).

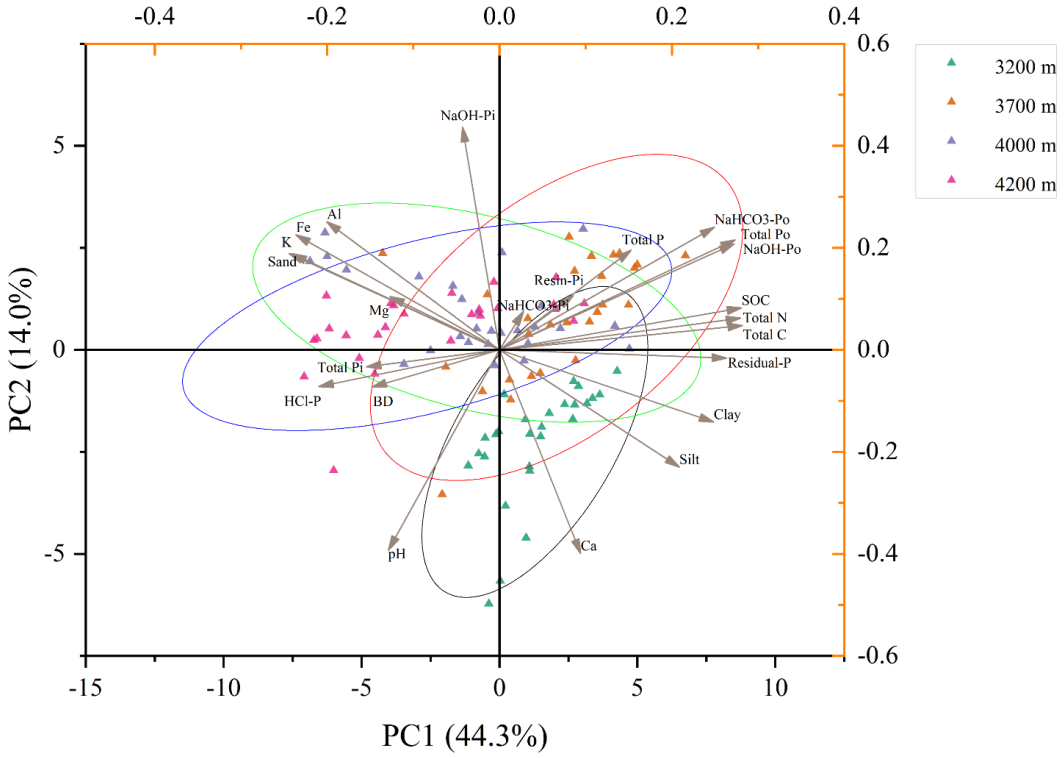

Fig. 12. Principal component analysis (PCA) shows the relationship between soil P fractions and soil properties at different altitudes. SOC: soil organic carbon; total N: total nitrogen. Total sample point (n = 107).

Table 8. Selected soil physical and chemical properties for different land uses at 0–10, 10–20 and 20–30 cm soil depths.

Soil properties	0-10 cm soil depth				10-20 cm soil depth				20-30 cm soil depth			
	3200 m	3700 m	4000 m	4200 m	3200 m	3700 m	4000 m	4200 m	3200 m	3700 m	4000 m	4200 m
pH	6.65 ± 0.54	6.20 ± 0.44	6.16 ± 0.46	6.32 ± 0.27	6.89 ± 0.57a	6.19 ± 0.47b	6.36 ± 0.39b	6.52 ± 0.33b	7.02 ± 0.53a	6.24 ± 0.55b	6.46 ± 0.35b	6.78 ± 0.40a
BD (g cm^{-3})	0.80 ± 0.11	0.77 ± 0.09	0.73 ± 0.12	0.87 ± 0.17	0.88 ± 0.28	0.82 ± 0.12	0.85 ± 0.20	1.08 ± 0.26	0.94 ± 0.28b	0.94 ± 0.11b	0.88 ± 0.23b	1.19 ± 0.29a
Al (g kg^{-1})	66.60 ± 3.19a	69.99 ± 2.82a	72.35 ± 5.02b	73.41 ± 5.37b	67.04 ± 4.43c	72.58 ± 2.54b	79.57 ± 5.36a	77.69 ± 4.82a	68.46 ± 3.05a	72.72±14.13a	81.21 ± 4.87b	80.35 ± 4.67b
Fe (g kg^{-1})	33.00 ± 3.50a	37.08 ± 2.51a	39.47 ± 2.92b	39.00 ± 3.92b	33.99 ± 3.11b	39.70 ± 2.69b	46.04 ± 4.14a	42.04 ± 4.26a	35.27 ± 3.20b	42.72 ± 5.79a	48.43 ± 4.86a	45.17 ± 4.26a
Ca (g kg^{-1})	14.82 ± 9.10a	10.47 ± 1.22b	9.48 ± 2.09b	7.56 ± 2.38c	17.88±13.40a	9.34 ± 1.32b	6.58 ± 2.56c	6.81 ± 2.50c	17.95±11.68a	8.43 ± 1.69b	5.88 ± 2.57c	6.11 ± 3.85c
Mg (g kg^{-1})	12.16 ± 1.29b	12.98 ± 1.39b	14.08 ± 1.75b	14.89 ± 1.72a	12.37 ± 1.47b	13.28 ± 1.85b	15.83±4.04a	15.72 ± 1.43a	12.51 ± 1.31b	13.38 ± 3.00b	15.54 ± 4.89a	16.96 ± 2.35a
Clay (%)	54.62 ± 2.72a	54.09 ± 9.19a	52.61 ± 4.33a	42.83 ± 5.69b	55.48 ± 3.60a	49.19±11.74a	41.79±10.90b	38.78 ± 7.32b	53.68 ± 3.52a	46.69±14.26a	41.13±10.85b	38.25 ± 8.50b
Silt (%)	34.71 ± 3.26a	30.23 ± 2.54b	29.64 ± 2.49b	21.07 ± 4.61c	32.76 ± 2.81a	29.31 ± 5.67b	25.34 ± 7.83b	19.11 ± 4.49c	33.66 ± 3.27a	28.33 ± 7.51b	26.84 ± 4.73b	20.73 ± 5.21c
Sand (%)	10.53 ± 3.85c	15.73±10.81b	17.99 ± 5.62b	35.93 ± 8.50a	11.80 ± 4.64c	21.46±17.28b	32.71±18.80b	42.14±11.06a	12.34 ± 4.77c	24.99±21.56b	31.85±15.09b	41.03± 10.11a
SOC (g kg^{-1})	63.22 ± 17.44	77.79 ± 5.62	64.39 ± 26.12	62.08 ± 25.56	51.80±17.63a	57.67±13.30a	32.62±16.75b	32.30±26.58b	43.22±15.73a	40.24±14.87a	23.95±13.06b	17.67±17.71b

Note BD: bulk density; Al: aluminum; Fe: iron; Ca: calcium; Mg: magnesium; SOC: soil organic carbon. Values indicate mean ± standard deviation (SD). Different letters after the values indicate significant differences among altitude gradients in the same soil layer at $p < 0.05$.

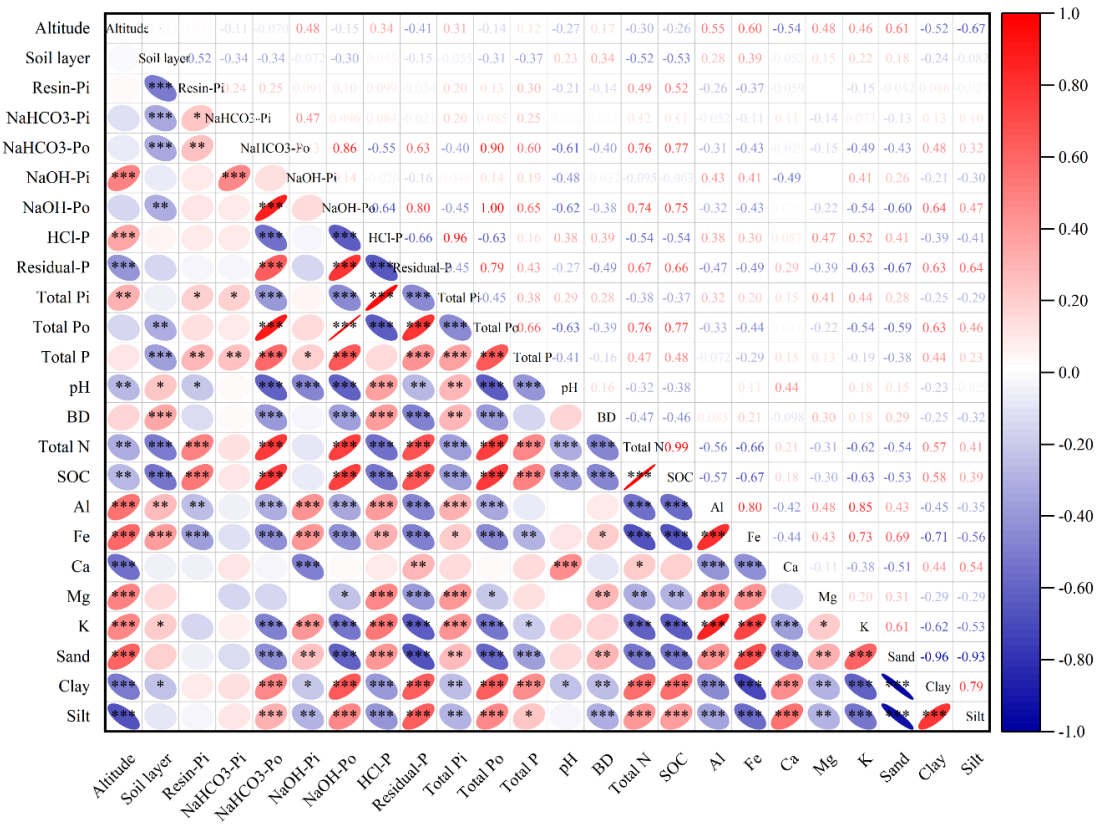

Fig. 13. Pearson correlation analysis of soil P fractions with selected soil properties for all soil samples. Note: Values in the graph represent correlation coefficients (r), while gradient colors represent the Pearson correlation coefficient (r) range from –1 to 1. Red denotes a positive correlation, while blue denotes a negative correlation. Asterisks denote the extent of the significance level: *** indicates $P \leq 0.001$, ** indicates $P \leq 0.01$, and * indicates $P \leq 0.05$. Total sample point (n = 107).

The strong correlation between SOC and total Po (Fig. 14) indicates that SOC plays a vital role in soil P accumulation (Li et al., 2021), as observed in studies on the Himalayan tree line (Müller et al., 2017) and in private research conducted across the Tibetan Plateau (Chen et al., 2017). Although soil properties differ between subtropical forest soil and alpine grassland, studies by Hou et al. (2015) and Yang et al. (2021) have shown a positive relationship between SOC and the concentration of Po fractions. Furthermore, the total Po pool and NaOH-Po fraction showed a significant negative correlation with soil pH (r = -0.63, $p < 0.001$) and Fe content (r = -0.44, $p < 0.001$; Fig. 13), primarily taken up by the oxides of Al and Fe (Hedley et al., 1982). Soil pH is positively associated with total soil Pi fractions, as the P in the soil of this area binds with the Al, Fe, and clay surfaces (Fig. 13). As a result when pH changed, the

concentration of total Pi and $HCl_{conc.}$-P (Ca-associated phosphates) increased, while NaOH-Po fraction and total Po pool decreased, as supported by Fu et al. (2021) and Yang et al. (2021). The resin-Pi fraction also showed a strong positively correlated with SOC (r = 0.52, $p < 0.001$) and total N (r = 0.49, $p < 0.001$; Fig. 13), indicating that the available P to plants depends on the availability of the soil parent material and the nutrient supply.

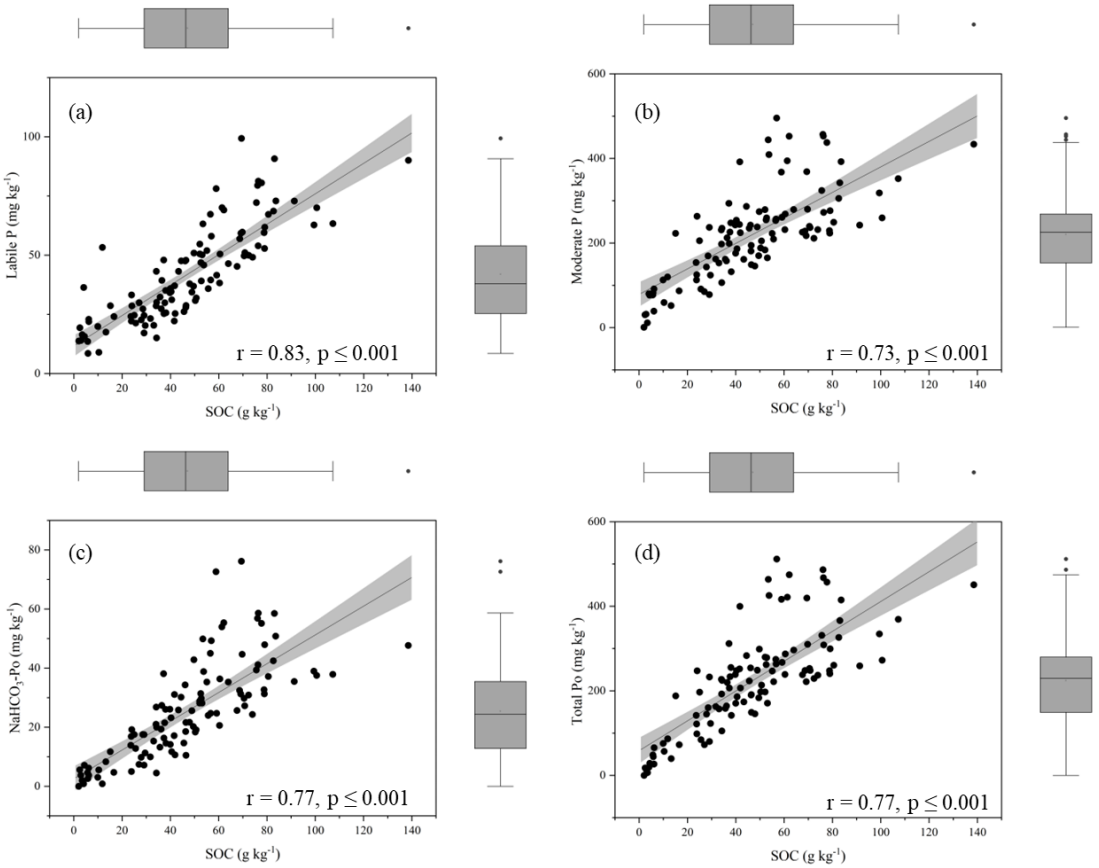

Fig. 14. Relationship between different P pools (a and b, respectively), P fraction (c) and total Po (d) with SOC content.

The RDA results showed that the SOC, total N and clay contents were positively correlated with total Po, moderate P and labile P pools. Meanwhile, the total Pi and stable P pools were also significantly correlated with soil bulk density, Mg and Al concentrations (Fig. 15). The RDA 1 and RDA 2 explained 80.84% of the variation based on all the factors, respectively. This result, together with the above analyses, indicated that the effect of soil factors on soil P pools might vary on different slopes and altitudes. Moreover, the clay content in the soil could mediate the soil fractions, especially the Po and moderate P pools (Fig. 15). In summary, the contents of Al, Fe,

Ca, and sand proportions were strongly correlated with soil P fractions at a lower elevation, indicating the physical protection of soils affects soil P availability and transformation, while at higher altitudes above the grass line, the soil development (i.e., nutrient supply) limits the shifting distribution of plants, which also overrides the effects of factors such as warming. Unfortunately, the loss of plant samples and the lack of moisture control experiments do not allow us to further understand the processes involved.

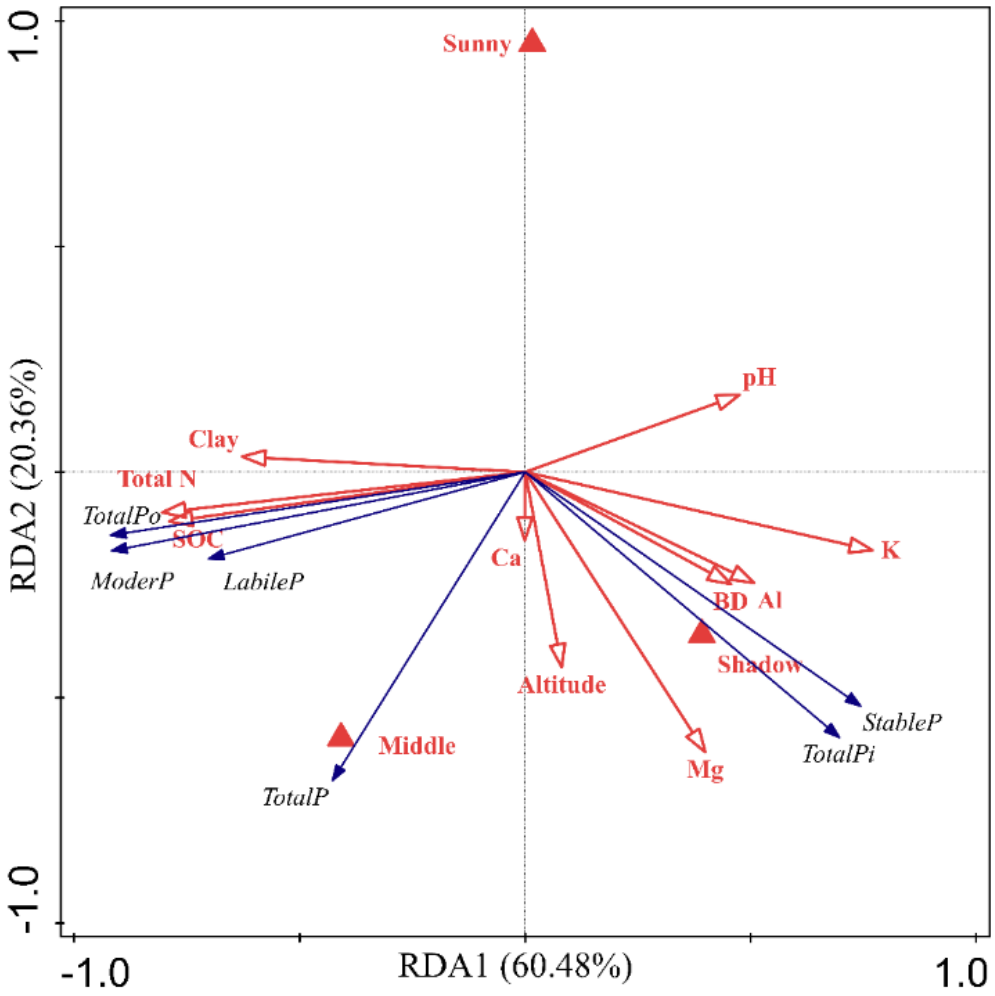

Fig. 15. Redundancy analysis (RDA) ordination graph for the relationship between soil P pools and soil properties along elevational gradients (altitude) and slopes (sunny, middle and shadow).

5. Summary and outlook

This thesis aimed to investigate the impact of global changes, specifically N deposition, warming and land use change through grazing, on the soil P transformation and plant P uptake in an alpine grassland on the Tibetan Plateau. Additionally, this study examined whether P was the limited nutrient factor in driving grasses toward higher elevations. The experiments were carried out using the modified Hedley P fractionation for soil P determination in nutrient addition (gathered with grazing treatment), OTC warming experiments combined with the random soil sampling along elevation gradients.

The studies found that N addition increased N availability but decreased available P in the soil while promoting the mineralization of the labile and moderate Po pools by stimulating the secretion of microbial extracellular phosphatase. Combined N and P additions increased SOC content but did not alter total N content. Plant shoot biomass was higher in plots with N addition regardless of soil P availability, and N addition decreased the root/shoot biomass ratio. With the increasing N input rate, greater P storage in plant shoots and litter and reduced microbial P pool were observed. Changes in root morphology observed in the study reflected the optimization of C costs and not an effective P acquisition strategy in alpine grassland ecosystems.

Warming had little effect on soil total P concentration in the upper 0-20 cm depth of all elevational positions. However, the content of labile P fraction increased, likely due to the enhanced soil phosphatase activities beneficial to the mineralization of Po into labile Pi. In short, the study provides insights into the role of soil properties in accumulating and modifying soil P fractions and identifies SOC as a vital component in soil P accumulation. Results further showed that winter grazing decreased soil Po content and its contribution to the total P pool with increasing N addition and interfered with Po accumulation by reducing litter in the field, which decreased litter P stocks, but on the other hand, trampling by grazing animals promoted the germination and growth of plants the following year.

There were also strong correlations between certain soil properties and soil P fractions that differ significantly along the altitude gradient. SOC played a vital role in soil P accumulation, while soil pH remained stable in all treatments, indicating abundant exchangeable Ca^{2+} and Mg^{2+} as an important factor in buffering against N-induced soil acidification. The effect of soil factors on soil P pools might vary on different slopes and altitudes. The contents of Al, Fe, Ca, and sand proportions were strongly correlated with soil P fractions at lower elevations, indicating that the physical protection of soils affects P availability and transformation. At higher altitudes, soil development (i.e., nutrient supply) limits the shifting distribution of plants, which also overrides the effects of factors such as warming.

Nevertheless, the type of chemical grouping on P fractions, like Hedley fractionation, can only characterize the stability and availability of different P fractions and cannot show the compound composition of Pi and Po, nor is it possible to quantify the contribution of the different fractions to the effective soil nutrients. Thus, to investigate P molecules, such as phytate in the soil and the compound composition, ^{31}P-nuclear magnetic resonance (^{31}P-NMR) or X-ray absorption near edge structure (XANES) spectroscopy (Lambers, 2022) should be used instead of the traditional fractionation techniques only. Additionally, the study using FT-NIRS to predict soil P pools was limited by the instability of P in soil solutions and other disturbances. An attempt was made to use Fourier transform mid-infrared spectroscopy (FT-MIRS) by compression after mixing with potassium bromide (KBr) to analyze soil samples from elevation gradients, which brought unexpected results due to the unquantifiable and uneven mixing. This thesis is also limited by the loss of plant samples and the need for moisture control experiments.

Future research should concentrate on multi-factor experiments with N addition, moisture change and warming to simulate the integrated impacts of global change on soil P dynamics in alpine grassland ecosystems. The functions of microorganisms in the soil related to P transformation and uptake by roots could also be further analyzed by

high-throughput sequencing. Investigating the plant P uptake, microbial communities, function, soil P dynamic, and their interactions driven by global changes will lead to new insights into the stability and productivity of alpine grassland ecosystems.

References

1. Alt, F., Oelmann, Y., Herold, N., Schrumpf, M., & Wilcke, W. (2011). Phosphorus partitioning in grassland and forest soils of Germany as related to land-use type, management intensity, and land-use-related pH. *Journal of Plant Nutrition and Soil Science*, *174*(2), 195–209. https://doi.org/10.1002/jpln.201000142
2. Antelo, J., Fiol, S., Pérez, C., Mariño, S., Arce, F., Gondar, D., & López, R. (2010). Analysis of phosphate adsorption onto ferrihydrite using the CD-MUSIC model. *Journal of Colloid and Interface Science*, *347*(1), 112–119. https://doi.org/10.1016/j.jcis.2010.03.020
3. Averill, C., Bhatnagar, J. M., Dietze, M. C., Pearse, W. D., & Kivlin, S. N. (2019). Global imprint of mycorrhizal fungi on whole-plant nutrient economics. *Proceedings of the National Academy of Sciences*, *116*(46), 23163–23168. https://doi.org/10.1073/pnas.1906655116
4. Azene, B., Qiu, P., Zhu, R., Pan, K., Sun, X., Nigussie, Y., Yigez, B., Gruba, P., Wu, X., & Zhang, L. (2022). Response of soil phosphorus fractions to land use change in the subalpine ecosystems of Southeast margin of Qinghai-Tibet Plateau, Southwest China. *Ecological Indicators*, *144*, 109432. https://doi.org/10.1016/j.ecolind.2022.109432
5. Barry, R. G., & Hall-McKim, E. A. (2018). 8 The Third Pole. In *Polar Environments and Global Change* (pp. 339–377). Cambridge University Press. https://doi.org/10.1017/9781108399708.009
6. Baumann, F., He, J.-S., Schimdt, K., Kühn, P., & Scholten, T. (2009). Pedogenesis, permafrost, and soil moisture as controlling factors for soil nitrogen and carbon contents across the Tibetan Plateau. *Global Change Biology*, *15*(12), 3001–3017. https://doi.org/10.1111/j.1365-2486.2009.01953.x

7. Baumann, F., Schmidt, K., Dörfer, C., He, J.-S., Scholten, T., & Kühn, P. (2014). Pedogenesis, permafrost, substrate and topography: Plot and landscape scale interrelations of weathering processes on the central-eastern Tibetan Plateau. *Geoderma*, *226-227*, 300–316. https://doi.org/10.1016/j.geoderma.2014.02.019
8. Boily, J.-F., Lützenkirchen, J., Balmès, O., Beattie, J., & Sjöberg, S. (2001). Modeling proton binding at the goethite (α-FeOOH)–water interface. *Colloids and Surfaces A: Physicochemical and Engineering Aspects*, *179*(1), 11–27. https://doi.org/10.1016/s0927-7757(00)00712-3
9. Bosch, A., Schmidt, K., He, J.-S., Doerfer, C., & Scholten, T. (2017). Potential CO2 emissions from defrosting permafrost soils of the Qinghai-Tibet Plateau under different scenarios of climate change in 2050 and 2070. *CATENA*, *149*, 221–231. https://doi.org/10.1016/j.catena.2016.08.035
10. Bowman, W. D., Cleveland, C. C., Halada, Ĺ., Hreško, J., & Baron, J. S. (2008). Negative impact of nitrogen deposition on soil buffering capacity. *Nature Geoscience*, *1*(11), 767–770. https://doi.org/10.1038/ngeo339
11. Bünemann, E. K. (2015). Assessment of gross and net mineralization rates of soil organic phosphorus – A review. *Soil Biology and Biochemistry*, *89*, 82–98. https://doi.org/10.1016/j.soilbio.2015.06.026
12. Callaway, R. M., Brooker, R. W., Choler, P., Kikvidze, Z., Lortie, C. J., Michalet, R., Paolini, L., Pugnaire, F. I., Newingham, B., Aschehoug, E. T., Armas, C., Kikodze, D., & Cook, B. J. (2002). Positive interactions among alpine plants increase with stress. *Nature*, *417*(6891), 844–848. https://doi.org/10.1038/nature00812
13. Cao, Z., Kühn, P., He, J.-S., Bauhus, J., Guan, Z.-H., & Scholten, T. (2022). Calibration of near-infrared spectra for phosphorus fractions in grassland soils on

the Tibetan Plateau. *Agronomy*, *12*(4), 783. https://doi.org/10.3390/agronomy12040783

14. Cao, Z., Xu, L., Zong, N., Zhang, J., & He, N. (2022). Impacts of Climate Warming on Soil Phosphorus Forms and Transformation in a Tibetan Alpine Meadow. *Journal of Soil Science and Plant Nutrition*, *22*. https://doi.org/10.1007/s42729-022-00826-8
15. Carson, L. C., & Ozores-Hampton, M. (2013). Factors affecting nutrient availability, placement, rate, and application timing of controlled-release fertilizers for Florida vegetable production using seepage irrigation. *HortTechnology*, *23*(5), 553–562. https://doi.org/10.21273/horttech.23.5.553
16. Chai, Y. N., & Schachtman, D. P. (2021). Root exudates impact plant performance under abiotic stress. *Trends in Plant Science*, 27(1), 80–91. https://doi.org/10.1016/j.tplants.2021.08.003
17. Chen, D., Xu, B., Yao, T., Guo, Z., Cui, P., Chen, F., Zhang, R., Zhang, X., Zhang, Y., Fan, J., Hou, Z., & Zhang, T. (2015). Assessment of past, present and future environmental changes on the Tibetan Plateau. *Chinese Science Bulletin*, *60*(32), 3025–3035. https://doi.org/10.1360/n972014-01370
18. Chen, I., Hill, J. K., Ohlemuller, R., Roy, D. B., & Thomas, C. D. (2011). Rapid range shifts of species associated with high levels of climate warming. *Science*, *333*(6045), 1024–1026. https://doi.org/10.1126/science.1206432
19. Chen, J., Luo, Y., Xia, J., Wilcox, K. R., Cao, J., Zhou, X., Jiang, L., Niu, S., Estera, K. Y., Huang, R., Wu, F., Hu, T., Liang, J., Shi, Z., Guo, J., & Wang, R.-W. (2016). Warming Effects on Ecosystem Carbon Fluxes Are Modulated by Plant Functional Types. *Ecosystems*, *20*(3), 515–526.

https://doi.org/10.1007/s10021-016-0035-6

20. Chen, L., Jing, X., Flynn, D. F. B., Shi, Y., Kühn, P., Scholten, T., & He, J.-S. (2017). Changes of carbon stocks in alpine grassland soils from 2002 to 2011 on the Tibetan Plateau and their climatic causes. *Geoderma*, *288*, 166–174. https://doi.org/10.1016/j.geoderma.2016.11.016
21. Chinese Soil Taxonomy Research Group, 1995. Chinese soil taxonomy. Beijing: Science Press.
22. CMA Climate Change Centre, 2022. Blue Book on Climate Change in China (2022). Beijing: Science Press.
23. Condron, L. M., & Tiessen, H. (2004). Interactions of organic phosphorus in terrestrial ecosystems. *Organic Phosphorus in the Environment*, 295–307. https://doi.org/10.1079/9780851998220.0295
24. Cuo, L., Zhang, Y., Wang, Q., Zhang, L., Zhou, B., Hao, Z., & Su, F. (2013). Climate change on the northern Tibetan Plateau during 1957–2009: Spatial patterns and possible mechanisms. *Journal of Climate*, *26*(1), 85–109. https://doi.org/10.1175/jcli-d-11-00738.1
25. Dong, Z., Hu, G., Qian, G., Lu, J., Zhang, Z., Luo, W., & Lyu, P. (2017). High-altitude aeolian research on the Tibetan Plateau. *Reviews of Geophysics*, *55*(4), 864–901.

    https://doi.org/10.1002/2017rg000585
26. Elser, J. J., Bracken, M. E. S., Cleland, E. E., Gruner, D. S., Harpole, W. S., Hillebrand, H., Ngai, J. T., Seabloom, E. W., Shurin, J. B., & Smith, J. E. (2007). Global analysis of nitrogen and phosphorus limitation of primary producers in freshwater, marine and terrestrial ecosystems. *Ecology Letters*, *10*(12), 1135–1142. https://doi.org/10.1111/j.1461-0248.2007.01113.x
27. Fu, D., Xu, Z., Wu, X., Zhao, L., Zhu, A., Duan, C., Chadwick, D. R., & Jones, D. L. (2021). Land use effects on soil phosphorus behavior characteristics in the

eutrophic aquatic-terrestrial ecotone of Dianchi Lake, China. *Soil and Tillage Research*, *205*, 104793.

https://doi.org/10.1016/j.still.2020.104793

28. Ganjurjav, H., Gao, Q., Gornish, E. S., Schwartz, M. W., Liang, Y., Cao, X., Zhang, W., Zhang, Y., Li, W., Wan, Y., Li, Y., Danjiu, L., Guo, H., & Lin, E. (2016). Differential response of alpine steppe and alpine meadow to climate warming in the central Qinghai–Tibetan Plateau. *Agricultural and Forest Meteorology*, *223*, 233–240.

    https://doi.org/10.1016/j.agrformet.2016.03.017

29. Ganjurjav, H., Gornish, E., Hu, G., Wu, J., Wan, Y., Li, Y., & Gao, Q. (2020). Phenological changes offset the warming effects on biomass production in an alpine meadow on the Qinghai–Tibetan Plateau. *Journal of Ecology, 109*(2), 1014–1025.

    https://doi.org/10.1111/1365-2745.13531

30. Geng, Y., Baumann, F., Song, C., Zhang, M., Shi, Y., Kühn, P., Scholten, T., & He, J.-S. (2017). Increasing temperature reduces the coupling between available nitrogen and phosphorus in soils of Chinese grasslands. *Scientific Reports*, *7*. https://doi.org/10.1038/srep43524

31. Gong, S., Zhang, T., Guo, R., Cao, H., Shi, L., Guo, J., & Sun, W. (2015). Response of soil enzyme activity to warming and nitrogen addition in a meadow steppe. *Soil Research*, *53*(3), 242.

    https://doi.org/10.1071/sr14140

32. Gregory, P. J. (2005). Organic Phosphorus in the Environment. In B. L. Turner, E. Frossard, & D. S. Baldwin (Eds.), *Experimental Agriculture* (Issue 1, p. 399). Cambridge University Press.

    https://doi.org/10.1017/s0014479705313330

33. Grman, E. (2012). Plant species differ in their ability to reduce allocation to non-beneficial arbuscular mycorrhizal fungi. *Ecology*, *93*(4), 711–718. https://doi.org/10.1890/11-1358.1

34. Gruselle, M.-C., & Bauhus, J. (2010). Assessment of the species composition of forest floor horizons in mixed spruce-beech stands by Near Infrared Reflectance Spectroscopy (NIRS). *Soil Biology and Biochemistry*, *42*(8), 1347–1354. https://doi.org/10.1016/j.soilbio.2010.03.011

35. Guan, S., An, N., Zong, N., He, Y., Shi, P., Zhang, J., & He, N. (2018). Climate warming impacts on soil organic carbon fractions and aggregate stability in a Tibetan alpine meadow. *Soil Biology and Biochemistry*, *116*, 224–236. https://doi.org/10.1016/j.soilbio.2017.10.011

36. Han, D., Huang, J., Ding, L., Zhang, G., Liu, X., Li, C., & Yang, F. (2022). Breaking the ecosystem balance over the Tibetan Plateau. *Earth's Future*, *10*(10). https://doi.org/10.1029/2022ef002890

37. Hao, L., Pan, C., Fang, D., Zhang, X., Zhou, D., Liu, P., Liu, Y., & Sun, G. (2018). Quantifying the effects of overgrazing on mountainous watershed vegetation dynamics under a changing climate. Science of the Total Environment, 639, 1408–1420. https://doi.org/10.1016/j.scitotenv.2018.05.224

38. He, H., Wu, M., Guo, L., Fan, C., Zhang, Z., Su, R., Peng, Q., Pang, J., & Lambers, H. (2020). Release of tartrate as a major carboxylate by alfalfa (*Medicago sativa L.*) under phosphorus deficiency and the effect of soil nitrogen supply. *Plant and Soil*, *449*(1-2), 169–178. https://doi.org/10.1007/s11104-020-04481-9

39. He, X., Chu, C., Yang, Y., Shu, Z., Li, B., & Hou, E. (2021). Bedrock and climate jointly control the phosphorus status of subtropical forests along two elevational gradients. *CATENA*, *206*, 105525.

https://doi.org/10.1016/j.catena.2021.105525

40. Hedley, M. J., Stewart, J. W. B., & Chauhan, B. S. (1982). Changes in Inorganic and Organic Soil Phosphorus Fractions Induced by Cultivation Practices and by Laboratory Incubations. *Soil Science Society of America Journal*, *46*(5), 970–976. https://doi.org/10.2136/sssaj1982.03615995004600050017x
41. Hidaka, A., & Kitayama, K. (2011). Allocation of foliar phosphorus fractions and leaf traits of tropical tree species in response to decreased soil phosphorus availability on Mount Kinabalu, Borneo. *Journal of Ecology*, *99*(3), 849–857. https://doi.org/10.1111/j.1365-2745.2011.01805.x
42. Hou, E., Chen, C., Luo, Y., Zhou, G., Kuang, Y., Zhang, Y., Heenan, M., Lu, X., & Wen, D. (2018). Effects of climate on soil phosphorus cycle and availability in natural terrestrial ecosystems. *Global Change Biology*, *24*(8), 3344–3356. https://doi.org/10.1111/gcb.14093
43. Hou, E., Chen, C., Wen, D., & Liu, X. (2015). Phosphatase activity in relation to key litter and soil properties in mature subtropical forests in China. *Science of the Total Environment*, *515-516*, 83–91. https://doi.org/10.1016/j.scitotenv.2015.02.044
44. Hou, E., Tan, X., Heenan, M., & Wen, D. (2018). A global dataset of plant available and unavailable phosphorus in natural soils derived by Hedley method. *Scientific Data*, *5*(1). https://doi.org/10.1038/sdata.2018.166
45. Hou, F., Jia, Q., Lou, S., Yang, C., Ning, J., Li, L., & Fan, Q. (2021). Grassland agriculture in China—a review. *Frontiers of Agricultural Science and Engineering*, *8*(1), 35. https://doi.org/10.15302/j-fase-2020378

46. Huang, L., Jia, X., Zhang, G., & Shao, M. (2017). Soil organic phosphorus transformation during ecosystem development: A review. *Plant and Soil*, *417*(1-2), 17–42. https://doi.org/10.1007/s11104-017-3240-y

47. Jackson, L. E., Burger, M., & Cavagnaro, T. R. (2008). Roots, Nitrogen Transformations, and Ecosystem Services. *Annual Review of Plant Biology*, *59*(1), 341–363. https://doi.org/10.1146/annurev.arplant.59.032607.092932

48. Jia, X., Zhao, Y., Wang, W., & He, Y. (2015). Elevated temperature altered photosynthetic products in wheat seedlings and organic compounds and biological activity in rhizopshere soil under cadmium stress. *Scientific Reports*, *5*(1). https://doi.org/10.1038/srep14426

49. Jiang, M., Caldararu, S., Zaehle, S., Ellsworth, D. S., & Medlyn, B. E. (2019). Towards a more physiological representation of vegetation phosphorus processes in land surface models. *New Phytologist*, *222*(3), 1223–1229. https://doi.org/10.1111/nph.15688

50. Jobbágy, E. G., & Jackson, R. B. (2000). The vertical distribution of soil organic carbon and its relation to climate and vegetation. *Ecological Applications*, *10*(2), 423–436. https://doi.org/10.1890/1051-0761(2000)010[0423:tvdoso]2.0.co;2

51. Kirchgesser, J., Hazarika, M., Bachmann-Pfabe, S., Dehmer, K. J., Kavka, M., & Uptmoor, R. (2023). Phenotypic variation of root-system architecture under high P and low P conditions in potato (Solanum tuberosum L.). *BMC Plant Biology*, *23*(1). https://doi.org/10.1186/s12870-023-04070-9

52. Klein, J. A., Harte, J., & Zhao, X.-Q. (2004). Experimental warming causes large and rapid species loss, dampened by simulated grazing, on the Tibetan Plateau. *Ecology Letters*, *7*(12), 1170–1179.

https://doi.org/10.1111/j.1461-0248.2004.00677.x

53. Klein, J. A., Harte, J., & Zhao, X.-Q. (2007). Experimental warming, not grazing, decreases rangeland quality on the Tibetan Plateau. *Ecological Applications*, *17*(2), 541–557. https://doi.org/10.1890/05-0685

54. Kuang, X., & Jiao, J. J. (2016). Review on climate change on the Tibetan Plateau during the last half century. *Journal of Geophysical Research: Atmospheres*, *121*(8), 3979–4007. https://doi.org/10.1002/2015jd024728

55. Lal, R. (2004). Soil Carbon Sequestration Impacts on Global Climate Change and Food Security. *Science*, 304(5677), 1623–1627. https://doi.org/10.1126/science.1097396

56. Lambers, H. (2022). Phosphorus Acquisition and Utilization in Plants. *Annual Review of Plant Biology*, *73*(1). https://doi.org/10.1146/annurev-arplant-102720-125738

57. Lehmann, J., & Kleber, M. (2015). The contentious nature of soil organic matter. *Nature*, *528*(7580), 60–68. https://doi.org/10.1038/nature16069

58. Li, J., Jian, S., Koff, J. P., Lane, C. S., Wang, G., Mayes, M. A., & Hui, D. (2018). Differential effects of warming and nitrogen fertilization on soil respiration and microbial dynamics in switchgrass croplands. *GCB Bioenergy*, *10*(8), 565–576. https://doi.org/10.1111/gcbb.12515

59. Li, M., Kang, E., Wang, J., Yan, Z., Zhang, K., Hu, Z., & Kang, X. (2021). Phosphorus accumulation poses less influence than soil physicochemical properties on organic phosphorus adsorption on ferrasol. *Geoderma*, *402*, 115324. https://doi.org/10.1016/j.geoderma.2021.115324

60. Li, Q., Wang, Y., Li, Y., Li, L., Tang, M., Hu, W., Chen, L., & Ai, S. (2022). Speciation of heavy metals in soils and their immobilization at micro-scale interfaces among diverse soil components. *Science of the Total Environment*, *825*, 153862.
https://doi.org/10.1016/j.scitotenv.2022.153862

61. Li, Y., Fang, Z., Yang, F., Ji, B., Li, X., & Wang, S. (2022). Elevational changes in the bacterial community composition and potential functions in a Tibetan grassland. *Frontiers in Microbiology*, *13*.
https://doi.org/10.3389/fmicb.2022.1028838

62. Liao, D., Zhang, C., Lambers, H., & Zhang, F. (2021). Changes in soil phosphorus fractions in response to long-term phosphate fertilization under sole cropping and intercropping of maize and faba bean on a calcareous soil. *Plant and Soil*. https://doi.org/10.1007/s11104-021-04915-y

63. Lie, Z., Zhou, G., Huang, W., Kadowaki, K., Tissue, David T., Yan, J., Peñuelas, J., Sardans, J., Li, Y., Liu, S., Chu, G., Meng, Z., He, X., & Liu, J. (2022). Warming drives sustained plant phosphorus demand in a humid tropical forest. *Global Change Biology*, *28*(13), 4085–4096.
https://doi.org/10.1111/gcb.16194

64. Liu, H., Mi, Z., Lin, L., Wang, Y., Zhang, Z., Zhang, F., Wang, H., Liu, L., Zhu, B., Cao, G., Zhao, X., Sanders, N. J., Classen, A. T., Reich, P. B., & He, J.-S. (2018). Shifting plant species composition in response to climate change stabilizes grassland primary production. *Proceedings of the National Academy of Sciences*, *115*(16), 4051–4056.
https://doi.org/10.1073/pnas.1700299114

65. Liu, H., Wang, R., Wang, H., Cao, Y., Dijkstra, F. A., Shi, Z., Cai, J., Wang, Z., Zou, H., & Jiang, Y. (2019). Exogenous phosphorus compounds interact with

nitrogen availability to regulate dynamics of soil inorganic phosphorus fractions in a meadow steppe. *Biogeosciences*, *16*(21), 4293–4306. https://doi.org/10.5194/bg-16-4293-2019

66. Liu, J., Zhang, X., Wang, H., Hui, X., Wang, Z., & Qiu, W. (2017). Long-term nitrogen fertilization impacts soil fungal and bacterial community structures in a dryland soil of Loess Plateau in China. *Journal of Soils and Sediments*, *18*(4), 1632–1640. https://doi.org/10.1007/s11368-017-1862-6
67. Liu, S., Zamanian, K., Schleuss, P.-M., Zarebanadkouki, M., & Kuzyakov, Y. (2018). Degradation of Tibetan grasslands: Consequences for carbon and nutrient cycles. *Agriculture, Ecosystems & Environment*, *252*, 93–104. https://doi.org/10.1016/j.agee.2017.10.011
68. Liu, X., Han, R., Cao, Y., Turner, B. L., & Ma, L. Q. (2022). Enhancing phytate availability in soils and phytate-P acquisition by plants: a review. *Environmental Science & Technology*, *56*(13), 9196–9219. https://doi.org/10.1021/acs.est.2c00099
69. Liu, X., Zhang, Y., Han, W., Tang, A., Shen, J., Cui, Z., Vitousek, P., Erisman, J. W., Goulding, K., Christie, P., Fangmeier, A., & Zhang, F. (2013). Enhanced nitrogen deposition over China. *Nature*, *494*(7438), 459–462. https://doi.org/10.1038/nature11917
70. Liu, Y., Lu, M., Yang, H., Duan, A., He, B., Yang, S., & Wu, G. (2020). Land–atmosphere–ocean coupling associated with the Tibetan Plateau and its climate impacts. *National Science Review*. https://doi.org/10.1093/nsr/nwaa011
71. Liu, Y., Wang, Y., Pan, Y., & Piao, S. (2015). Wet deposition of atmospheric inorganic nitrogen at five remote sites in the Tibetan Plateau. *Atmospheric*

Chemistry and Physics, *15*(20), 11683–11700. https://doi.org/10.5194/acp-15-11683-2015

72. Mamantov, M. A., Gibson-Reinemer, D. K., Linck, E. B., & Sheldon, K. S. (2021). Climate-driven range shifts of montane species vary with elevation. *Global Ecology and Biogeography*, *30*(4), 784–794. https://doi.org/10.1111/geb.13246

73. Margalef, O., Sardans, J., Maspons, J., Molowny-Horas, R., Fernández-Martínez, M., Janssens, I. A., Richter, A., Ciais, P., Obersteiner, M., & Peñuelas, J. (2021). The effect of global change on soil phosphatase activity. *Global Change Biology*, *27*(22), 5989–6003. https://doi.org/10.1111/gcb.15832

74. Mei, L., Yang, X., Zhang, S., Zhang, T., & Guo, J. (2019). Arbuscular mycorrhizal fungi alleviate phosphorus limitation by reducing plant N:P ratios under warming and nitrogen addition in a temperate meadow ecosystem. *Science of the Total Environment*, *686*, 1129–1139. https://doi.org/10.1016/j.scitotenv.2019.06.035

75. Miehe, G., Miehe, S., Kaiser, K., Jianquan, L., & Zhao, X. (2008). Status and Dynamics of the *Kobresia pygmaea* Ecosystem on the Tibetan Plateau. *AMBIO: A Journal of the Human Environment*, *37*(4), 272–279. https://doi.org/10.1579/0044-7447(2008)37[272:sadotk]2.0.co;2

76. Miehe, G., Schleuss, P.-M., Seeber, E., Babel, W., Biermann, T., Braendle, M., Chen, F., Coners, H., Foken, T., Gerken, T., Graf, Hans-F., Guggenberger, G., Hafner, S., Holzapfel, M., Ingrisch, J., Kuzyakov, Y., Lai, Z., Lehnert, L., Leuschner, C., & Li, X. (2019). The Kobresia pygmaea ecosystem of the Tibetan highlands – Origin, functioning and degradation of the world's largest pastoral alpine ecosystem. *Science of the Total Environment*, *648*, 754–771. https://doi.org/10.1016/j.scitotenv.2018.08.164

77. Mou, X. M., Wu, Y., Niu, Z., Jia, B., Guan, Z.-H., Chen, J., Li, H., Cui, H., Kuzyakov, Y., & Li, X. G. (2020). Soil phosphorus accumulation changes with decreasing temperature along a 2300 m altitude gradient. *Agriculture, Ecosystems & Environment*, *301*, 107050. https://doi.org/10.1016/j.agee.2020.107050

78. Müller, M., Oelmann, Y., Schickhoff, U., Böhner, J., & Scholten, T. (2017). Himalayan treeline soil and foliar C:N:P stoichiometry indicate nutrient shortage with elevation. *Geoderma*, *291*, 21–32. https://doi.org/10.1016/j.geoderma.2016.12.015

79. Nannipieri, P., Ascher, J., Ceccherini, M. T., Landi, L., Pietramellara, G., & Renella, G. (2017). Microbial diversity and soil functions. *European Journal of Soil Science*, *68*(1), 12–26. https://doi.org/10.1111/ejss.4_12398

80. Niederberger, J., Kohler, M., & Bauhus, J. (2019). Distribution of phosphorus fractions with different plant availability in German forest soils and their relationship with common soil properties and foliar P contents. *SOIL*, *5*(2), 189–204. https://doi.org/10.5194/soil-5-189-2019

81. Niederberger, J., Todt, B., Boča, A., Nitschke, R., Kohler, M., Kühn, P., & Bauhus, J. (2015). Use of near-infrared spectroscopy to assess phosphorus fractions of different plant availability in forest soils. *Biogeosciences*, *12*(11), 3415–3428. https://doi.org/10.5194/bg-12-3415-2015

82. Niu, Y., Chai, R., Jin, G., Wang, H., Tang, C., & Zhang, Y. (2013). Responses of root architecture development to low phosphorus availability: a review. *Annals of Botany*, *112*(2), 391–408. https://doi.org/10.1093/aob/mcs285

83. Pätzold, S., Hejcman, M., Barej, J., & Schellberg, J. (2013). Soil phosphorus fractions after seven decades of fertilizer application in the Rengen Grassland Experiment. *Journal of Plant Nutrition and Soil Science*, *176*(6), 910–920. https://doi.org/10.1002/jpln.201300152

84. Prescott, C. E., Grayston, S. J., Helmisaari, H.-S., Kaštovská, E., Körner, C., Lambers, H., Meier, I. C., Millard, P., & Ostonen, I. (2020). Surplus Carbon Drives Allocation and Plant–Soil Interactions. *Trends in Ecology & Evolution*, *35*(12), 1110–1118. https://doi.org/10.1016/j.tree.2020.08.007

85. Qiu, J. (2008). China: The third pole. *Nature*, *454*(7203), 393–396. https://doi.org/10.1038/454393a

86. Ren, F., Yang, X., Zhou, H., Zhu, W., Zhang, Z., Chen, L., Cao, G., & He, J.-S. (2016). Contrasting effects of nitrogen and phosphorus addition on soil respiration in an alpine grassland on the Qinghai-Tibetan Plateau. *Scientific Reports*, *6*(1). https://doi.org/10.1038/srep34786

87. Ren, H., Kang, J., Yuan, Z., Xu, Z., & Han, G. (2018). Responses of nutrient resorption to warming and nitrogen fertilization in contrasting wet and dry years in a desert grassland. *Plant and Soil*, *432*(1-2), 65–73. https://doi.org/10.1007/s11104-018-3775-6

88. Richter, D. D., Allen, H. L., Li, J., Markewitz, D., & Raikes, J. (2006). Bioavailability of slowly cycling soil phosphorus: major restructuring of soil P fractions over four decades in an aggrading forest. *Oecologia*, *150*(2), 259–271. https://doi.org/10.1007/s00442-006-0510-4

89. Rui, Y., Wang, Y., Chen, C., Zhou, X., Wang, S., Xu, Z., Duan, J., Kang, X., Lu, S., & Luo, C. (2012). Warming and grazing increase mineralization of organic P in an alpine meadow ecosystem of Qinghai-Tibet Plateau, China. *Plant and Soil*, *357*(1-2), 73–87.

https://doi.org/10.1007/s11104-012-1132-8

90. Sardans, J., Peñuelas, J., & Estiarte, M. (2006). Warming and drought alter soil phosphatase activity and soil P availability in a Mediterranean shrubland. *Plant and Soil*, *289*(1-2), 227–238.

https://doi.org/10.1007/s11104-006-9131-2

91. Schleuss, P. M., Widdig, M., Heintz-Buschart, A., Kirkman, K., & Spohn, M. (2020). Interactions of nitrogen and phosphorus cycling promote P acquisition and explain synergistic plant-growth responses. *Ecology*, *101*(5).

https://doi.org/10.1002/ecy.3003

92. Shen, H., Dong, S., Di Tommaso, A., Xiao, J., Lu, W., & Zhi, Y. (2022). Nitrogen deposition shifts grassland communities through directly increasing dominance of graminoids: a 3-year case study from the Qinghai-Tibetan Plateau. *Frontiers in Plant Science*, *13*.

https://doi.org/10.3389/fpls.2022.811970

93. Shen, H., Wang, S., & Tang, Y. (2013). Grazing alters warming effects on leaf photosynthesis and respiration in Gentiana straminea, an alpine forb species. *Journal of Plant Ecology*, *6*(5), 418–427.

https://doi.org/10.1093/jpe/rtt010

94. Shen, J., Yuan, L., Zhang, J., Li, H., Bai, Z., Chen, X., Zhang, W., & Zhang, F. (2011). Phosphorus dynamics: from soil to plant. *Plant Physiology*, *156*(3), 997–1005.

https://doi.org/10.1104/pp.111.175232

95. Shen, M., Piao, S., Jeong, S.-J., Zhou, L., Zeng, Z., Ciais, P., Chen, D., Huang, M., Jin, C.-S., Li, L. Z. X., Li, Y., Myneni, R. B., Yang, K., Zhang, G., Zhang, Y., & Yao, T. (2015). Evaporative cooling over the Tibetan Plateau induced by vegetation growth. *Proceedings of the National Academy of Sciences*, *112*(30), 9299–9304.

https://doi.org/10.1073/pnas.1504418112

96. Shi, G., Yao, B., Liu, Y., Jiang, S., Wang, W., Pan, J., Zhao, X., Feng, H., & Zhou, H. (2017). The phylogenetic structure of AMF communities shifts in response to gradient warming with and without winter grazing on the Qinghai–Tibet Plateau. *Applied Soil Ecology*, *121*, 31–40.

https://doi.org/10.1016/j.apsoil.2017.09.010

97. Shukla, P. R., Skea, J., Calvo Buendia, E., Masson-Delmotte, V., Pörtner, H.-O., Roberts, D. C., Zhai, P., Slade, R., Connors, S., Van Diemen, R., Ferrat, M., Haughey, E., Luz, S., Neogi, S., Pathak, M., Portugal Pereir, J., Vyas, P., Huntley, E., Kissick, K., & Belkacemi, M. (2019). ***IPCC, 2019****: Climate Change and Land: an IPCC special report on climate change, desertification, land degradation, sustainable land management, food security, and greenhouse gas fluxes in terrestrial ecosystems. In press*.

98. Shulse, C. N., Chovatia, M., Agosto, C., Wang, G., Hamilton, M., Deutsch, S., Yoshikuni, Y., & Blow, M. J. (2019). Engineered root bacteria release plant-available phosphate from phytate. *Applied and Environmental Microbiology*, *85*(18), e01210-19.

https://doi.org/10.1128/AEM.01210-19

99. Spain, A. V., Tibbett, M., Ridd, M., & McLaren, T. I. (2018). Phosphorus dynamics in a tropical forest soil restored after strip mining. *Plant and Soil*, *427*(1-2), 105–123.

https://doi.org/10.1007/s11104-018-3668-8

100. Speißer, B., Wilschut, R. A., & van Kleunen, M. (2022). Number of simultaneously acting global change factors affects composition, diversity and productivity of grassland plant communities. *Nature Communications*, *13*(1).

https://doi.org/10.1038/s41467-022-35473-1

101. Spohn, M. (2020). Increasing the organic carbon stocks in mineral soils sequesters large amounts of phosphorus. *Global Change Biology*, *26*(8), 4169–4177. https://doi.org/10.1111/gcb.15154

102. Stauch, G., IJmker, J., Pötsch, S., Zhao, H., Hilgers, A., Diekmann, B., Dietze, E., Hartmann, K., Opitz, S., Wünnemann, B., & Lehmkuhl, F. (2012). Aeolian sediments on the north-eastern Tibetan Plateau. *Quaternary Science Reviews*, *57*, 71–84.

https://doi.org/10.1016/j.quascirev.2012.10.001

103. Sun, Y., Schleuss, P.-M., Pausch, J., Xu, X., & Kuzyakov, Y. (2018). Nitrogen pools and cycles in Tibetan Kobresia pastures depending on grazing. *Biology and Fertility of Soils*, *54*(5), 569–581.

https://doi.org/10.1007/s00374-018-1280-y

104. Tian, D., & Niu, S. (2015). A global analysis of soil acidification caused by nitrogen addition. *Environmental Research Letters*, *10*(2), 024019. https://doi.org/10.1088/1748-9326/10/2/024019

105. Tian, J., Ge, F., Zhang, D., Deng, S., & Liu, X. (2021). Roles of Phosphate Solubilizing Microorganisms from Managing Soil Phosphorus Deficiency to Mediating Biogeochemical P Cycle. *Biology*, *10*(2), 158. https://doi.org/10.3390/biology10020158

106. Tian, L., Zhao, L., Wu, X., Hu, G., Fang, H., Zhao, Y., Sheng, Y., Chen, J., Wu, J., Li, W., Ping, C.-L., Pang, Q., Liu, Y., Shi, W., Wu, T., & Zhang, X. (2019). Variations in soil nutrient availability across Tibetan grassland from the 1980s to 2010s. *Geoderma*, *338*, 197–205.

https://doi.org/10.1016/j.geoderma.2018.12.009

107. Tian, Y., Shi, C., Malo, C. U., Kwatcho Kengdo, S., Heinzle, J., Inselsbacher, E., Ottner, F., Borken, W., Michel, K., Schindlbacher, A., & Wanek, W. (2023). Long-term soil warming decreases microbial phosphorus utilization by increasing

abiotic phosphorus sorption and phosphorus losses. *Nature Communications*, *14*(1). https://doi.org/10.1038/s41467-023-36527-8

108. Tissen, H., & Moir, J. O. (2007). *Characterization of available P by sequential extraction. In: Carter MR (ed) Soil sampling and methods of analysis.* (pp. 293–306). Lewis publishers.

109. Turner, A. G., & Annamalai, H. (2012). Climate change and the South Asian summer monsoon. *Nature Climate Change*, *2*(8), 587–595. https://doi.org/10.1038/nclimate1495

110. Turner, B., Cade-Menun, B., Condron, L., & Newman, S. (2005). Extraction of soil organic phosphorus. *Talanta*, *66*(2), 294–306. https://doi.org/10.1016/j.talanta.2004.11.012

111. Vance, C. P., Uhde-Stone, C., & Allan, D. L. (2003). Phosphorus acquisition and use: critical adaptations by plants for securing a nonrenewable resource. *New Phytologist*, *157*(3), 423–447. https://doi.org/10.1046/j.1469-8137.2003.00695.x

112. Ven, A., Verlinden, M. S., Verbruggen, E., & Vicca, S. (2019). Experimental evidence that phosphorus fertilization and arbuscular mycorrhizal symbiosis can reduce the carbon cost of phosphorus uptake. *Functional Ecology*, *33*(11), 2215–2225. https://doi.org/10.1111/1365-2435.13452

113. Vitousek, P. M., Menge, D. N. L., Reed, S. C., & Cleveland, C. C. (2013). Biological nitrogen fixation: rates, patterns and ecological controls in terrestrial ecosystems. *Philosophical Transactions of the Royal Society B: Biological Sciences*, *368*(1621), 20130119. https://doi.org/10.1098/rstb.2013.0119

114. Vitousek, P. M., Porder, S., Houlton, B. Z., & Chadwick, O. A. (2010). Terrestrial phosphorus limitation: mechanisms, implications, and nitrogen–phosphorus interactions. *Ecological Applications*, *20*(1), 5–15. https://doi.org/10.1890/08-0127.1

115. Wang, R., Creamer, C. A., Wang, X., He, P., Xu, Z., & Jiang, Y. (2016). The effects of a 9-year nitrogen and water addition on soil aggregate phosphorus and sulfur availability in a semi-arid grassland. *Ecological Indicators*, *61*, 806–814. https://doi.org/10.1016/j.ecolind.2015.10.033

116. Wei, W., Zhang, Y., Tang, Z., An, S., Zhen, Q., Qin, M., He, J., & Oosthuizen, M. K. (2022). Suitable grazing during the regrowth period promotes plant diversity in winter pastures in the Qinghai-Tibetan plateau. *Frontiers in Ecology and Evolution*, *10*. https://doi.org/10.3389/fevo.2022.991967

117. Wen, Z., Li, H., Shen, Q., Tang, X., Xiong, C., Li, H., Pang, J., Ryan, M. H., Lambers, H., & Shen, J. (2019). Tradeoffs among root morphology, exudation and mycorrhizal symbioses for phosphorus-acquisition strategies of 16 crop species. *New Phytologist*, *223*(2), 882–895. https://doi.org/10.1111/nph.15833

118. Wrb, World Reference Base for Soil Resources, 2014 (update 2015). International soil classification system for naming soils and creating legends for soil maps. FAO/ISRIC/ISSS, Rome.

119. Wu, G., Duan, A., Liu, Y., Mao, J., Ren, R., Bao, Q., He, B., Liu, B., & Hu, W. (2014). Tibetan Plateau climate dynamics: recent research progress and outlook. *National Science Review*, *2*(1), 100–116. https://doi.org/10.1093/nsr/nwu045

120. Wu, L., Jiang, Y., Zhao, F., He, X., Liu, H., & Yu, K. (2020). Increased organic fertilizer application and reduced chemical fertilizer application affect the soil

properties and bacterial communities of grape rhizosphere soil. *Scientific Reports*, *10*(1). https://doi.org/10.1038/s41598-020-66648-9

121. Wu, Y., Zhou, J., Yu, D., Sun, S., Luo, J., Bing, H., & Sun, H. (2013). Phosphorus biogeochemical cycle research in mountainous ecosystems. *Journal of Mountain Science*, *10*(1), 43–53. https://doi.org/10.1007/s11629-013-2386-1

122. Yan, Z., Chen, S., Dari, B., Sihi, D., & Chen, Q. (2018). Phosphorus transformation response to soil properties changes induced by manure application in a calcareous soil. *Geoderma*, *322*, 163–171. https://doi.org/10.1016/j.geoderma.2018.02.035

123. Yang, C., Zhang, Y., Hou, F., Millner, J. P., Wang, Z., & Chang, S. (2019). Grazing activity increases decomposition of yak dung and litter in an alpine meadow on the Qinghai-Tibet plateau. *Plant and Soil*, *444*(1-2), 239–250. https://doi.org/10.1007/s11104-019-04272-x

124. Yang, L., Yang, Z., Zhong, X., Xu, C., Lin, Y., Fan, Y., Wang, M., Chen, G., & Yang, Y. (2021). Decreases in soil P availability are associated with soil organic P declines following forest conversion in subtropical China. *CATENA*, *205*, 105459. https://doi.org/10.1016/j.catena.2021.105459

125. Yao, T., Thompson, L., Yang, W., Yu, W., Gao, Y., Guo, X., Yang, X., Duan, K., Zhao, H., Xu, B., Pu, J., Lu, A., Xiang, Y., Kattel, D. B., & Joswiak, D. (2012). Different glacier status with atmospheric circulations in Tibetan Plateau and surroundings. *Nature Climate Change*, *2*(9), 663–667. https://doi.org/10.1038/nclimate1580

126. Yu, L., Caldararu, S., Ahrens, B., Wutzler, T., Schrumpf, M., Helfenstein, J., Pistocchi, C., & Zaehle, S. (2023). Improved representation of phosphorus exchange on soil mineral surfaces reduces estimates of phosphorus limitation in

temperate forest ecosystems. *Biogeosciences*, *20*(1), 57–73. https://doi.org/10.5194/bg-20-57-2023

127. Zhang, G., Chen, Z., Zhang, A., Chen, L., & Wu, Z. (2013). Influence of climate warming and nitrogen deposition on soil phosphorus composition and phosphorus availability in a temperate grassland, China. *Journal of Arid Land*, *6*(2), 156–163. https://doi.org/10.1007/s40333-013-0241-4

128. Zhang, J., Yan, X., Su, F., Li, Z., Wang, Y., Wei, Y., Ji, Y., Yang, Y., Zhou, X., Guo, H., & Hu, S. (2018). Long-term N and P additions alter the scaling of plant nitrogen to phosphorus in a Tibetan alpine meadow. *Science of the Total Environment*, *625*, 440–448. https://doi.org/10.1016/j.scitotenv.2017.12.292

129. Zhang, Y., Li, B., & Zheng, D. (2021). Boundary Data of the Tibetan Plateau. *Journal of Global Change Data & Discovery*, *5*(3), 322–332. https://doi.org/doi.org/10.3974/geodp.2021.03.10.

130. Zhang, Y., Tang, Y., Jiang, J., & Yang, Y. (2007). Characterizing the dynamics of soil organic carbon in grasslands on the Qinghai-Tibetan Plateau. *Science in China Series D: Earth Sciences*, *50*(1), 113–120. https://doi.org/10.1007/s11430-007-2032-2

131. Zhang, Y., Wang, C., & Li, Y. (2019). Contrasting effects of nitrogen and phosphorus additions on soil nitrous oxide fluxes and enzyme activities in an alpine wetland of the Tibetan Plateau. *PLOS ONE*, *14*(5), e0216244. https://doi.org/10.1371/journal.pone.0216244

132. Zhao, Q., & Zeng, D.-H. (2019). Nitrogen addition effects on tree growth and soil properties mediated by soil phosphorus availability and tree species identity. *Forest Ecology and Management*, *449*, 117478. https://doi.org/10.1016/j.foreco.2019.117478

133. Zhou, J., Li, X., Peng, F., Li, C., Lai, C., You, Q., Xue, X., Wu, Y., Sun, H., Chen, Y., Zhong, H., & Lambers, H. (2021). Mobilization of soil phosphate after 8 years of warming is linked to plant phosphorus-acquisition strategies in an alpine meadow on the Qinghai-Tibetan Plateau. *Global Change Biology*, *27*(24), 6578–6591. https://doi.org/10.1111/gcb.15914

134. Zong, N., Shi, P., Jiang, J., Song, M., Xiong, D., Ma, W., Fu, G., Zhang, X., & Shen, Z. (2013). Responses of Ecosystem CO_2 Fluxes to Short-Term Experimental Warming and Nitrogen Enrichment in an Alpine Meadow, Northern Tibet Plateau. *The Scientific World Journal*, *2013*, 1–11. https://doi.org/10.1155/2013/415318

135. Zuccarini, P., Asensio, D., Sardans, J., Ogaya, R., & Peñuelas, J. (2021). Changes in soil enzymatic activity in a P-limited Mediterranean shrubland subject to experimental nitrogen deposition. *Applied Soil Ecology*, *168*, 104159. https://doi.org/10.1016/j.apsoil.2021.104159

Appendix

Manuscript 1

Calibration of Near-Infrared Spectra for Phosphorus Fractions in Grassland Soils on the Tibetan Plateau

Agronomy 2022, 12(4), 783

Zuonan Cao [1], Peter Kühn [1], Jin-Sheng He [2,3], Jürgen Bauhus [4], Zhen-Huan Guan [2] and Thomas Scholten [1,*]

[1] Department of Geosciences, Soil Science and Geomorphology, University of Tübingen,
72070 Tuebingen, Germany

[2] State Key Laboratory of Grassland Agro-ecosystems, College of Pastoral Agriculture Science and Technology, Lanzhou University, 730020 Lanzhou, China

[3] Department of Ecology, College of Urban and Environmental Sciences, Peking University, 100871 Beijing, China

[4] Chair of Silviculture, Faculty of Environment and Natural Resources, University of Freiburg,
79106 Freiburg, Germany

* Correspondence: thomas.scholten@uni-tuebingen.de

Submitted: February 9, 2022; Accepted: March 22, 2022; Published: March 24, 2022

Abstract:

Soil phosphorus (P) is essential for plant growth and influences biological processes. Determining the amounts of available P to plants has been challenging, and many different approaches exist. The traditional Hedley sequential extraction method and its subsequent modification are applied to determine different soil P forms, which is critical for understanding its dynamics and availability. However, quantifying organic and inorganic P (Po & Pi) in different extracts is labor-intensive and rarely used with large sample numbers. As an alternative, near-infrared spectroscopy (NIRS) has been employed to determine different P fractions at reasonable costs in a short time. This study aimed to test whether the analysis of P fractions with NIRS is an appropriate method to disentangle the effects of P limitation on high-altitude grassland ecosystems, particularly with fertilizer amendments. We explored NIRS in soils from the grassland soil samples on the northern Tibetan Plateau. First, we extracted the P fractions of 191 samples from the Haibei Alpine Meadow Ecosystem Research Station at four depth increments (0–10 cm, 10–20 cm, 20–40 cm, and 40–70 cm), including nutrient additions of nitrogen (N) and P. We compared the results of the Hedley extraction with the laboratory-based NIRS model. The fractionation data were correlated with the corresponding NIRS soil spectra; the coefficient of determination (R^2) of the NIRS calibrations to predict P in P fractions ranged between 0.12 and 0.90; the ratio of (standard error of) prediction to the standard deviation (RPD) ranged between 1.07 and 3.21; the ratio of performance to inter-quartile distance (RPIQ) ranged from 0.3 to 4.3; and the model prediction quality was higher for Po than Pi fractions, and decreased with fertilizer amendment. However, the external-validation results were not precise enough for the labile P fractions (RPD < 1.4) due to the limited number of samples. The results indicate that using NIRS to predict the more stable P pools, combined with Hedley fractionation focusing on the labile P pool, can be a promising approach for soils in alpine grasslands on the Tibetan Plateau.

Keywords: phosphorus; P fractions; grassland soil; Hedley sequential extraction; NIRS; Tibetan Plateau

1. Introduction

Phosphorus (P) is essential for all life forms, especially plant growth [1–3]. It is one of the plant's essential nutrients that influences biological processes, and a deficiency of P, when combined with nitrogen (N), can impede plant growth in terrestrial environments around the world [4,5]. P in soil occurs in two distinct pools: inorganic P (Pi, minerals, and mineral-bound P) and organic P (Po, organic matter, and organic-bound P) [6]. Forms of soil P range from ions in solution to very stable inorganic and organic compounds, which typically include: primary P minerals (apatite, strengite, variscite); secondary P minerals (Ca−, Mg−, Fe−, or Al-phosphates); P adsorbed on the edges of clay minerals; mineral- and organic-associated P; and dissolved P in the form of $H_2PO_4^-$, HPO_4^{2-}, and PO_4^{3-} [2]. The last two parts are the primary forms that can be assimilated by plants and microbes [6]. Soil P plays a vital role in determining ecosystems' structures, functions, and processes [5,7,8]. It is essential to distinguish between Pi and Po, since Po, although not directly available for plant uptake, plays a vital role in plant nutrition in forest ecosystems [9,10]. In alpine environments, soil P and its bioavailability also influence the establishment of timber lines [11]. In addition, there is increasing interest in the role of soil P and other nutrients, such as soil N and carbon (C), in alpine grassland ecosystems that are vulnerable to climate warming and nutrient enrichment [12–15].

In cold and high-altitude regions such as the Tibetan Plateau—which covers an area of more than 2.4 million km^2 and has an average altitude exceeding 4000 m above sea level [16], with young soils that are at the beginning of their formation [17,18]—weathering coincides with the onset of primary succession; Pi is slowly released from parent material as the primary source [19]. Concerns have been expressed that the ecosystems and plant productivity on the Tibetan Plateau may suffer from P and N

limitations [20,21]. Related research shows that nutrient application in the meadow could increase primary plant productivity. It suppresses topsoil microbial activity [22], especially for P enrichment with N; meanwhile, P addition more efficiently increases the N uptake capacity of grasses, since N is an essential limiting nutrient for plant productivity [23]. On the other hand, P is essential for the organization of alpine meadow soil fungal communities; however, the addition of P may reduce soil fungal diversity and long-term ecosystem stability in fragile alpine environments [13]. Furthermore, factors such as overgrazing and fertilization of grassland; the foundation of settlement; and road and railway construction interfere with the fragile ecosystem of the Tibetan Plateau [24–27]. When the temperature increases in the Tibetan grassland, total N, total P, and available P in the soil decrease, and the coupling between available N and P is lost [28]. This effect has also been shown in high-altitude tree-line systems south of the Tibetan Plateau in the Himalayas [11]. In contrast, Huang et al. [29] reported that the distribution of alpine grasslands on the north Tibetan Plateau did not show an upward shift despite rapid climate warming having occurred from 2000 to 2014. In summary, it would be valuable to explore the role of P in the response of the meadow ecosystem on the Tibetan Plateau to climate change and nutrient enrichment; moreover, the determination of soil P fractions that reflect its bioavailability is also an essential basis for evaluating the influence of soil P on the alpine grassland ecosystem.

Kruse et al. [30] reviewed advanced methods currently used in soil P research. Nevertheless, for a long time, extraction methods such as the Olsen bicarbonate method have been developed to analyze the different P fractions [31]. These methods focus only on the soil labile-P but do not quantify Pi and Po into fractions of different plant availability. The sequential extraction of P after Hedley et al. [32], which was further modified by Tiessen and Moir [33], has become standard in ecosystem research. This method provides seven Pi and four Po fractions. These P fractions are usually grouped into pools of distinct plant availability as follows [9,34]:

(a) Labile P, which is considered to supply the short-term P demand of plants, including Resin-P, $NaHCO_3$-Pi and Po;

(b) Moderately labile P, which can be transformed into labile P forms, including NaOH-Pi and Po;

(c) Stable P, including HCl-P and residual-P, which hardly contributes to bioavailable P.

However, compared to other methods, Hedley fractionation has a high workload that requires technical expertise, and high costs in the laboratory, making it time-consuming, error-prone, and unsuitable for routine soil analysis [35,36]. Therefore, it would be helpful to determine Hedley P extraction by utilizing a less expensive and time-saving technique. A promising approach is the measurement of near-infrared spectra (NIRS) as proxies for P fractions in the soil fractions with reasonable accuracy [9,37–40]. In contrast to traditional soil chemical, biological and physical methods, NIRS allows the measurement of large sample numbers in a relatively short time and does not require complicated sample pretreatment [41]. However, there have been no studies focusing on the use of NIRS to predict organic and inorganic Hedley P fractions in meadow soils on the Tibetan Plateau.

The specific objectives of this study are (i) to adapt the Hedley method modified by Tiessen and Moir [33] to the specifics of the grassland soils of the Tibetan Plateau, and (ii) to examine whether P fractions determined by the Hedley method can be predicted from the spectral properties of soils determined by NIRS as applied by Niederberger et al. [9], which serves as a reference method.

2. Materials and Methods

2.1. Soil Samples

Soil samples were provided by the Northwest Institute of Plateau Biology, Chinese Academy of Sciences, and were taken from the long-term field experiment at the Haibei Alpine Meadow Ecosystem Research Station in the northeastern part of the Tibetan Plateau (37° 37′ N, 101° 12′ E). The mean annual temperature is 1.1 °C, and the mean annual precipitation is 485 mm at 3.200 m a.s.l [42]. Thirty-six plots (6 m × 6 m) using the randomized block design were set up with 6 repeats and 6 treatments. Fertilizers (urea and triple superphosphate, Table 1) were evenly distributed by hand on the soil surface in the plots, after sunset (for higher moisture), during the growing season in early June, July, and August, each year since 2011 [43]. The buffer strip between each block was 2 m wide, and that between each plot was 1 m wide. Each fertilization treatment was divided into two parts: with and without grazing by yak. The soil samples were taken from four depth increments (0–10, 10–20, 20–40, and 40–70 cm) in 2016 from 4 repeats. All samples were air-dried and sieved (<2 mm), and 191 samples (one N25 treatment sample was missing) in total were analyzed.

Table 1. Design of the nutrient addition experiment on the alpine grassland since 2012 (N: nitrogen, P: phosphorous).

Treatments	**Fertilizer**	**Amount (ha^{-1} $year^{-1}$)**
Control	No	0
P	Triple Superphosphate (TSP)	50 kg
NP	Carbamide $CO(NH_2)^2$ + TSP	50 kg P + 100 kg N
N25	Carbamide $CO(NH_2)^2$	25 kg
N50	Carbamide $CO(NH_2)^2$	50 kg
N100	Carbamide $CO(NH_2)^2$	100 kg

2.2. Hedley Fractionation

Soil samples were air-dried, sieved to a fine fraction (<2 mm), and extracted in different fractions, according to Hedley et al. [32], Alt et al. [44], and Niederberger et al. [9]. An amount of 0.5 g from each sample was weighed into a 50 mL centrifuge tube for extraction. The fractionation steps are given in Table 2. For the regular Hedley fractions, the amount of organically bound P in the 1 M HCl extracts was considered negligible [33] and, therefore, not analyzed. The concentrated HCl ($HCl_{conc.}$) fraction was applied.

All Pi fractions were determined by continuous flow analysis (CFA, SEAL Auto Analyzer AA3, SEAL Analytical GmbH, Norderstedt, Germany). Total $NaHCO_3$-P and NaOH-P were determined by inductively coupled plasma–optical emission spectrometry (ICP–OES, Optima 5300 DV, PerkinElmer, Waltham, MA, USA). To evaluate differences in P fractions between the treatments and soil depth increments, one-way ANOVA and independent-sample *t*-tests were used.

Table 2. Experimental procedure for the Hedley fractionation steps and assignment of Hedley P fractions to soil P pools.

P Pools and Fractions		**Extraction Procedure [9,43]**	**Properties and Bonding Forms of Pi and Po in the Fractions [45]**
Labile P	Resin-P	Anion-exchange resin in resin bag, 0.5 M HCl	Mainly Pi, marginal Po; biologically most available P form; adsorbed on the surface of crystalline compounds.
	$NaHCO_3$-P	0.5 M $NaHCO_3$, pH 8.5	Highly labile P; Pi likely to be plant-available, associated with Fe and Al oxides; Po easily mineralized.
Moderate P	NaOH-P	0.1 M NaOH	Moderately labile P; Pi associated with Fe and Al oxides; Po involved in slow transformation processes.

Stable P	HCl_{conc}.-P	HCl_{conc}. 85 °C	Very stable Pi; covers P in primary minerals; Po in very stable pools, eventually also derived from particulate organic matter.
	Residual-P	0.5 M H_2SO_4	Highly resistant and occluded P forms.

2.3. Near-Infrared Spectroscopy

All soil samples were scanned with an integrating sphere measured by diffuse reflectance using a Fourier transform near-infrared reflectance spectrometer (Tensor 37, with a resolution better than 0.6 cm^{-1}, a wavenumber accuracy better than 0.01 cm^{-1} at 2000 cm^{-1} and a photometric accuracy better than 0.1%; Bruker Optik GmbH, Ettlingen, Germany). The sample was inserted into a glass sample cup with a flat bottom, placed on the scanner, and measured as it rotated. Each spectrum consisted of 64 independent scans. Five replicate measurements were made for each sample, and a mean spectrum was created over the entire spectrum from 12,000 to 3800 cm^{-1} wavenumbers, i.e., 800–2500 nm wavelength with a resolution of 16 cm^{-1}. The spectral data and model development were processed with the spectroscopic software OPUS/QUANT (Version 7.5, Bruker Optik GmbH, Ettlingen, Germany, 2014). The data pre-processing of a combination of the first derivative and vector normalization (SNV) in the software was used to find the best fit with the value of the respective component (Bruker Optik User Manual version 6, 2006). Corrected partial least square (PLS) regressions then proceeded to regress the information contained in the spectrum of the calibration sample with the P fraction values, which is a popular chemometrics method in NIR analysis [9].

Calibration was performed with leave-one-out cross-validation for the small data sets to determine the accuracy of the NIRS models [46]: one sample was removed from the data set and validated against the remaining subset. This process was repeated until every sample was used once for validation. For each data set, 80% of the samples were

used to build the models with cross-validation, and 20% were set aside for external validation to test the prediction [9]; these were chosen by an automatic function in the software (Bruker Optik User Manual, version 6, 2006). Different treatments of N and P were considered in the calibration, but not in the external-validation due to the limit of the samples. No outliers were removed in the model development process, since new outliers were detected after removing the old ones. The differences in performance of the model were compared using the following parameters: coefficient of determination (R^2) (Equation (1)); root mean standard error (RMSE) (Equation (2)); the ratio of (standard error of) prediction to the standard deviation (RPD) (Equation (3)); and the ratio of performance to inter-quartile distance (RPIQ) (Equation (4)):

$$R^2 = \frac{\sum_{i=1}^{n}(\hat{y}_i - \bar{y}_i)^2}{\sum_{i=1}^{n}(y_i - \bar{y}_i)^2} \quad (1)$$

$$RMSE = \sqrt{\frac{1}{n}\sum_{i=1}^{n}(\hat{y}_i - y_i)^2} \quad (2)$$

$$RPD = \frac{\text{standard deviation of analyzed data}}{RMSE} \quad (3)$$

$$RPIQ = \frac{(Q3 - Q1)}{RMSE} \quad (4)$$

in which $\hat{y}$ = predicted value; $\bar{y}$ = mean measured values; y = measured values; n = number of samples with i = 1, 2, …, n; Q1, Q3 are the upper bounds of the first and third quartiles of the measurements, respectively; and $Q3 - Q1$ represents the interval responsible for 50% of the population around the median [47]. The range of RPIQ might represent the soil attributes' values better than the standard deviation, since the distribution of soil attributes is usually skewed [47,48]. However, the RPD value has been adopted extensively when using NIRS, and several limits have been suggested and applied [9,40,49]. Hence, we included RPD as one of the evaluation criteria, and bias—the mean of residuals—did not occur very often [47]. Generally, a robust model achieves high R^2, RPD and RPIQ values and a low RMSE [9,48–51]. The performance of the models can be judged as follows:

RPD: (i) ≥2.0, suitable for predicting P in soils; (ii) 1.4–2.0, limited; and (iii) ≤1.4, not reliable [40];

RPIQ: (i) >2.5, excellent; (ii) 2.0–2.5, good model with predictive ability; (iii) 1.7–2.0, good model; (iv) 1.4–1.7, fair model that needs improvement; and (v) <1.4, very poor predictive ability [51].

All other statistical analyses were conducted using Origin v.2021 and Excel 2019.

3. Results

3.1. Hedley P Fractions

No significant differences in grazing treatment were found in Hedley fractionation, so we kept the data volume support for modeling, and the final data of P fractions were averaged. The average total P concentration by Hedley fractionation of all the samples covered a wide range from 381 to 950 μg g^{-1}, and significant differences in total P between treatments were found after N and P amendment. In comparison, each P fraction ranged from 0 to 460.5 μg g^{-1} (Table S1). The complete P fractionation results at different soil depths are displayed in Table 3, separately summarized for P pools (labile P, moderate P, and stable P). The highest P concentrations were found in the stable P pool for each depth increment (Table 3). Different reactions of P fractions between treatments and soil depths were detected. In the treatments with P application (P and NP additions), Pi contents (Resin-P, $NaHCO_3$-P, NaOH-P, and $HCl_{conc.}$-P) at 0–10 cm and 10–20 cm exceeded those without P input (Table 3). However, the difference

between means was more distinct in those fractions in which the 0 to 10 cm depth had higher *p* values than the other layers. Notably, the contents of Po fractions ($NaHCO_3$-Po and NaOH-Po) only increased significantly with the addition of the NP combination. The residual fraction was the only part in which no highly significant differences ($p < 0.1$) between treatments were found.

Table 3. Soil P contents (µg g^{-1}) from each soil depth for seven Hedley fractionations in different treatments with N (N25: 25 kg nitrogen, N50: 50 kg nitrogen, N100: 100 kg nitrogen ha^{-1} $year^{-1}$), P (50 kg phosphorous), and their combination NP (100 kg nitrogen + 50 kg phosphorous).

Fractions	**Labile P (µg g^{-1})**			**Moderate P (µg g^{-1})**		**Stable P (µg g^{-1})**	
Treatments	Resin-P	$NaHCO_3$-Pi	$NaHCO_3$-Po	NaOH-Pi	NaOH-Po	$HCl_{conc.}$-P	Residual-P
0–10 cm							
Control	20.9 (1.1)	19.0 (1.9)	21.4 (2.1)	28.1 (2.4)	177.5 (2.5)	219.0 (6.8)	86.8 (3.6)
P	183.8 (22.3) ***	112.4 (8.5) ***	68.5 (6.7) ***	82.1 (7.5) ***	181.2 (4.4)	332.3 (14.7) ***	80.5 (1.9) *
NP	139.5 (12.7) ***	96.4 (5.4) ***	49.4 (7.7) **	84.0 (3.6) ***	196.2 (5.0) **	326.1 (19.3) ***	83.5 (3.8)
N25	19.1 (1.7)	23.4 (2.4)	24.0 (3.4)	28.1 (2.0)	178.6 (3.7)	252.9 (18.9)	85.0 (2.9)
N50	14.8 (3.0)	23.2 (1.8)	25.5 (3.0)	27.1 (2.3)	172.8 (4.5)	230.2 (7.4)	79.3 (3.3)
N100	13.6 (1.9)**	20.5 (2.3)	21.4 (2.6)	27.6 (2.3)	179.4 (8.4)	230.8 (8.0)	83.6 (3.0)
10–20 cm							
Control	11.1 (1.1)	6.6 (0.7)	14.4 (1.2)	11.5 (0.5)	142.8 (4.1)	203.2 (5.7)	81.0 (3.9)
P	31.2 (5.7) **	24.0 (5.3) *	24.2 (4.3)	20.9 (3.2) *	150.0 (7.7)	257.3 (16.2) *	75.8 (2.5)
NP	29.3 (2.6) ***	21.4 (2.1) ***	20.0 (2.3) *	24.8 (1.9) ***	166.3 (5.8) **	222.8 (7.1) *	72.8 (6.8)
N25	12.0 (1.4)	9.0 (1.0)	16.5 (1.5)	12.4 (1.6)	158.7 (5.7) *	232.7 (14.9)	74.7 (1.7) *
N50	10.8 (1.2)	9.3 (0.7) **	15.0 (1.4)	12.1 (0.8)	143.2 (4.8)	227.5 (8.3) *	75.5 (1.8) *
N100	10.5 (0.8)	8.3 (0.8)	14.0 (0.9)	12.7 (1.1)	153.4 (6.0)	215.6 (7.8)	74.7 (2.1)
20–40 cm							
Control	8.6 (1.1)	2.7 (0.4)	8.8 (0.9)	4.6 (0.3)	96.2 (4.2)	273.8 (10.2)	67.1 (2.3)
P	15.5 (2.3) *	10.0 (2.0) **	14.1 (1.6) *	7.2 (1.2)	102.2 (8.1)	298.5 (23.1)	68.6 (3.5)
NP	13.7 (0.9) ***	8.4 (0.7) ***	12.9 (1.4) *	7.0 (0.6) **	106.3 (7.4)	269.4 (12.6)	68.0 (1.8)
N25	7.6 (1.0)	4.2 (0.5) *	10.0 (1.4)	4.7 (0.7)	92.7 (9.4)	288.6 (20.4)	68.3 (2.4)

N50	9.0 (1.1)	4.7 (0.9)	10.9 (1.4)	5.1 (0.5)	93.9 (7.4)	274.9 (16.4)	69.9 (3.4)
N100	8.2 (1.4)	3.7 (0.3) *	9.2 (0.9)	5.5 (0.9)	93.3 (7.2)	283.5 (12.0)	65.3 (2.6)
40–70 cm							
Control	7.9 (0.9)	1.4 (0.3)	3.0 (1.1)	3.1 (0.3)	28.9 (8.1)	408.8 (20.3)	43.7 (3.5)
P	9.7 (0.8)	5.3 (0.7) ***	4.8 (0.8)	3.9 (0.4)	34.4 (5.2)	403.8 (11.0)	48.2 (2.7)
NP	9.4 (0.6)	3.7 (0.7) *	4.7 (1.3)	3.5 (0.6)	57.0 (20.6)	395.4 (15.1)	51.4 (1.9) **
N25	6.0 (0.9)	2.6 (0.5)	3.7 (0.7)	2.7 (0.3)	36.8 (14.0)	398.3 (19.6)	48.4 (3.0)
N50	6.4 (1.0)	1.6 (0.4)	2.0 (0.8)	2.9 (0.3)	19.6 (3.7)	437.7 (6.6) **	39.5 (1.7) *
N100	6.5 (1.1)	1.6 (0.3)	3.4 (0.8)	3.0 (0.3)	28.6 (3.7)	420.0 (11.6)	45.3 (2.6)

Asterisks denote significant differences among the treatments at $p = 0.05$; * <0.1; ** <0.01; or *** <0.001. Values are the mean ± SE, df = 7; treatment with N25 at 10–20 cm, df = 6.

The proportion of P in each fraction varied distinctly from different soil depth increments, highlighting some effects more clearly (Figure 1 and Table S1). Similarly, changes occurred mainly in the topsoil (Figure 1a,b). P addition, after several years, increased the proportion of Pi at 0–20 cm. The proportion of moderate and stable P pools also increased with increasing depth. For the labile P pool, the contribution of Resin-P and $NaHCO_3$-Pi was significantly increased by P addition (6.3% to 10.2% compared with 1.9% to 2.7%), which led to no change in $NaHCO_3$-Po. NaOH-Pi in the moderate P pool also increased with P addition (4.8–4.9% to 2.6%), but the contents of NaOH-Po were stable (Figure 1 and Table S1). Intriguingly, the contribution of Po to total Hedley-P was higher in the treatments without P addition. Overall, stable P formed the central part of the total P concentration for all nutrient amendments and soil depth increments; meanwhile, phosphate addition significantly changed labile and moderate Pi's contributions.

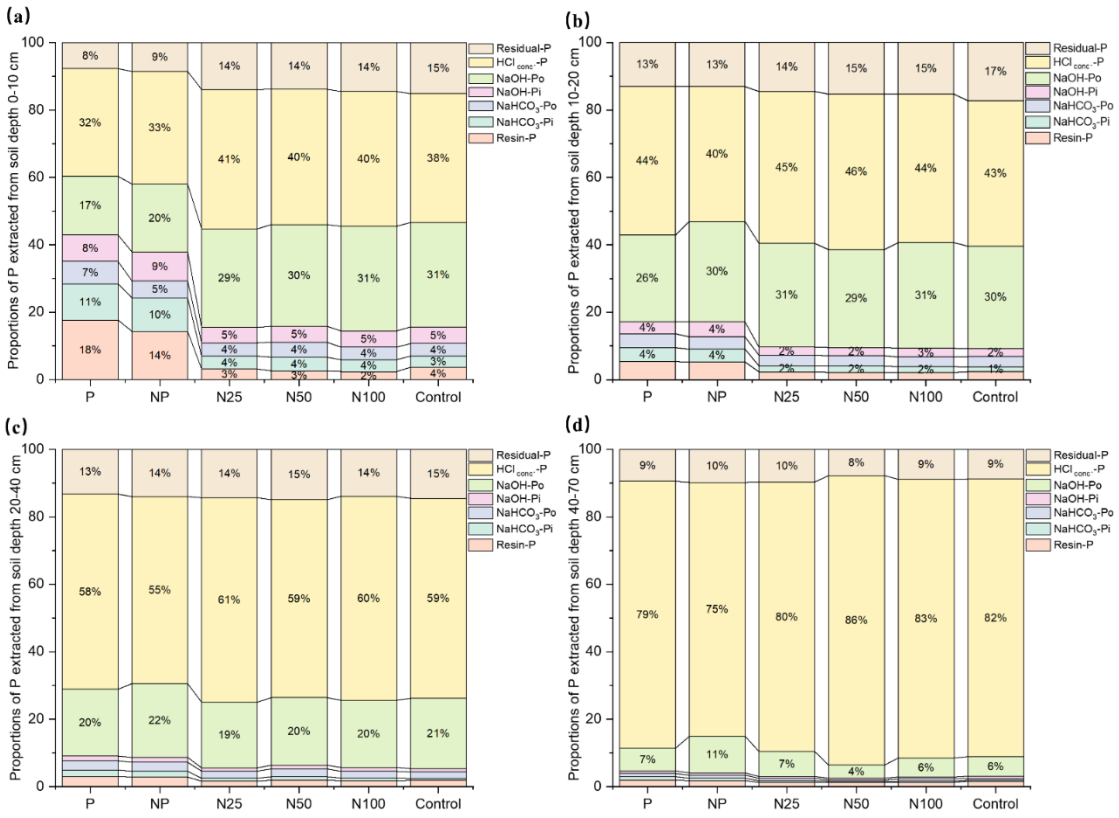

Figure 1. Proportions of P-extracted Hedley fractions from soil depth increments: (**a**) 0–10 cm; (**b**) 10–20 cm; (**c**) 20–40 cm; and (**d**) 40–70 cm.

3.2. NIRS Models

The quality measures of the NIRS models varied to a great extent over the cross-validation (calibration) data set with different treatments (Table 4). N and P amendments significantly reduced the performance of the models, especially the addition of P, which had higher RMSECV (RMSE of cross-validation) but lower RPD and RPIQ compared with the control. Among all the treatments with N and P, better calibration models achieved for NaOH-Po than others such as Resin-P (R^2 = 0.02–0.59; RPD = 0.92–1.57; RPIQ = 0.6–2.1; RMSECV = 4.21–74.9), $NaHCO_3$-Pi (R^2 = 0.42–0.81; RPD = 1.32–2.28; RPIQ = 1.3–2.8; RMSECV = 3.93–34.6) and $NaHCO_3$-Po (R^2 = 0.37–0.70; RPD = 1.26–1.82; RPIQ = 1.1–2.3; RMSECV = 4.26–20.2). In particular, when nutrient amendments were not considered, the fraction of NaOH-Po (R^2 = 0.90, RPD = 3.21, RPIQ = 4.3), HCl_{conc}.-P (R^2 = 0.79; RPD = 2.19; RPIQ = 2.4), and Residual-P (R^2 = 0.78; RPD = 2.16; RPIQ = 2.6) in the regression model performed better in calibriation compared with other fractions (Table 5). Overall, the best

calibration models were achieved for the control data without nutrient amendments (Table 4), and especially for the NaOH-Po, HCl_{conc}.-P and Residual-P fractions. In addition, the RPD values were higher for cross-validation than for external validation for all seven Hedley fractions—confirming that external validation requires a larger dataset (Table S2)—which ranged from 1.16–2.29, and RMSEP (RMSE of prediction) ranged from 9.97–59.8. According to the judgment of performance [40,51], all the P fractions, except Resin-P from the non-NP addition samples (control), showed better predictive ability in cross-validation, as well as NaOH-Po in all treatments (Table 4) and in external-validation (Table S2). Notably, the RMSECV of stable P fractions was generally higher than others.

Table 4. Quality parameters for NIRS model calibration in the cross-validation process for all Hedley fractions with different treatments.

P Pools		**Labile P**			**Moderate P**		**Stable P**	
P fractions and treatments		Resin-P	$NaHCO_3$-Pi	$NaHCO_3$-Po	NaOH-Pi	NaOH-Po	HCl_{conc}.-P	Residual-P
Control	R^2	0.52	0.82	0.67	0.86	0.95	0.79	0.67
	RPD	1.44	2.33	1.73	1.99	4.43	2.24	1.74
	Bias	0.137	0.023	0.344	0.605	0.517	8.15	−0.417
	RMSECV	4.09	3.21	4.47	3.97	12.9	39.7	10.9
	RPIQ	1.5	3.1	2.1	3.4	5.9	2.7	1.9
P	R^2	0.08	0.42	0.43	0.53	0.86	0.06	0.66
	RPD	1.04	1.32	1.33	1.46	2.74	0.99	1.71
	Bias	−2.3	−0.164	0.096	0.0252	−3.94	8.15	−0.268
	RMSECV	74.9	34.6	20.2	23	21.5	70.5	8.36
	RPIQ	0.9	1.3	1.1	1.5	3.5	0.7	2.0
NP	R^2	0.59	0.62	0.37	0.74	0.75	0.40	0.26
	RPD	1.57	1.63	1.26	1.97	2.04	1.29	1.17
	Bias	0.33	0.397	0.528	0.414	0.865	−0.989	−0.668
	RMSECV	35.7	23.5	16	16.6	30.4	57.8	13.7
	RPIQ	2.1	2.5	1.6	2.9	3.0	1.0	1.4
N25	R^2	0.48	0.81	0.54	0.87	0.91	0.70	0.80

	RPD	1.39	2.28	1.48	2.75	3.35	1.83	2.22
	Bias	−0.045	−0.15	0.3	−0.347	−4.45	1.49	−0.179
	RMSECV	4.43	4	6.3	3.9	18.8	43.9	6.83
	RPIQ	1.2	2.1	1.9	3.3	3.8	1.5	2.4
	R^2	0.02	0.65	0.57	0.77	0.91	0.82	0.69
	RPD	0.92	1.69	1.53	2.1	3.35	2.36	1.8
N50	Bias	0.422	0.209	0.294	0.893	2.02	5.24	0.241
	RMSECV	6.1	5.2	6.35	4.87	17.9	38.7	9.58
	RPIQ	0.6	1.7	1.4	2.1	3.7	2.6	2.2
	R^2	0.10	0.76	0.70	0.80	0.90	0.71	0.72
	RPD	1.06	2.03	1.82	2.26	3.25	1.85	1.88
N100	Bias	0.424	0.0426	0.15	0.203	−1.23	−0.862	0.723
	RMSECV	4.21	3.93	4.26	4.54	18.7	45.9	8.44
	RPIQ	1.3	2.8	2.3	3.0	4.0	2.1	2.3

R^2: coefficient of determination; RPD: ratio of (standard error of) prediction to the standard deviation; RMSECV: root mean squared error of cross-validation; RPIQ: ratio of performance to inter-quartile range.

Table 5. Quality parameters for NIRS model calibration in the cross-validation process for all Hedley fractions.

P Pools		**Labile P**			**Moderate P**		**Stable P**	
P fractions		Resin-P	$NaHCO_3$-Pi	$NaHCO_3$-Po	NaOH-Pi	NaOH-Po	$HCl_{conc.}$-P	Residual-P
	R^2	0.12	0.31	0.44	0.48	0.90	0.79	0.78
	RPD	1.07	1.2	1.34	1.39	3.21	2.19	2.16
Cross-validation	Bias	0.0314	−0.00023	0.0233	0.0975	0.0348	−0.611	0.0418
	RMSECV	42.1	22.1	11.3	15.2	18.8	38	7.51
	RPIQ	0.3	0.8	1.2	2.3	4.3	2.4	2.6

R^2: coefficient of determination; RPD: ratio of (standard error of) prediction to the standard deviation; RMSECV: root mean squared error of cross-validation; RPIQ: ratio of performance to inter-quartile range.

We compared the results of the treatments of P addition, NP addition and the Control set after grouping the Hedley fractions into different P pools. Better predictions with R^2 were shown when no P inputs were considered (Figure 2). The moderate and stable P fractions could effectively be predicted ($R^2 > 0.86$), while only the result of the labile P pool in the control was acceptable, albeit barely (Figure 2g, $R^2 = 0.72$). The Po and Pi fractions from labile and moderate P pools were also compared to assess the model. For the Po fractions, R^2 was higher than for the Pi fractions (Figure S1). The prediction accuracy decreased when the P and NP additions were applied.

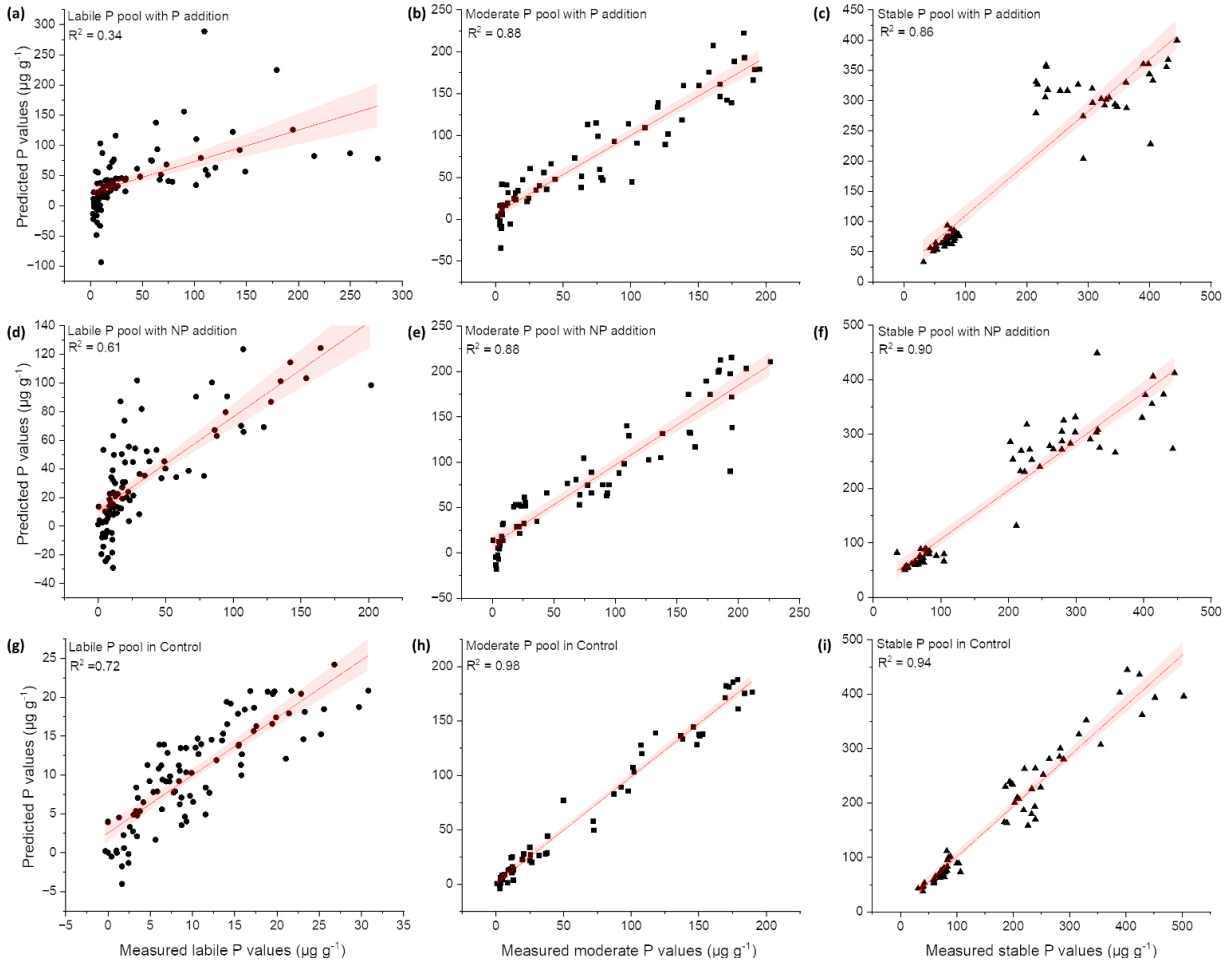

Figure 2. Comparisons of measured P pools (labile P: **a**, **d** and g; moderate P: **b**, **e** and h; stable P: **c**, **f** and i) and the predicted P contents (μg g^{-1}) by NIRS modeling with P addition (**a**–**c**), NP addition (**d**–**f**), and control (**g**–**i**). Red lines indicate a significant correlation (all $p < 0.05$). Shaded areas represent 95% confidence intervals.

4. Discussion

4.1. Influence of Nutrient Amendments on Soil P Pools

Research on nutrient addition to different natural ecosystems is becoming a key issue worldwide [52–54]. In tropical forest ecosystems with highly weathered soils, atmospheric P deposition can lead to P fertilization effects through direct input. It can accelerate P release from organic matter and increase P availability [55]. It has been reported that in subtropical forest ecosystems, N addition significantly increased the content of available soil P, but decreased the content of moderately labile P [56]. However, fertilization and plant species composition on the Tibetan Plateau could play a substantial role in P pools in grassland soils. In alpine grasslands, the relative availability of soil N and soil P has been indicated as an important determinant in regulating plants' N and P contents, controlling plant metabolic and growth rates [57]. As shown for some legumes, N additions could also significantly increase the aboveground net primary production (ANPP) [43]. The addition of P and N during the experiment at the Haibei station also significantly reduced fungal species richness and changed the fungal community composition [13]. Overall, N addition can affect the P fractions in three ways: First, N addition to ammonium compounds can lower the soil pH and promote the dissolution of recalcitrant Ca-bound Pi into moderately occluded Pi and available P fractions [58]; second, N also promotes the secretion of microbial extracellular phosphatase, which enhances the mineralization of Po, thereby increasing the leaching of available P [59]. In addition, plants and mycorrhizal communities are also the driving force behind soil P cycling [60]. Our results partly verify that Po contents were increased by the second way, with NP addition at a 0–20 cm depth (Table 3), indicating the P-limit on the research area. In addition, the P contents of Pi and Po increased significantly under the P additions, but there were no notable changes in the proportions of Po fractions (Table 3). Plant-species composition must be considered to estimate plant access to soil P, as Pätzhold et al. [45] showed in long-term grassland experiments in Germany. P and N additions also significantly influenced the labile and moderate P fractions (Figure 1 & Table 3). Regarding the proportion of each fraction, our study showed values of 8.7% for plant-available labile P pools, and 31% for the moderate P pool (28.4% for Po in this pool) for the control samples (Table S1). In addition, most of the soil P was present in stable P forms (all fractions made up almost 65% of the total P, Table S1), which can be attributed to the formation of the relatively young soil on the Tibetan Plateau [17]. This pool also differed at least between depths.

However, significant differences were observed between the P ratios of all the pools compared to different soil depths.

The distinct differences between all depths of the stable P pool could probably be explained by the large C content and soil development difference. In soils with less organic matter, the Pi fractions can have equal importance in controlling Resin-P [61]. Furthermore, strong correlations between the $NaHCO_3$ and NaOH fractions have been found, suggesting that these fractions do not represent separate pools [33]. The contribution of individual fractions to total P in soils varies substantially between grassland, pasture, arable land, and forest. Significant differences were observed mainly in moderately labile P and stable P fractions. As shown in Figure 1 and the P content for the control samples in our study, the increase in P pools after nutrient amendment is inconsistent with findings from other studies worldwide (Table S3). However, recent research has pointed out different results to determining bioavailable soil P (labile P) using Hedley fractionation. Wu et al. [62] provided better results for labile P fractions using this method than synchrotron-based X-ray absorption near edge structure (XANES) spectroscopy. Hou et al. [63] highlighted the value of soil P dynamics and availability worldwide to predict the response of terrestrial ecosystems to global changes. On the other hand, Negassa & Leinweber [64] reviewed the limit of Hedley fractionation for different land uses. Klotzbücher et al. [65] argued that this method could not provide information to understand P bioavailability, because the sequential extraction using individual steps could not be related to a specific mineral source or its binding strength. In addition, the labile P measured by Hedley fractionation should not be generally defined as plant-available P because most of the P pool is immobilized by microbes [19]. We suppose this difference is mainly related to whether P fertilizer is applied. In summary, in our experiment, the results of Hedley fractionation can provide an indication of the amount of bioavailable P in grassland soils.

4.2. NIRS Models

Chodak [66] and Cécillon et al. [67] emphasized that P calibration rarely performs well in soil, with an R^2 value between 0.4–0.5 only; this is because P has no direct vibrational response in NIRS. Therefore, its proper prediction depends on the correlation with the soil components absorbed in the spectral range of wavelengths, such as total C and N, particle size, and water content. Our calibration models of

individual P fractions achieved relatively satisfactory results for some, but not all, individual P fractions (Tables 4 and 5). It is obvious that nutrient amendments increased the data redundancy (higher heterogeneity) significantly, resulting in reduced accuracy (Table 4). Generally, the precision and reproducibility of the results of the Hedley fractionation method are of crucial importance for the quality of predictions of NIRS models [9]. All the fractions of the labile P pool (Resin-P, $NaHCO_3$-P) performed poorly in the cross-validation (Tables 4 and 5), and fractions of moderate and stable P pools performed better. Richter et al. [68] hypothesized that organic acids slowly displace Pi because many naturally occurring acids, such as citric acid and oxalic acid, compete with phosphates for sorption sites. The poor external-validation results were due to an insufficient sample size and complex external conditions, i.e., heterogeneous sets. The results of NIRS for P determination allow approximate quantitative predictions or the grouping of samples into different categories based on RPD and RPIQ values, at least under our experimental conditions [9,40,49,51]. We attribute the higher RMSE values (Tables 4, 5 and S2) to the significant differences caused in the fractionation and the high concentrations. For many agricultural and engineering applications (such as soil fertility assessments), it is usually sufficient to classify soils as basic test values without requiring an accurate estimate of soil properties. To use NIRS to determine P fractions in grassland-soil-monitoring studies, the precision of the reference values and NIRS measurements has to be improved; the grinding of soil samples is a possibility for the development of improved NIRS measurements. Overall, soil particle sizes influence the spectral absorbance, introducing an error for P measurements [69–71]. Additionally, the homogeneity of soil samples, which have lower data redundancy, provides a better quality of P prediction in the NIRS model [9]. Thus, it is necessary to classify the soil samples appropriately.

In addition, we note that our model showed little variance in performance with inorganic and Po fractions, indicating that both P forms are bound to primary soil properties detected directly by NIRS (Figure S1). However, this reproducibility could not provide information about the distribution of Pi and Po within individual fractions. The regressions of the NaOH-Po and $HCl_{conc.}$-P fractions exhibited the best performance of all the regressions, and showed similar statistical values for both validations. According to present knowledge, P or phosphate are not excited through NIR light waves to reflect in a particular part of the NIR spectrum. Hence recognizable

excitation of P depends on organic or mineral compounds. It can be hypothesized that the separation of the HCl_{conc}. fraction in Pi and Po does not give reliable estimates of these P fractions. In general, the information on the P forms extracted using the NaOH and HCl_{conc}. steps are vague, describing these forms only as recalcitrant Pi and Po [33]. Overall, from the Hedley results, it can be interpreted that the effect of depth is more durable than the impact of nutrition addition in the data set. Chang et al. [72] reported that the ability to predict levels of extractable cations varied with the extraction method without explaining the differences; however, spectral changes associated with soil P content are usually associated with organic matter or crystal water. The quality of the Po fraction model is related to the underlying mechanism that produces near-infrared spectroscopy, because organic compounds are more easily irradiated than inorganic compounds [9]; this is because the organic compounds have characteristic infrared absorptions such as carbon-hydrogen bonds [73], while the P compounds correlated with organic matter in soil are detectable in NIRS [74]. In contrast to the Po fraction, the relationship between the Pi fraction and other soil properties detectable by NIRS is insufficient to predict Pi using NIRS [40]. If the model is improved, NIRS can help to evaluate the data obtained with the Hedley method, which means that the model based on the large sample numbers could be more precise. However, even with the results of this study, some trends are shown; for example, although the parent material and nutrient content influence the P status of the soil, other factors become more important.

As noted in previous studies, the labile P pool (Resin-P, $NaHCO_3$-Pi, and Po) could be recognized as a plant-available form [75,76]. Our results show that with P fertilization, the Resin-P fraction, in particular, increases strongly (Figure 1); this can only be inadequately predicted in the NIRS model. It can be concluded that a combination of NIRS modeling and chemical extraction for the labile P pool, such as an anion-exchange resin, provides the best results overall. Additionally, Reijneveld et al. [77] showed that a combination of chemical extraction using $CaCl_2$ and NIRS gave the best results compared to conventional soil chemical techniques.

In summary, we showed that the model prediction quality was better for Po than Pi fractions and the moderate, stable P pool than in the labile P pool (Tables 4). Since the P content in the nutrient addition experiment was mainly concentrated in the Resin-P fraction of the topsoil, the modeling of Hedley P fractions with NIRS may be a

promising method for determining plant-available P from soils with similar properties. Combining the measurement of Pi using Hedley fractionation and using the measurement of the more stable P pool with NIRS also appears promising in the natural grassland without nutrient additions.

5. Conclusions

Hedley fractionation was adapted to the specifics of the grassland soils of the Tibetan Plateau, and showed reliable results of soil available-P for plants. Additionally, the prediction of the Hedley fractions by the NIRS spectra gave satisfactory results for the moderate and stable P pools, except for the labile fraction. When P was added to the soils by fertilizer application, the labile Resin-P pool increased from below 3% in total to rates of to 18%, which was accompanied by a decrease in the model quality. Therefore, NIRS modeling may suit large-scale experiments requiring substantial spatial and temporal replication of soil samples within similar soil physical and chemical properties in combination with chemical soil extractions—such as the resin-P fractionation or the $CaCl_2$ extraction for labile P pools in soils—to lower the costs and increase the value of soil analysis results.

This study yielded basic P data and a specific description of Hedley fractionation and NIRS modeling for alpine grassland soils on the Tibetan Plateau. It will support the continuation of possible future studies that will help to investigate the responses of soil to environmental factors, such as climate warming and the stability of the alpine ecosystem. Hence, its implementation in extensive inventories would significantly improve data gathering. Further research should improve the accuracy of NIRS models for predicting Hedley precision in determining P fractions and their relationships to other soil parameters.

Supplementary Materials: The following supporting information can be downloaded at: https: //www.mdpi.com/article/10.3390/agronomy12040783/s1, Figure S1: Comparisons of measured Pi contents (a,c,e) and Po contents (b,d,f), and the predicted P contents (μg g−1) using NIRS modeling with P addition (a,b), NP addition (c,d), and control (e,f); Table S1: soil P contents (μg g−1) and proportions (% of total Hedley-P) for seven Hedley fractions in different treatments of N, P, and an NP combination; Table S2: quality parameters for NIRS model in external validation (20% of total samples)

for all Hedley fractions (predicted vs. measured external validation); Table S3: Review: concentrations (µg g−1) of soil P fractions in different ecosystems worldwide [78–81].

Author Contributions: Conceptualization, T.S.; methodology, P.K.; J.B. and T.S.; formal analysis, Z.C.; investigation, Z.C.; resources, J.-S.H.; P.K. and J.B.; writing—original draft preparation, Z.C.; writing—review and editing, P.K.; J.-S.H.; J.B.; Z.-H.G. and T.S. All authors have read and agreed to the published version of the manuscript.

Funding: This research received no external funding.

Institutional Review Board Statement: Not applicable.

Informed Consent Statement: Not applicable.

Data Availability Statement: Data are contained within the article or Supplementary Material.

Acknowledgments: We thank Zhenghua Zhang from the Northwest Institute of Plateau Biology, the Chinese Academy of Sciences (CAS), and Chao Wang from Peking University, for cooperating and sharing the soil samples. Many thanks go to Renate Nitschke and Michael Witt from the University of Freiburg, and to Sabine Flaiz, and Rita Mögenburg from the University of Tübingen, for introducing the methods used in the laboratory and analysis work. We acknowledge support by Open Access Publishing Fund of University of Tuebingen.

Conflicts of Interest: The authors declare no conflict of interest.

References

1. Correll, D.L. The Role of Phosphorus in the Eutrophication of Receiving Waters: A Review. *J. Environ. Qual*. **1998**, *27*, 261–266. https://doi.org/10.2134/jeq1998.00472425002700020004x.
2. Renneson, M.; Barbieux, S.; Colinet, G. Indicators of phosphorus status in soils: Significance and relevance for crop soils in southern Belgium. A review. *Biotechnol. Agron. Soc. Envir.* **2016**, *20*, 257–272.
3. Hou, E.; Wen, D.; Jiang, L.; Luo, X.; Kuang, Y.; Lu, X.; Chen, C.; Allen, K.T.; He, X.; Huang, X.; Luo, Y. Latitudinal patterns of terrestrial phosphorus

limitation over the blobe. *Ecol. Lett.* **2021**, *24*, 1420–1431. https://doi.org/10.1111/ele.13761

4. Augusto, L.; Achat, D.L.; Jonard, M.; Vidal, D.; Ringeval, B. Soil parent material—A major driver of plant nutrient limitations in terrestrial ecosystems. *Glob. Change Biol*. **2017**, *23*, 3808–3824. https://doi.org/10.1111/gcb.13691.

5. Vitousek, P.M.; Porder, S.; Houlton, B.Z.; Chadwick, O.A. Terrestrial phosphorus limitation: Mechanisms, implications, and nitrogen-phosphorus interactions. *Ecol. Appl.* **2010**, *20*, 5–15. https://doi.org/10.1890/08-0127.1.

6. Walker, T.W.; Syers, J.K. The fate of phosphorus during pedogenesis. *Geoderma* **1976**, *15*, 1–19. https://doi.org/10.1016/0016-7061(76)90066-5.

7. Peñuelas, J.; Poulter, B.; Sardans, J.; Ciais, P.; Van Der Velde, M.; Bopp, L.; Boucher, O.; Godderis, Y.; Hinsinger, P.; Llusia, J.; et al. Human-Induced nitrogen-phosphorus imbalances alter natural and managed ecosystems across the globe. *Nat. Commun.* **2013**, *4*, 2934. https://doi.org/10.1038/ncomms3934.

8. Wang, Y.P.; Law, R.M.; Pak, B. A global model of carbon, nitrogen and phosphorus cycles for the terrestrial biosphere. *Biogeosciences* **2010**, *7*, 2261–2282. https://doi.org/10.5194/bg-7-2261-2010.

9. Niederberger, J.; Todt, B.; Boča, A.; Nitschke, R.; Kohler, M.; Kühn, P.; Bauhus, J. Use of near-infrared spectroscopy to assess phosphorus fractions of different plant availability in forest soils. *Biogeosciences* **2015**, *12*, 3415–3428. https://doi.org/10.5194/bg-12-3415-2015.

10. Shen, J.; Yuan, L.; Zhang, J.; Li, H.; Bai, Z.; Chen, X.; Zhang, W.; Zhang, F. Phosphorus Dynamics: From Soil to Plant. *Plant Physiol.* **2011**, *156*, 997–1005. https://doi.org/10.1104/pp.111.175232.

11. Müller, M.; Oelmann, Y.; Schickhoff, U.; Böhner, J.; Scholten, T. Himalayan tree-line soil and foliar C:N:P stoichiometry indicate nutrient shortage with elevation. *Geoderma* **2017**, *291*, 21–32. https://doi.org/10.1016/j.geoderma.2016.12.015.

12. Guan, S.; An, N.; Zong, N.; He, Y.; Shi, P.; Zhang, J.; He, N. Climate warming impacts on soil organic carbon fractions and aggregate stability in a Tibetan

alpine meadow. *Soil Biol. Biochem*. **2018**, *116*, 224–236. https://doi.org/10.1016/j.soilbio.2017.10.011.

13. He, D.; Xiang, X.; He, J.-S.; Wang, C.; Cao, G.; Adams, J.; Chu, H. Composition of the soil fungal community is more sensitive to phosphorus than nitrogen addition in the alpine meadow on the Qinghai-Tibetan Plateau. B*iol. Fertil. Soils*. **2016**, *52*, 1059–1072. https://doi.org/10.1007/s00374-016-1142-4.

14. Jiang, J.; Shi, P.; Zong, N.; Fu, G.; Shen, Z.; Zhang, X.; Song, M. Climatic patterns modulate ecosystem and soil respiration responses to fertilization in an alpine meadow on the Tibetan Plateau, China. *Ecol. Res.* **2014**, *30*, 3–13. https://doi.org/10.1007/s11284-014-1199-1.

15. Wang, H.; Sun, J.; Li, W.; Wu, J.; Chen, Y.; Liu, W. Effects of soil nutrients and climate factors on belowground biomass in an alpine meadow in the source region of the Yangtze-Yellow rivers, Tibetan Plateau of China. *J. Arid Land* **2016**, *8*, 881–889. https://doi.org/10.1007/s40333-016-0055-2.

16. Wang, D.; Wang, L.; Liu, J.; Zhu, H.; Zhong, Z. Grassland ecology in China: Perspectives and challenges. *Front Agric. Sci. Eng*. **2018**, *5*, 24–43. https://doi.org/10.15302/J-FASE-2018205.

17. Baumann, F.; He, J.S.; Schmidt, K.; Kühn, P.; Scholten, T. Pedogenesis, permafrost, and soil moisture as controlling factors for soil nitrogen and carbon contents across the Tibetan Plateau. *Glob. Change Biol.* **2019**, *15*, 3001–3017. https://doi.org/10.1111/j.1365-2486.2009.01953.x.

18. Baumann, F.; Schmidt, K.; Dörfer, C.; He, J.S.; Scholten, T.; Kühn, P. Pedogenesis, permafrost, substrate and topography: Plot and landscape scale interrelations of weathering processes on the central-eastern Tibetan Plateau. *Geoderma* **2014**, *226–227*, 300–316. https://doi.org/10.1016/j.geoderma.2014.02.019.

19. Yang, X.; Post, W.M. Phosphorus transformations as a function of pedogenesis: A synthesis of soil phosphorus data using Hedley fractionation

method. *Biogeosciences* **2011**, *8*, 2907–2916. https://doi.org/10.5194/bg-8-2907-2011.

20. Du, E.; Terrer, C.; Pellegrini, A.F.A.; Ahlström, A.; van Lissa, C.J.; Zhao, X.; Xia, N.; Wu, X.; Jackson, R.B. Global patterns of terrestrial nitrogen and phosphorus limitation. *Nat. Geosci.* **2020**, *13*, 221–226. https://doi.org/10.1038/s41561-019-0530-4.

21. Hou, E.; Luo, Y.; Kuang, Y.; Chen, C.; Lu, X.; Jiang, L.; Luo, X.; Wen, D. Global meta-analysis shows pervasive phosphorus limitation of aboveground plant production in natural terrestrial ecosystems. *Nat. Commun.* **2020**, *11*, 1–9. https://doi.org/10.1038/s41467-020-14492-w.

22. Jing, X.; Yang, X.; Ren, F.; Zhou, H.; Zhu, B.; He, J.S. Neutral effect of nitrogen addition and negative effect of phosphorus addition on topsoil extracellular enzymatic activities in an alpine grassland ecosystem. *Appl. Soil Ecol.* **2016**, *107*, 205–213. https://doi.org/10.1016/j.apsoil.2016.06.004.

23. Luo, R.; Fan, J.; Wang, W.; Luo, J.; Kuzyakov, Y.; He, J.S.; Chu, H.; Ding, W. Nitrogen and phosphorus enrichment accelerates soil organic carbon loss in alpine grassland on the Qinghai-Tibetan Plateau. *Sci. Total Environ***. 2019**, *650*, 303–312. https://doi.org/10.1016/j.scitotenv.2018.09.038.

24. He, S.; Richards, K. Impact of Meadow Degradation on Soil Water Status and Pasture Management-A Case Study in Tibet. *Land Degrad Dev.* **2015**, *26*, 468–479. https://doi.org/10.1002/ldr.2358.

25. Shen, M.; Piao, S.; Cong, N.; Zhang, G.; Jassens, I.A. Precipitation impacts on vegetation spring phenology on the Tibetan Plateau. *Glob. Change Biol.* **2015**, *21*, 3647–3656. https://doi.org/10.1111/gcb.12961.

26. Wang, Y.; Wesche, K. Vegetation and soil responses to livestock grazing in Central Asian grasslands: A review of Chinese literature. *Biodivers. Conserv.* **2016**, *25*, 2401–2420. https://doi.org/10.1007/s10531-015-1034-1.

27. Yang, Y.; Fang, J.; Smith, P.; Tang, Y.; Chen, A.; Ji, C.; Hu, H.; Rao, S.; Tan, K.; He, J.S. Changes in topsoil carbon stock in the Tibetan grasslands between

the 1980s and 2004. *Glob. Change Biol.* **2009**, *15*, 2723–2729. https://doi.org/10.1111/j.1365-2486.2009.01924.x.

28. Geng, Y.; Baumann, F.; Song, C.; Zhang, M.; Shi, Y.; Kühn, P.; Scholten, T.; He, J.-S. Increasing temperature reduces the coupling between available nitrogen and phosphorus in soils of Chinese grasslands. *Sci. Rep.* **2017**, *7*, srep43524. https://doi.org/10.1038/srep43524.

29. Huang, N.; He, J.S.; Chen, L.; Wang, L. No upward shift of alpine grassland distribution on the Qinghai-Tibetan Plateau despite rapid climate warming from 2000 to 2014. *Sci. Total Environ.* **2018**, *625*, 1361–1368. https://doi.org/10.1016/j.scitotenv.2018.01.034.

30. Kruse, J.; Abraham, M.; Amelung, W.; Baum, C.; Bol, R.; Kühn, O.; Lewandowski, H.; Niederberger, J.; Oelmann, Y.; Rüger, C.; et al. Innovative methods in soil phosphorus research: A review. *J. Plant. Nutr. Soil Sci.* **2015**, *178*, 43–88. https://doi.org/10.1002/jpln.201400327.

31. Olsen, S.R. *Estimation of Available Phosphorus in Soils by Extraction with Sodium Bicarbonate*; (No. 939); US Department of Agriculture: Washington, DC, USA, 1954.

32. Hedley, M.J.; Stewart, J.W.B.; Chauhan, B.S. Changes in Inorganic and Organic Soil Phosphorus Fractions Induced by Cultivation Practices and by Laboratory Incubations. *Soil Sci. Soc. Am. J.* **1982**, *46*, 970–976. https://doi.org/10.2136/sssaj1982.03615995004600050017x.

33. Tiessen, H.; Moir, J. *Characterization of Available P by Sequential Extraction.* In: *Soil Sampling and Methods of Analysis*; Carter, M.R., and Gregorich, E.G., 2nd Ed.; Boca Raton: Florida, USA, 2007; Chapter 25, pp. 293–306. https://doi.org/10.1201/9781420005271.

34. Johnson, A.H.; Frizano, J.; Vann, D.R. Biogeochemical implications of labile phosphorus in forest soils determined by the Hedley fractionation procedure. *Oecologia* **2013**, *135*, 487–499. https://doi.org/10.1007/s00442-002-1164-5.

35. Lajtha, K.; Driscoll, C.T.; Jarrell, W.M.; Elliott, E.T. Soil phosphorus: Characterization and total element analysis. *Stand. Soil Methods Long Term Ecol. Res.* **1999**, *7*, 115–143.

36. Bogrekci, I.; Lee, W.S. Improving phosphorus sensing by eliminating soil particle size effect in spectral measurement. *Am. Soc. Agric. Eng.* **2005**, *48*, 1971–1978.

37. Gruselle, M.C.; Bauhus, J. Assessment of the species composition of forest floor horizons in mixed spruce-beech stands by Near Infrared Reflectance Spectroscopy (NIRS). *Soil Biol. Biochem*. **2010**, *42*, 1347–1354. https://doi.org/10.1016/j.soilbio.2010.03.011.

38. Stevens, A.; Nocita, M.; Tóth, G.; Montanarella, L.; van Wesemael, B. Prediction of Soil Organic Carbon at the European Scale by Visible and Near InfraRed Reflectance Spectroscopy. *PLoS ONE* **2013**, *8(6)*: e66409. https://doi.org/10.1371/journal.pone.0066409.

39. Galasso, H.L.; Callier, M.D.; Bastianelli, D.; Blancheton, J.P.; Aliaume, C. The potential of near infrared spectroscopy (NIRS) to measure the chemical composition of aquaculture solid waste. *Aquaculture* **2017**, *476*, 134–140. https://doi.org/10.1016/j.aquaculture.2017.02.035.

40. Zhang, L.e.i.; Zhang, R. Effect of soil moisture and particle size on soil total phosphorus estimation by near-infrared spectroscopy. *Pol. J. Environ. Stud.* **2017**, *26*, 395–401. https://doi.org/10.15244/pjoes/64930.

41. Viscarra Rossel, R.A.; Behrens, T.; Ben-Dor, E.; Brown, D.J.; Demattê, J.A.M.; Shepherd, K.D.; Shi, Z.; Stenberg, B.; Stevens, A.; Adamchuk, V.; et al. A global spectral library to characterize the world's soil. *Earth-Sci. Rev.* **2016**, *155*, 198–230. https://doi.org/10.1016/j.earscirev.2016.01.012.

42. Suonan, J.; Classen, A.T.; Zhang, Z.; He, J.S. Asymmetric winter warming advanced plant phenology to a greater extent than symmetric warming in an alpine meadow. *Funct. Ecol.* **2017**, *31*, 2147–2156. https://doi.org/10.1111/1365-2435.12909.

43. Ren, F.; Song, W.; Chen, L.; Mi, Z.; Zhang, Z.; Zhu, W.; Zhou, H.; Cao, G.; He, J.-S. Phosphorus does not alleviate the negative effect of nitrogen enrichment on legume performance in an alpine grassland. *J. Plant Ecol.* **2016**, *9*, 1–9. https://doi.org/10.1093/jpe/rtw089.

44. Alt, F.; Oelmann, Y.; Herold, N.; Schrumpf, M.; Wilcke, W. Phosphorus partitioning in grassland and forest soils of Germany as related to land-use type, management intensity, and land use-related pH. *J. Plant. Nutr. Soil Sci*. **2011**, *174*, 195–209. https://doi.org/10.1002/jpln.201000142.

45. Pätzold, S.; Hejcman, M.; Barej, J.; Schellberg, J. Soil phosphorus fractions after seven decades of fertilizer application in the Rengen Grassland Experiment. *J. Plant. Nutr. Soil Sci.* **2013**, *176*, 910–920. https://doi.org/10.1002/jpln.201300152.

46. Stolter, C.; Julkunen-tiitto, R.; Ganzhorn, U. Application of near infrared reflectance spectroscopy (NIRS) to assess some properties of a sub-arctic ecosystem. *Basic Appl. Ecol.* **2006**, *7*, 167–187. https://doi.org/10.1016/j.baae.2005.05.002.

47. Bellon-Maurel, V.; Fernandez-Ahumada, E.; Palagos, B.; Roger, J.-M.; McBratney, A. Critical review of chemometric indicators commonly used for assessing the quality of the prediction of soil attributes by NIR spectroscopy. *TrAC Trend. Anal. Chem*. **2010**, *29*, 1073–1081. https://doi.org/10.1016/j.trac.2010.05.006.

48. Jabadi, S.H.; Mouazen, A.M. Data Fusion of XRF and Vis-NIR using Outer Product Analysis, Granger-Ramanathan, and Least Squares for Prediction of Key Soil Attributes. *Remote Sens.* **2021**, *13*, 2023. https://doi.org/10.3390/rs13112023.

49. Zornoza, R.; Guerrero, C. Near infrared spectroscopy for determination of various physical, chemical and biochemical properties in Mediterranean soils. Soil Biol. Biochem. 2008, 40, 1923–1930. https://doi.org/10.1016/j.soilbio.2008.04.003.

50. Wan, M.; Hu, W.; Qu, M.; Li, W.; Zhang, C.; Kang, J.; Hong, Y.; Chen, Y.; Huang, B. Rapid estimation of soil cation exchange capacity through sensor data fusion of portable XRF spectrometry and Vis-NIR spectroscopy. *Geoderma* **2020**, *363*, 114163. https://doi.org/10.1016/j.geoderma.2019.114163.

51. Nawar, S.; Mouazen, A.M. Predictive performance of mobile vis-near infrared spectroscopy for key soil properties at different geographical scales by using spiking and data mining techniques. *Catena* **2017**, *151*, 118–129. https://doi.org/10.1016/j.catena.2016.12.014.

52. Mao, J.; Mao, Q.; Zheng, M.; Mo, J. Responses of Foliar Nutrient Status and Stoichiometry to Nitrogen Addition in Different Ecosystems: A Meta-analysis. *J. Geophys. Res. Biogeosci.* **2020**, *125*, 1–16. https://doi.org/10.1029/2019JG005347.

53. Midolo, G.; Alkemade, R.; Schipper, A.M.; Benítez-López, A.; Perring, M.P.; De Vries, W. Impacts of nitrogen addition on plant species richness and abundance: A global meta-analysis. *Glob. Ecol. Biogeogr.* **2019**, *28*, 398–413. https://doi.org/10.1111/geb.12856.

54. Sardans, J.; Grau, O.; Chen, H.Y.H.; Janssens, I.A.; Ciais, P.; Piao, S.; Peñuelas, J. Changes in nutrient concentrations of leaves and roots in response to global change factors. *Glob. Chang. Biol. Bioenergy.* **2017**, *23*, 3849–3856. https://doi.org/10.1111/gcb.13721.

55. Dietrich, K.; Spohn, M.; Villamagua, M.; Oelmann, Y. Nutrient addition affects net and gross mineralization of phosphorus in the organic layer of a tropical montane forest. *Biogeochemistry* **2017**, *136*, 223–236. https://doi.org/10.1007/s10533-017-0392-z.

56. Fan, Y.; Zhong, X.; Lin, F.; Liu, C.; Yang, L.; Wang, M.; Chen, G.; Chen, Y.; Yang, Y. Responses of soil phosphorus fractions after nitrogen addition in a subtropical forest ecosystem: Insights from decreased Fe and Al oxides and increased plant roots. *Geoderma* **2019**, *337*, 246–255. https://doi.org/10.1016/j.geoderma.2018.09.028.

57. Zhang, J.; Yan, X.; Su, F.; Li, Z.; Wang, Y.; Wei, Y.; Ji, Y.; Yang, Y.; Zhou, X.; Guo, H.; et al. Long-Term N and P additions alter the scaling of plant nitrogen to phosphorus in a Tibetan alpine meadow. *Sci. Total Environ.* **2018**, *625*, 440–448. https://doi.org/10.1016/j.scitotenv.2017.12.292.

58. Liu, H.; Wang, R.; Wang, H.; Cao, Y.; Dijkstra, F.A.; Shi, Z.; Cai, J.; Wang, Z.; Zou, H.; Jiang, Y. Exogenous phosphorus compounds interact with nitrogen availability to regulate dynamics of soil inorganic phosphorus fractions in a meadow steppe. *Biogeosciences* **2019**, *16*, 4293–4306. https://doi.org/10.5194/bg-16-4293-2019.

59. Schleuss, P.M.; Widdig, M.; Heintz-Buschart, A.; Kirkman, K.; Spohn, M. Interactions of nitrogen and phosphorus cycling promote P acquisition and explain synergistic plant-growth responses. *Ecology*. **2020**, *101*, 1–14. https://doi.org/10.1002/ecy.3003.

60. Lambers, H.; Shane, M.W.; Cramer, M.D.; Pearse, S.J.; Veneklaas, E.J. Root structure and functioning for efficient acquisition of phosphorus: Matching morphological and physiological traits. *Ann. Bot.* **2006**, *98*, 693–713. https://doi.org/10.1093/aob/mcl114.

61. Thomas, S.M.; Johnson, A.H.; Frizano, J.; Vann, D.R.; Zarin, D.J.; Joshi, A. Phosphorus fractions in montane forest soils of the Cordillera de Piuchue, Chile: Biogeochemical implications. *Plant Soil.* **1999**, *211*, 139–148. https://doi.org/10.1023/A:1004686213319.

62. Wu, Y.H.; Prietzel, J.; Zhou, J.; Bing, H.J.; Luo, J.; Yu, D.; Sun, S.Q.; Liang, J.H.; Sun, H.Y. Soil phosphorus bioavailability assessed by XANES and Hedley sequential fractionation technique in a glacier foreland chronosequence in Gongga Mountain, Southwestern China. *Sci. China Earth Sci.* **2014**, *57*, 1860–1868. https://doi.org/10.1007/s11430-013-4741-z.

63. Hou, E.; Tan, X.; Heenan, M.; Wen, D. A global dataset of plant available and unavailable phosphorus in natural soils derived by Hedley method. *Sci. Data* **2018**, *5*, 180166. https://doi.org/10.1038/sdata.2018.166.

64. Negassa, W.; Leinweber, P. How does the Hedley sequential phosphorus fractionation reflect impacts of land use and management on soil phosphorus: A review. *J. Plant. Nutr. Soil Sci.* **2009**, *172*, 305–325. https://doi.org/10.1002/jpln.200800223.

65. Klotzbücher, A.; Kaiser, K.; Klotzbücher, T.; Wolff, M.; Mikutta, R. Testing mechanisms underlying the Hedley sequential phosphorus extraction of soils. *J. Plant. Nutr. Soil Sci.* **2019**, *182*, 570–577. https://doi.org/10.1002/jpln.201800652.

66. Chodak, M. Application of near infrared spectroscopy for analysis of Soils, litter and Plant materials. *Pol. J. Environ. Stud.* **2008**, *17*, 631–642.

67. Cécillon, L.; Barthès, B.G.; Gomez, C.; Ertlen, D.; Genot, V.; Hedde, M.; Stevens, A.; Brun, J.J. Assessment and monitoring of soil quality using near-infrared reflectance spectroscopy (NIRS). *Eur. J. Soil Sci.* **2009**, *60*, 770–784. https://doi.org/10.1111/j.1365-2389.2009.01178.x.

68. Richter, D.D.; Allen, H.L.; Li, J.; Markewitz, D.; Raikes, J. Bioavailability of slowly cycling soil phosphorus: Major restructuring of soil P fractions over four decades in an aggrading forest. *Oecologia* **2006**, *150*, 259–271. https://doi.org/10.1007/s00442-006-0510-4.

69. Ji, W.; Viscarra Rossel, R.A.; Shi, Z. Accounting for the effects of water and the environment on proximally sensed vis-NIR soil spectra and their calibrations. *Eur. J. Soil Sci.* **2015**, *66*, 555–565. https://doi.org/10.1111/ejss.12239.

70. Nocita, M.; Stevens, A.; Noon, C.; Van Wesemael, B. Prediction of soil organic carbon for different levels of soil moisture using Vis-NIR spectroscopy. *Geoderma* **2013**, *199*, 37–42. https://doi.org/10.1016/j.geoderma.2012.07.020.

71. Sadeghi, M.; Babaeian, E.; Tuller, M.; Jones, S.B. Particle size effects on soil reflectance explained by an analytical radiative transfer model. *Remote Sens. Environ.* **2018**, *210*, 375–386. https://doi.org/10.1016/j.rse.2018.03.028.

72. Chang, C.; Laird, D.; Mausbach, M.J. Near-Infrared Reflectance Spectroscopy—Principal Components Regression Analyses of Soil Properties. *Soil Sci. Soc. Am. J.* **2001**, *65*, 480–490. https://doi.org/10.2136/sssaj2001.652480x.

73. Barth, A. Infrared Spectroscopy of Proteins. *Biochim. Biophys. Acta Bioenerget.* **2007**, *1767*, 1073–1101. https://doi.org/10.1016/j.bbabio.2007.06.004.

74. Stenberg, B.; Viscarra-Rossel, R.A.; Mouazen, A.M.; Wetterlind, J. Visible and Near Infrared Spectorscopy in Soil Science. In *Advances in Agronomy*; Sparks, D.L., Ed.; Academica Press: Burlington, MA, USA, 2010; Vol. 107, Chapter 5, pp 163–215. https://doi.org/10.1016/S0065-2113(10)07005-7.

75. Cross, A.F.; Schlesinger, W.H. A literature review and evaluation of the. Hedley fractionation: Applications to the biogeochemical cycle of soil phosphorus in natural ecosystems. *Geoderma* **1995**, *64*, 197–214. https://doi.org/10.1016/0016-7061(94)00023-4.

76. Cross, A.F.; Schlesinger, W.H. Biological and geochemical controls on phosphorus fractions in semiarid soils. *Biogeochemistry* **2001**, *52*, 155–172. https://doi.org/10.1023/A:1006437504494.

77. Reijneveld, J.A.; van Oostrum, M.J.; Brolsma, K.M.; Fletcher, D.; Oenema, O. Empower Innovations in Routine Soil Testing. *Agronomy* **2022**, *12*, 191. https://doi.org/10.3390/agronomy12010191.

Manuscript 2

Soil phosphorus availability mediates the effects of nitrogen addition on community- and species-level phosphorus-acquisition strategies in alpine grasslands

Science of The Total Environment, 2024, 906, 167630

Zhen-Huan Guan[1, #], Zuonan Cao[2, #], Xiao Gang Li[3], Thomas Scholten[2], Peter Kühn[2], Lin Wang[3], Rui-Peng Yu[4] & Jin-Sheng He[1, 5, *]

[1]State Key Laboratory of Herbage Improvement and Grassland Agro-ecosystems, College of Pastoral Agriculture Science and Technology, Lanzhou University, Lanzhou 730000, China

[2]Department of Geosciences, Soil Science and Geomorphology, University of Tübingen, Tübingen 72070, Germany

[3]College of Ecology, Lanzhou University, Lanzhou 730000, China

[4]Beijing Key Laboratory of Biodiversity and Organic Farming, Key Laboratory of Plant–Soil Interactions, Ministry of Education, College of Resources and Environmental Sciences, China Agricultural University, Beijing 100193, China

[5]Institute of Ecology, College of Urban and Environmental Sciences, Peking University, Beijing, 100871, China

[#]These authors contributed equally to the work

* Corresponding author: Jin-Sheng He

State Key Laboratory of Herbage Improvement and Grassland Agro-ecosystems, College of Pastoral Agriculture Science and Technology, and College of Ecology, Lanzhou University, Lanzhou 730000, China

E-mail addresses: jshe@pku.edu.cn

Abbreviations: Phosphorus (P), nitrogen (N), Qinghai–Tibet Plateau (QTP), arbuscular mycorrhizal fungi (AMF), specific root length (SRL), carbon (C), inorganic P (Pi), organic P (Po), phospholipid fatty acid (PLFA), high-performance liquid chromatography (HPLC), soil organic carbon (SOC), root dry weight (RDW).

Abstract

Plants modulate their phosphorus (P) acquisition strategies (i.e., change in root morphology, exudate composition, and mycorrhizal symbiosis) to adapt to varying soil P availability. However, how community- and species-level P-acquisition strategies change in response to nitrogen (N) supply under different P levels remain unclear. To address this research gap, we conducted an 8-year fully factorial field experiment in an alpine grassland on the Qinghai–Tibet Plateau (QTP) combined with a 12-week glasshouse experiment with four treatments (N addition, P addition, combined N and P addition, and control). In the field experiment (community-level), when P availability was low, N addition increased the release of carboxylate from roots and led to a higher percentage of colonisation by arbuscular mycorrhizal fungi (AMF), along with decreased root length, specific root length (SRL), and total root length colonised by AMF. When P availability was higher, N addition resulted in an increase in the plant's demand for P, accompanied by an increase in root diameter and phosphatase activity. In the glasshouse experiment (species-level), the P-acquisition strategies of grasses and sedge in response to N addition alone mirrored those observed in the field, exhibiting a reduction in root length, SRL, and total root length colonised, but an increased percentage of AMF colonisation. Forbs responded to N addition alone with increased investment in all P-acquisition strategies, especially increased root biomass and length. P-acquisition strategies showed consistent changes among all species in response to combined N and P addition. Our results suggest that increased carboxylate release and AMF colonisation rate are common P-acquisition strategies of plants in alpine grasslands under N-induced P limitation. The main difference in P-acquisition strategies between forbs and grasses/sedges in response to N addition under low-P conditions was an increase in root biomass and length.

Keywords

Alpine grassland, Nitrogen addition, Phosphorus-acquisition strategy, Plant root, Soil

phosphorus availability, Qinghai–Tibetan Plateau

1. Introduction

The alpine grassland ecosystem of the Qinghai-Tibet Plateau (QTP) has extreme weather conditions and is particularly susceptible to N deposition (Baumann et al., 2009; Han et al., 2019). Field measurements, simulations using atmospheric chemical transport models, and interpolations based on limited field observations have revealed that N deposition on the plateau has increased over the past decade (Dentener et al., 2006; Jia et al., 2014; Liu et al., 2015; Lü & Tian, 2007). Continuous N input to terrestrial ecosystems increases plant P requirements and intensifies competition for P among plant species (Phoenix et al., 2004; Lü et al., 2013; DeMalach, 2018; Wan et al., 2019; Li et al., 2022), which can lead to a shift in plant nutrient requirements from N limitation to P limitation, particularly in areas with low soil P availability (Li et al., 2016; Müller et al., 2017; Zhao & Zeng, 2019; He et al., 2020; Chen et al., 2021). Such changes inevitably influence the stability and productivity of grassland ecosystems.

Under P-limited conditions, plants may increase their root biomass and form thinner, longer, and shallower roots to access a larger soil volume. Plants can upregulate the amounts of P-mobilising exudates (i.e., carboxylates and acid phosphatase [APase]) in the rhizosheath. Additionally, P deficiency is associated with an increase in the percentage of colonisation by arbuscular mycorrhizal fungi (AMF), which form an interface (through intraradical hyphae, e.g., arbuscules) for the exchange of inorganic nutrients for photosynthates and provide access to critical inorganic nutrients (via extraradical hyphae) that roots or even root hairs are unable to access (Zhu et al., 2001; Vance et al., 2003; Blank & Derner, 2004; Lambers et al., 2006; Wen et al., 2019; Liu et al., 2021; Pang et al., 2021; Lambers, 2022). However, it is unclear how plants regulate their P-acquisition strategies in response to N addition under varying soil P levels, which hinders predictions of vegetation dynamics under these conditions.

Except for P limitation, N enrichment could directly affect plant root biomass,

morphology, exudates, and colonisation by AMF; moreover, changes in root biomass and morphology would indirectly affect AMF colonisation (Ding et al., 2021; Pang et al., 2021; Lambers, 2022). The process of plant nutrient acquisition is a fundamental trade-off between maximising resource uptake and minimising associated costs (Wurzburger & Wright, 2015; Wen et al., 2019; Oldroyd & Leyser, 2020). As N gradually accumulates in the soil, plants modulate growth and metabolism following their N status and balance carbon (C) assimilation and N uptake (Oldroyd & Leyser, 2020). Furthermore, plant responses to N are influenced by the resources that limit their growth, such as radiation, precipitation, temperature, and other soil nutrients (Pregitzer et al., 1993; Xie et al., 2021). Owing to multiple factors, N addition may increase (Wang et al., 2017; Liu et al., 2021), decrease (Li et al., 2015; Wurzburger & Wright, 2015), or have no effect on the growth of fine roots (<2 mm diameter, Yan et al., 2021). Similarly, there is no consistent evidence on the response of root metrics, such as fine root length, root diameter, specific root length (SRL), and the release of carboxylate and APase in the rhizosheath (Wurzburger & Wright, 2015; He et al., 2020; Ding et al., 2021; Liu et al., 2021). The relationship between root traits and AMF colonisation is complex, leading to uncertainty in the response of the percentage of colonisation by AMF to N addition, showing an increase (Grman & Robinson, 2013) or decrease (Jiang et al., 2018).

When soil P availability is low, N-induced P limitation contributes to the positive regulation of plant P starvation signals (Li et al., 2022), and plants upregulate C allocation for P acquisition (Luo et al., 2022). In this situation, it is unclear whether the P-acquisition strategy is influenced by N addition or P limitation. Under conditions of high soil P availability, even if the N-induced increases in P demand do not lead to P limitation, the mass flow of plant-available P could never satisfy the increased P demand, requiring the root system to explore the wider space or mobilise more of the inorganic P (Pi) and organic P (Po) fractions (Gahoonia et al., 1994; Lambers et al., 2006). However, higher level of available P are more likely to be absorbed by plants;

thus, plant P-acquisition strategies may be influenced by N addition rather than P limitation. But N addition increased plant rhizosheath APase activity independent of soil P availability (Schleuss et al., 2020). In grassland communities, plant responses to N addition are inconsistent among plant species compared to crops and model plants (i.e. *Arabidopsis*) in glasshouse (Li et al., 2015; You et al., 2017; Chen et al., 2018; Oldroyd & Leyser, 2020), as different species have different nutrient requirements and costs at the individual level (Lynch & Ho, 2005). Different plant species exhibit contrasting root functional traits in response to nutrient limitation (Pang et al., 2021), species with thick-root species primarily relying on mycorrhizal fungi and/or more P-mobilizing exudates for nutrient uptake, while thin-root species rely more on root spreading (Wen et al., 2019). In the grasslands, the roots of forbs are usually thicker compared to grasses and sedges (Zheng et al., 2019). How does the response to N addition differ among species in soils with different P availability? Further studies are needed to answer this question.

Our study area was located on the QTP, where the average annual temperature is below 0 °C, which leads to a slower mineralisation rate of Po in the soil; the amount of plant-available P in the soil is less than 3% of the total P content (Rui et al., 2011; Zhou et al., 2021). With the application of P in this area, the effect of increasing P availability can be sustained over a long period because of the low iron- and aluminium-oxide contents (Gao et al., 2019). We investigated the effects of N addition on plant-community- and species-level P-acquisition strategies, including root morphology, exudate release, and AMF dynamics, under varying levels of soil P availability. Using data from a long-term field experiment (community-level) in alpine grassland of the QTP combined with a 12-week glasshouse experiment (species-level), we tested the following hypotheses:

(1) At low P level, changes in plant P-acquisition strategies are mainly influenced by N-induced P limitation; at high P level, gradual N saturation is the key factor causing changes in plant P-acquisition strategies.

(2) Different species display diverse P-acquisition strategies in response to N-induced P limitation. Forbs would primarily enhance the percentage of colonisation by AMF in response to N-induced P limitation, while grasses and sedges would primarily modify their root morphology.

Our findings contribute to the accurate prediction of nutrient limitations in grassland plants under the influence of N accumulation and provide insights into the community dynamics of alpine grassland ecosystems.

2. Materials and Methods

2.1 Site description

The field experiment was conducted at the Haibei National Field Research Station of Alpine Grassland Ecosystem (37°37′ N, 101°19′ E, 3250 m above sea level) of the Chinese Academy of Sciences in the north-eastern QTP. The region experiences a continental monsoon climate, with an average annual temperature of −1.7 °C, ranging from a mean monthly temperature of −14.8 °C in January to 9.8 °C in July. The mean annual precipitation is 489.0 mm, with over 80% occurring from May to September (Liu et al., 2018). The soil in the area is classified as Mat-Cryic Cambisol (Chinese Soil Taxonomy Research Group, 1995), corresponding to Gelic Cambisol (WRB, 2015), with a mean depth of 0.70 m (Ren et al., 2017). The dominant plant species at the site include *Kobresia humilis*, *Stipa aliena*, *Elymus nutans*, and *Festuca ovina*.

The long-term field experiment, conducted from 2011 to 2018, followed a two-factor (soil P and N supply) fully randomised design with six replications. Each plot was 6 m × 6 m in size with a 2 m buffer strip separating the blocks, and a 1 m buffer strip separating the plots within each block to minimise interference from neighbouring plots (Fig. **S1**). The fertilisers (triple superphosphate supplied at 50 kg P ha^{-1} yr^{-1} and urea supplied at 100 kg N ha^{-1} yr^{-1}) were divided into three equal parts and evenly distributed by hand on the soil surface after sunset in early June, July, and August during

the growing season of each year (Ren et al., 2017).

2.2 Field sampling

2.2.1 Soil sampling

Soil samples (0–10 cm depth) were collected in early August 2018. Five soil cores (Ø 50 mm) were randomly taken from each plot and mixed into a composite bulk sample. Samples were packed in polyethene bags and stored in an ice box before being shipped to the laboratory. All visible roots, residues, and stones were removed from the samples by sieving (2 mm). Approximately 10 g soil of each sample was aseptically collected and stored at −80 °C for phospholipid fatty acid (PLFA) determination, and the remaining material was air-dried for soil property analysis.

2.2.2 Vegetation harvest

Plant communities were surveyed in mid-August 2018 at the peak of the growing season. Three species richness surveys were conducted for each plot, covering an area of 1 m^2. Within each plot, plants were harvested in a randomly selected 0.5 m × 0.5 m quadrat. Shoots (leaves and stems) were cut at the base with scissors and sorted into three functional groups (grasses, forbs, and sedges) to measure aboveground biomass. All plant species within the quadrat were pooled into a mixed community sample to measure C, N, and P concentrations.

2.2.3 Rhizosheath sampling

After harvest, intact root samples of plant community from three replicate soil cores (0–10 cm) per plot were carefully extracted from the soil, using a root auger (Ø 70 mm). The root samples consisted of a mixed sample from different species, and then care was taken to separate the roots from the soil. Gentle shaking was applied to remove loosely adherent bulk soil, leaving only the soil firmly adhering to the rhizosheath around the roots, which was defined as rhizosheath soil (Pang et al., 2017). The roots and

rhizosheath soil were bulked and transferred to a beaker containing 0.2 mM $CaCl_2$ depending on root volume (Pearse et al., 2007). The roots were repeatedly submerged in the solution until all rhizosheath soil was removed. 0.5 mL aliquots of the soil suspension was transferred into 2 mL centrifuge tubes to measure APase activity (Neumann, 2006). Subsequently, a few drops of concentrated phosphoric acid were added into subsamples of 7–8 mL before storage at −20 °C for the analysis of carboxylates using high-performance liquid chromatography (HPLC) (Wen et al., 2019). After analysing the rhizosheath exudates, the soaked roots were collected and washed with tap water, placed in kraft paper bags, and kept at 4 °C for subsequent measurement of C, N, and P contents; root biomass and morphology; and percentage of colonisation by AMF as soon as possible.

2.3 Glasshouse experiment

In early May 2019, we selected eight dominant species from the three functional groups—grasses (*Stipa aliena*, *Elymus nutans*, *Poa pratensis*, and *Festuca rubra*), forbs (*Aster diplostephioides*, *Potentilla anserina*, and *Saussurea pulchra*), and sedge (*Kobresia humilis*)—to conduct a glasshouse pot experiment with comparable conditions at the artificial intelligence glasshouse of Lanzhou University (Fig. **S2**). These species collectively exceeded more than 70% of the aboveground biomass (Table S1). Soil substrate from the top 15 cm layer of natural grassland near the field site was collected, air-dried, sieved (2 mm) to remove debris such as plant roots and other organic matter, and mixed thoroughly. The soil properties were as follows: pH 7.2 (1:5, soil: water); total P, 692 mg kg^{-1}; organic C, 60.6 g kg^{-1}; total N, 11.5 g kg^{-1}; available N, 7.48 g kg^{-1}; and available P, 66.3 mg kg^{-1}. Each pot (16 × 13 × 14.5 cm^3) was filled with 2 kg of processed soil.

The eight species were divided into four treatments (N addition, P addition, combined N and P addition and a control). Each treatment was replicated four times, resulting in a total of 128 pots. N was added in the form of urea, with a transformation

ratio of 40 mg N kg soil^{-1} in a pot equivalent to 100 kg N ha^{-1} yr^{-1} in the field; P was added as KH_2PO_4, with a ratio of 20 mg P kg soil^{-1} in a pot equivalent to 50 kg P ha^{-1} yr^{-1} in the field. No additional fertilisers or AMF inoculants were used because the roots were already colonised by native AMF (Wen et al., 2019).

Seeds from the eight species were sterilised in a 30% (v/v) solution of hydrogen peroxide for 5 min, rinsed three times with deionised water, and placed on top of moistened filter papers in Petri dishes overnight. Each pot was planted with 10 germinated seedlings of single species. The potted soils were maintained at 80% field capacity by daily watering and monitoring the weight. The glasshouse temperatures were maintained between 17 and 20 °C during the day and 12–15 °C at night. All pot positions were randomised every 2 weeks. To reveal as much as possible the true picture of the response of single species to nutrient addition in the glasshouse experiment, the plants were harvested in batches after 12 weeks of glasshouse cultivation, when the morphology converged with that of the field plants at the peak of growth. Then, the aboveground shoots of all plants were cut at the base and separated into leaves and stems for biomass measurement. The rhizosheath exudates were collected using the same methods described above for field roots. All visible roots in each pot were individually wrapped in a kraft paper bag and kept at 4 °C until further processing. The soil from the pots was then removed and sieved (2 mm), and available nutrient indicators were immediately measured. In addition, 200 g of soil was stored at −80 °C for PLFA determination, while the remaining soil was air-dried and used for soil property determination.

2.4 Laboratory measurements

2.4.1 Soil properties and plant nutrients

Soil pH was determined by measuring a 1:5 soil: water suspension after shaking for 30 min. Soil organic carbon (SOC), total N, and plant C and N concentrations in plant

shoot and root samples were measured using an elemental analyser (Elementar Vario EL III, Elementar Analysensysteme GmbH, Langenselbold, Germany). Inorganic C was eliminated by treating the samples with 0.5 M HCl prior to SOC measurement. Total soil P and plant P concentrations were determined by colorimetric after digestion in an $HClO_4$–H_2SO_4 mixture. Soil available N (KCl-extractable ammonium [NH_4^+] and nitrate [NO_3^-]) was determined using a continuous flow analyser (Skalar San, Breda, the Netherlands). An anion-exchange resin bag soaked in 0.5 M HCl was used to measure labile resin-Pi directly from the soil solution, followed by extraction with 0.5 M $NaHCO_3$ (pH 8.5) to obtain relatively labile plant-available Pi and easily mineralised Po; these three P fractions were considered to collectively represent available P (Pätzold et al., 2013; Niederberger et al., 2015), which was determined through continuous flow analysis (SEAL Auto Analyzer AA3, SEAL Analytical GmbH, Norderstedt, Germany) for the Pi fractions, and inductively coupled plasma–optical emission spectrometry (Optima 5300 DV, PerkinElmer, Waltham, MA, USA) for the total $NaHCO_3$ fraction.

2.4.2 Root morphology

Fresh plant roots samples were washed to remove debris, spread in water without overlapping, and scanned on an Epson Expression 10,000 XL desktop scanner (resolution 300 dpi). The resulting root images were then analysed using WinRHIZO software (Regent Instruments, Quebec, QC, Canada) to determine average root diameter and total root length (given as m per m^2 in the field experiment and m per pot in the glasshouse experiment; Wurzburger and Wright 2015). Samples were then oven-dried to a constant weight at 80 °C and weighed, and SRL was calculated as total root length per unit root dry weight (RDW).

2.4.3 Rhizosheath exudates

Rhizosheath carboxylates content (relative to RDW) was analysed using a Waters 1525 HPLC equipped with a Waters 2489 detector and a Waters Symmetry C^{18} reverse-phase

column (Waters, Milford, MA, USA). The mobile phase was 20 M KH_2PO_4 adjusted to pH 2.5 with concentrated H_3PO_4 at a flow rate of 0.6 mL min^{-1} and 100% methanol at 0.01 mL min^{-1}. The working standards to identify carboxylates at 210 nm included oxalate, tartrate, formate, malate, malonate, lactate, acetate, citrate, succinate, and propionate (Cawthray, 2003). Each sample was injected at a volume of 10 μL, and the run time was set at 16 min.

APase activity was determined by colorimetric based on the release of p-nitrophenol released from the soil suspension during incubation with p-nitrophenyl phosphate (PNPP) in buffers of pH 6.5 for 1 h at 37 °C (Hopkins et al., 2008). Subsequently, the 0.5 mL aliquots of soil suspension were transferred into 2 mL centrifuge tubes, treated with 0.4 mL of Na-Ac buffer and 0.1 mL of substrate solution (Zhang et al., 2015). At the end of the incubation, 0.5 mL of 0.5 M NaOH was added to the slurries to terminate the enzymatic reactions. The absorbance of the enzyme extracts was measured at 410 nm (UV-1800, MAPADA, Shanghai, China) immediately after the filtration process was completed. Rhizosheath carboxylate content and APase activity were expressed as mmol per unit RDW.

2.4.4 AMF Colonisation

After root scanning, a sub-sample of roots was randomly taken from the root system. Root samples were cleaned with 10% (w/v) KOH solution in a water bath at 90 °C for 20 min, rinsed with water, acidified with 2% (v/v) HCl for 5 min at 18 °C, and stained with 0.05% (w/v) nonvital Trypan blue in a 90 °C water bath for 30 min (Phillips & Hayman, 1970). The stained root fragments were placed in a lactic acid–glycerol–water solution (v/v/v, 1: 1: 1) overnight to remove excess stain. For each sample, 30 stained root fragments from first- and second-order roots with an average length of 1 cm were randomly selected and mounted on two slides for observation with a light microscope (BX63, Olympus Corporation, Tokyo, Japan). Colonisation by AMF (%) was evaluated following the method described by Trouvelot et al. (1986). The total root length

colonised by AMF was calculated by multiplying total root length per unit (m m^{-2}) by the percentage of colonisation by AMF (Toth et al., 1991; Barceló et al., 2020).

2.4.5 Microbial community structure

Soil microbial PLFA were determined using a modified Bligh–Dyer method. Fatty acids were extracted from 10 g of soil sample using chloroform–methanol–citric acid buffer (Kourtev et al., 2002). The lipids in the concentrated extract were separated on solid-phase extraction cartridges and fractionated into neutral lipids, glycolipids, and polar lipids. The polar lipid fraction was eluted with methanol, dried under nitrogen gas, saponified, and methylated. The specific fatty acids were used as indicators of AMF biomass (Olsson et al., 1998). The individual fatty acid methyl esters were identified and quantified using a MIDI Sherlock Microbial Identification System (MIDI, Newark, DE, USA), where the 16:1ω5c content represented the AMF fatty acid fraction. Finally, the sample content was converted to nmol g^{-1} soil sample based on the water content.

2.5 Statistical analysis

Two-way repeated-measures ANOVA with least significant difference test for post hoc means comparison was used to test the effects of N and P addition and their interactions on soil parameters, P fractions, plant growth parameters, P-acquisition strategy indicators, species richness, and functional group biomass of plants in the field experiment. A three-way ANOVA was conducted to assess the effects of species, N and P additions, and their interactions on plant growth parameters, indicators of P-acquisition strategies, and soil P fractions. Following Ward's method, cluster analysis for root biomass and root traits in response to N addition among the eight dominant species was used as the P-acquisition strategy indicator (Yu et al., 2020). The above analyses were performed using SPSS 25.0 (IBM SPSS, Chicago, IL, USA), and differences were considered significant at $P < 0.05$.

3. Results

3.1 Soil and plant properties in the field experiment

After treatment for 8 years, neither N nor P addition had a significant effect on the soil pH (Table 1). Combined N and P addition increased SOC content compared to the control, but none of the treatments had a significant effect on soil total N content (Table 1). N addition increased soil available N content (sum of NH_4^+ and NO_3^- contents) but decreased available P content (sum of resin-Pi and $NaHCO_3$ Pi and $NaHCO_3$ Po contents; Table 1). P addition increased P availability and total P content in the soil (Table 1).

Grass species accounted for over 60% of the plant community biomass (Table S1). The average shoot biomass of the plant community in plots with N addition was 64% higher than in plots without N addition, regardless of soil P availability (Table 2). In plots with P addition, N addition decreased plant community species richness, but stimulated forbs growth and inhibited sedge growth (Tables S2 and S3). Root samples of the plant community in the field were collected from mixed root systems of different species. Plots with N addition significantly decreased the root/shoot biomass ratio compared to plots without N addition, while the shoot N/P ratio increased more in plots with N addition alone than in plots with combined N and P addition (Table 2). Shoot P uptake, root P storage, and total P pool of plant community exhibited a greater increase with the combined addition of N and P, compared to that with N addition alone (Table 2).

3.2 Root trait responses to nutrient addition in the field experiment

With N addition, plant community root biomass decreased in plots with low soil P availability but increased in plots with high soil P availability (Fig. **1a**; Table S4); root length decreased in plots with low soil P availability, and root diameter increased in plots with high soil P availability (Fig. **1b, c**; Table S4); and SRL decreased at both soil P levels (Fig. **1d**; Table S4).

N addition enhanced the secretion of APase in the rhizosheath, which was

inhibited by high P availability (Fig. **2a**; Table S4). N addition increased the release of rhizosheath carboxylates in plots with low P availability, but it had no effect in plots with P addition (Fig. **2b**; Table S4).

We observed that N addition led to an increase in the percentage of AMF colonisation in plots without P application, while it significantly inhibited AMF colonisation rate in plots with P application (Fig. **2c**; Table S4). N reduced the total root length colonised by AMF at both soil P levels (Fig. **2d**; Table S4). Plots with P addition decreased the percentage of AMF colonisation and total root length colonised compared to plots without P addition (Fig. **2c**, d; Table S4). In addition, N addition decreased the content of AMF PLFA in soils with high P availability (Fig. **S3**; Table S4).

3.3 Effects of nutrient addition on plant root traits in the glasshouse experiment

The three-way interaction between species, N, and P addition had a significant effect on plant root traits ($P < 0.005$). Moreover, the impact of N addition on plant root traits varied across species under both low and high soil P availability, revealing a two-way interaction between N addition and species ($P < 0.05$; Tables S5, S6, and S7). We observed that N addition increased/decreased the root biomass of grasses and sedge with/without P addition, while root biomass of forbs increased regardless of soil P level (Fig. **3a,b**; Table S7). In pots with low soil P availability, N addition led to a decrease in root length for grasses and sedge but an increase in root length for forbs. However, root length remained unaffected by N addition for all species under high soil P level (Fig. **3c, d**). Combined N and P addition resulted in an increase in root diameter across all species (Fig. **3e, f**; Table S7). For most grass and forb species, N addition decreased SRL regardless of P availability (Fig. **3g, h**; Table S7).

We also observed additional effects of three- and two-way interactions on rhizosheath APase activity, rhizosheath carboxylate release, percentage of colonisation by AMF, total root length colonised by AMF and soil AMF PLFA content (Table S7). N addition increased rhizosheath APase activity in all species, but this was inhibited by

P addition (Fig. **4a, b**; Table S7). N addition also increased the amounts of carboxylates in the rhizosheath for all species under low soil P level (Fig. **4c, d**; Tables S7 and S8).

We found that N addition increased the percentage of colonisation by AMF in grasses (*S. aliena*, *E. nutans*, *F. rubra*, and *P. pratensis*) and forbs (*P. anserina*) without P addition (Fig, **4e**; Table S7). However, when P was added, N addition resulted in a decrease in the percentage of colonisation by AMF in all species, except *K. humilis* (Fig. **4f**; Table S7). N addition decreased total root length colonised by AMF in grasses, independent of P addition (Fig. 4g, h, Table S7). N addition increased total root length colonised by AMF in forbs without P addition but decreased it with P addition (Fig. **4g**, **h**, Table S7). P addition decreased the percentage of colonisation and total root length colonised by AMF in all species regardless of N addition (Fig. **4f, h**; Table S7). Notably, the P-acquisition strategies of the grasses responding to N addition were consistent with those of the field experiment (Figs. **1–4**).

3.4 Cluster analysis among species in response to N addition

In the glasshouse experiment, the response of root traits to N addition showed significant differences among species when soil P availability was low (Figs. **3** and **4**). Consequently, we performed a cluster analysis among species based on the effect sizes of root traits that responded to N addition alone, including root biomass, SRL, root length, root diameter, carboxylate content, percentage of colonisation by AMF, and APase activity (Fig. **5**). Our analysis revealed that in pots without P addition, the relative trait values associated with P-acquisition strategies across all species in response to N addition could be categorised into two groups: (1) *E. nutans*, *S. aliena*, *P. pratensis*, *F. rubra*, and *K. humilis* and (2) *S. pulchra*, *P. anserina*, and *A. diplostephioides*. In summary, forbs exhibited more diverse P-acquisition strategies in terms of root traits than grasses and sedge, while the responses of grasses to N addition were consistent with those observed in the field experiment.

4. Discussion

In the community-level field experiment, we found that N-induced P limitation under conditions of low soil P availability resulted in increased percentage of AMF colonisation and carboxylate release in the rhizosheath but decreased root length, SRL, and total root length colonised by AMF. In contrast, when soil P availability was high, N addition resulted in an increase in root diameter and APase activity but had no effect on carboxylate release or percentage of AMF colonisation, which partially supported our first hypothesis (Fig. **6**). In the species-level glasshouse experiment, we observed that grasses and sedge primarily increased the percentage of colonisation by AMF in response to N-induced P limitation, whereas forbs showed increased investment in almost all P-acquisition strategies, partially contradicting our second hypothesis. We also noted that although the root biomass of forbs in the glasshouse was much higher than that of grasses (and sedge), not only exceeded the biomass of grasses in the field 60% of the total biomass of the community (Table S1), but also was the number of forb individuals with larger individual biomass much lower than grass individuals. Therefore, we inferred that the roots of grasses dominated the mixed-root samples of community plants obtained in the field experiment. In addition, the response of the plant community P-acquisition strategy to N addition under low P conditions was consistent with that of grasses and sedge to N addition in the glasshouse, which suggested that differences in environmental conditions between the glasshouse and field did not mask the effects of fertilizer application on root attributes of single species related to P-acquisition. Although this approach ignores the allelopathy effect of single species in the community.

4.1 Plant response to N-induced P limitation at low soil P availability

Under low P level, plant functional traits change in response to N addition in two main processes. First, plant traits change as the soil becomes more saturated with N, followed

by changes in plant traits in response to increasing P limitation (Luo et al., 2022). Adequate N supply has been shown to suppress belowground biomass allocation to lateral roots and root hairs (Hermans et al., 2006; Jackon et al., 2008; Oldroyd & Leyser, 2020). Conversely, low P availability in the soil promotes the growth of root hair and lateral roots, resulting in increased total root biomass and root length (Williamson et al., 2001; Lambers et al., 2006; Desnos, 2008; Lambers, 2022). In our field experiment, we found that the effects of N-induced P limitation on root biomass and morphology within the plant community did not align with the changes expected under low P availability. Instead, they reflected the optimisation of root C costs under sufficient N supply (Figs. 1 and 2; Jackson et al., 2008). This finding contrasts with those from studies conducted in subtropical forests, where high N administration induces similar changes in root morphology as low P availability in the soil (Song et al., 2016). Changes in root morphology are considered to be C-dependent processes and do not constitute an effective strategy for P acquisition in alpine grassland with high P fixation rates compared to the forests with high rates of Po mineralisation (Olsson et al., 1998; Ryan et al., 2012; Ven et al., 2019). This is because the kinetic mechanism of available P uptake by the root system plays only a minor role in the acquisition of P (Lambers, 2022). In addition, the decrease in root biomass and length in the plant community could be related to the increased percentage of AMF colonisation (Jiang et al., 2018; Pang et al., 2023). The results from the glasshouse experiment showed that not all species responded in the same way to N addition, while the response of grass root biomass and structure to N addition mirrored that of the plant community in the field (Figs. 1 and 3; detailed discussion in 4.3). Our study site is dominated by resource-acquiring grasses, which invest conservatively in their root systems to reduce the cost of photosynthetic products (McCormack et al., 2012; Zheng et al., 2012).

Carboxylates are important constituents of root exudates, particularly under conditions of N-induced P limitation, as they mobilise both Pi and Po (He et al., 2020; Prescott et al., 2020; He et al., 2021; Li et al., 2022). Our community- and species-level

results confirm that N addition increases carboxylate release under conditions of low P availability in the rhizosheath. This may be attributed to carboxylate release being a self-protective strategy under P-limited conditions, where the rate of cell division and shoot growth decline while photosynthesis continues, resulting in excess leaf photosynthates (Prescott et al., 2020). Plants excrete these excess photosynthates in the form of carboxylates through the root system to prevent feedback inhibition and sustain normal photosynthesis (Trouvelot et al., 1986; Koerner, 2015). Previous studies have also found that P limitation enhances ammonium uptake and triggers the accumulation of the STOP1 protein, promoting carboxylate release (Li et al., 2022).

Common carboxylates in grassland ecosystems include malate, citrate, tartrate, succinate, oxalate, and malonate (Lambers et al., 2006; Gerke, 2015; Kidd et al., 2018; He et al., 2020; He et al., 2021). We identified acetate, formate, lactate, and propionate in this study as well (Table S8). At the community level, we observed that roots increased the release of nine carboxylates in response to N addition alone, with lactate being predominant. Notably, the type of carboxylates released by plants under P-limiting conditions can vary (Wen et al., 2022). In the glasshouse experiment, all species were capable of releasing 5 of the 10 carboxylates (oxalate, tartrate, lactate, citrate, and succinate), with increased amounts of all carboxylates except for oxalate in response to N addition compared to the control (Table S8; He et al., 2020). Previous research has associated tartrate and citrate with plant responses to P limitation and their role in soil P mobilisation (He et al., 2020; Lambers et al., 2006). Additionally, we found that malate was only detected in the rhizosheath of *P. anserina*, which released most types of carboxylates in larger quantities than the other species, possibly due to the unique morphology of its tubercle (Table S8; Wen et al., 2019).

In our field experiments, we found that N-induced P limitation increased the percentage of colonisation by AMF but decreased total root length colonised by AMF (Fig. 2). The increased percentage of root colonisation by AMF is a typical response for plants to P deficiency (Hsieh et al., 2009; Smith et al., 2011; Floss et al., 2013; Ryan et

al., 2016), as symbiotic associations with AMF are generally considered the optimal strategy for plants to acquire available P under P-limited conditions (Treseder, 2013; Raven et al., 2018; Ven et al., 2019). However, several meta-analyses and field research have shown that N addition alone can reduce the percentage of AMF colonisation (Treseder, 2004; Li et al., 2015; Jiang et al., 2018; Pan et al., 2020). It is important to note that the reduction in AMF colonisation level was frequently attributed to soil acidification or alterations in plant community composition, with little consideration given to changes in species P-acquisition strategies (Mueller & Harrison, 2019; Ven et al., 2019; Oldroyd & Leyser, 2020). In the glasshouse experiment, grasses exhibited a significant increase in the percentage of colonisation by AMF and a decrease in the total root length colonised in response to N addition, consistent with the findings from the field experiment. In contrast to grasses, we found that N increased the total root length colonised of forbs, likely due to increased root biomass and length distribution (Figs. 3 and 4). We did not observe AMF colonisation among *K. humilis* roots, which aligns with previous research suggesting that although sedges seem to be readily colonised by AMF in Tibetan grasslands, no AMF were observed in any of the *K. humilis* ecotypes, whereby sedge roots are seldom mycorrhizal (Gai et al., 2006; Brundrett, 2009). Both field and glasshouse studies have shown that N addition alone has no significant effect on AMF abundance in the soil (expressed as soil PLFA concentrations, Table S4; Fig. S3). These results also confirm that N addition alone does not reduce plant investment in AMF, which is due to P limitation compensating for the reduced allocation of photosynthetic products from the plant to the root system caused by N addition (Barceló et al., 2020).

4.2 Plant response to increased P demand under high level of both N and P

The increase in root biomass and diameter was not due to root remodelling as a result of P limitation but rather because of suitable conditions with adequate N and P levels; thus, the root system grows along with the shoot (Chapin, 1980), which indirectly

increases the area of the plant–soil interface and facilitates the acquisition of available P.

In contrast to the increased release of carboxylates under N-induced P limitation, the release of carboxylates was inhibited under conditions with sufficient P. We also found that N addition enhanced APase activity in the rhizosheath at both high and low P availability (Figs. 2 and 4). This is consistent with the findings of He et al. (2020) and Schleuss et al. (2020), which indicated that under conditions of P limitation, plants use additional N to produce phosphatases to mineralise soil organic P.

The plant–AMF symbiotic association was inhibited by high nutrient conditions. Even though N increases plant demand for P, it can be found from leaf N:P that the main limiting nutrient for the plant is still N (Tables. 2 and S6). Below the P limitation threshold, plants can maximise short-term P uptake in response to P demand and may not decrease C allocation for P-acquisition (Luo et al., 2022), particularly through symbiosis with AMF (Ven et al., 2019). Our results showed that AMF abundance in soil (soil PLFA content) decreased with both N and P addition (Fig. S3), suggesting that the plants reduced the supply of photosynthetic C to AMF when nutrient level are adequate (Johnson, 2010; Grman, 2012). Therefore, we inferred that, under high P level, plants could use the gradual accumulation of N as an efficient strategy for P acquisition without needing to consume photosynthetic products.

4.3 Trade-offs between root traits and AMF symbiosis among different species

Our findings indicate that changes in root morphology, exudate composition and symbiosis with AMF do not respond uniformly to N addition at low P availability and based on the distinct clusters of species responses (Fig. **5**), the results suggest a trade-off between investment in root morphology and AMF colonisation (Smilauerova, 2001; Shen et al., 2011; Ostonen et al., 2011). N addition attenuate the N-dominated nutrient limitation and result in plants requiring fewer roots for nutrient uptake than those without fertilisation (Muller et al., 2000; Hermans et al., 2006; Lu et al., 2011). Under

P-limiting conditions, photosynthetic C is a valuable resource to mediate the costs of plant P-acquisition strategies (Noë & Kiers, 2018). Grasses (*S. aliena*, *E. nutans*, *P. pratensis*, and *F. rubra*) are resource-acquiring plants that outcompete smaller plants for light resources (Fig. **S4**; Hautier et al., 2009; Zheng et al., 2012). Compared to grasses, forbs (*A. diplostephioides*, *P. anserina*, and *S. pulchra*) are resource-conservative plants that compete for belowground nutrients (Zheng et al., 2012). Therefore, under conditions of P limitation, grasses need to allocate limited photosynthetic C to the most efficient pathway for P acquisition, with AMF colonisation showing the greatest return on investment (Noë & Kiers, 2018; Ven et al., 2019; Prescott et al., 2020; Bennett & Groten, 2022).

In contrast, resource-conservative plants have an abundance of belowground C stores, so they invest in most P-acquisition strategies under P-limited conditions. Compared with those in grasses, root biomass and length, as well as carboxylate release and APase activity were higher in forbs under the N-induced P limitation condition, reflecting the advantage of forbs in nutrient competition.

5. Conclusions

In this study, we elucidated potential mechanisms underlying the changes in plant community- and species-level P-acquisition strategies with altered nutrient supply, and herein, highlight the functional group-specific effects. Our findings have demonstrated that the change in P-acquisition strategies of alpine grassland community and dominant species in response to N addition depends on soil P availability (Fig. 6). Grasses prioritise efficient P acquisition through AMF colonisation, while forbs invest in diverse P-acquisition strategies. This also reflects the fact that not all plant species in alpine grassland plant communities exhibit the full range of P-acquisition strategies under P limitation, but rather the most efficient will be selected based on the limited C source. However, neither in the field nor in the glasshouse did we consider changes in plant communities and species during root growth and AMF infestation on different time

scales, which would also be important for estimating the functional response of grassland communities. Future studies should assess how nutrient enrichment affects the structure of plant communities and the long-term performance of different functional groups to better understand plant succession and the adaptation of alpine ecosystems to global change.

Acknowledgments

We appreciate the constructive comments from Dr Liang-Dong Guo from the Institute of Microbiology, Chinese Academy of Sciences, and Dr Shengjing Jiang from Lanzhou University on the manuscript. This work was conducted at the Haibei National Field Research Station of Alpine Grassland Ecosystem, managed by the Northwest Institute of Plateau Biology, Chinese Academy of Sciences. This study was financially supported by the National Natural Science Foundation of China (Grants: 32192461, 32130065, 42007078) and the Top Leading Talents Program of Gansu Province (No. 842016). The authors declare no competing interests.

Author's contributions

Z-H.G. and J-S.H. designed the study; Z-H.G. performed the field and laboratory work; Z-H.G. and Z.C. analysed the data; Z-H.G. and Z.C. wrote the manuscript with extensive discussion with X.L. and J-S.H., and critical input from all authors.

Declaration of competing interest

The authors declare that they have no known competing financial interests or personal relationships that could have appeared to influence the work reported in this paper.

Data availability statement

The data that support the findings of this study will be openly available in the Figshare digital repository.

References

Barceló, M., van Bodegom, P. M., Tedersoo, L., den Haan, N., Veen, G. F. (Ciska), Ostonen, I., Trimbos, K., & Soudzilovskaia, N. A. 2020. The abundance of arbuscular mycorrhiza in soils is linked to the total length of roots colonized at ecosystem level. PLOS ONE 15(9), e0237256.

Baumann, F., He, J-S., Schmidt, K., Kühn, P., Scholten, T., 2009. Pedogenesis, permafrost, and soil moisture as controlling factors for soil nitrogen and carbon contents across the Tibetan Plateau. Global Change Biology 15, 3001–3017.

Bennett, A.E., Groten, K., 2022. The Costs and Benefits of Plant–Arbuscular Mycorrhizal Fungal Interactions. Annual Review of Plant Biology 73, 649–672.

Blank, R.R., Derner, J.D., 2004. Effects of CO_2 enrichment on plant–soil relationships of Lepidium latifolium. Plant and Soil 262, 159–167.

Brundrett, M.C. 2009. Mycorrhizal Associations and Other Means of Nutrition of Vascular Plants: Understanding the Global Diversity of Host Plants by Resolving Conflicting Information and Developing Reliable Means of Diagnosis. Plant Soil 320, 37–77.

Cawthray, G.R., 2003. An improved reversed-phase liquid chromatographic method for the analysis of low-molecular mass organic acids in plant root exudates. Journal of Chromatography A 1011, 233–240.

Chapin, F.S., 1980. The mineral-nutrition of wild plants. Annual Review of Ecology and Systematics 11, 233–260.

Chen, Q., Yuan, Y., Hu, Y., Wang, J., Si, G., Xu, R., Zhou, J., Xi, C., Hu, A., Zhang, G., 2021. Excessive nitrogen addition accelerates N assimilation and P utilization by enhancing organic carbon decomposition in a Tibetan alpine steppe. Science of the Total Environment 764, 142848.

Chen, J.B., Dong, C.C., Yao, X.D., Wang, W., 2018. Effects of nitrogen addition on

plant biomass and tissue elemental content in different degradation stages of temperate steppe in northern China. Journal of Plant Ecology 11, 730–739.

Chinese Soil Taxonomy Research Group, 1995. Chinese soil taxonomy. Science Press, Beijing. pp. 58–147.

DeMalach, N., 2018. Toward a mechanistic understanding of the effects of nitrogen and phosphorus additions on grassland diversity. Perspectives in Plant Ecology, Evolution and Systematics 32, 65–72.

Dentener, F., Drevet, J., Lamarque, J.F., Bey, I., Eickhout, B., Fiore, A.M., Hauglustaine, D., Horowitz, L.W., Krol, M., Kulshrestha, U. C., Lawrence, M., Galy-Lacaux, C., Rast, S., Shindell, D., Stevenson, D., Van Noije, T., Atherton, C., Bell, N., Bergman, D., Butler, T., Cofala, J., Collins, B., Doherty, R., Ellingsen, K., Galloway, J., Gauss, M., Montanaro, V., Müller, J. F., Pitari, G., Rodriguez, J., Sanderson, M., Solmon, F., Strahan, S., Schultz, M., Sudo, K., Szopa, S., Wild O., 2006. Nitrogen and sulfur deposition on regional and global scales: A multimodel evaluation. Global Biogeochemical Cycles 20, GB4003.

Desnos, T., 2008. Root branching responses to phosphate and nitrate. Current Opinion in Plant Biology 11, 82–87.

Ding, W., Cong, W-F., Lambers, H., 2021. Plant phosphorus-acquisition and -use strategies affect soil carbon cycling. Trends in Ecology & Evolution 36, 899–906.

Floss, D.S., Levy, J.G., Levesque–Tremblay, V., Pumplin, N., Harrison, M.J., 2013. DELLA proteins regulate arbuscule formation in arbuscular mycorrhizal symbiosis. Proceedings of the National Academy of Sciences of the United States of America 110, E5025–E5034.

Gahoonia, T.S., Raza, S., Nielsen, N.E., 1994. Phosphorus depletion in the rhizospohere as influenced by soil moisture. Plant and Soil 159, 213-218.

Gai, J.P., Christie, P., Feng, G., Li, X.L., 2006. Twenty years of research on community

composition and species distribution of arbuscular mycorrhizal fungi in China: a review. Mycorrhiza 16, 229–239

Gao, X-L., Li, X.G., Zhao. L., Kuzyakov, Y., 2019. Regulation of soil phosphorus cycling in grasslands by shrubs. Soil Biology and Biochemistry 133, 1–11.

Gerke, J., 2015. The acquisition of phosphate by higher plants: Effect of carboxylate release by the roots. A critical review. Journal of Plant Nutrition and Soil Science 178, 351–364.

Grman, E., 2012. Plant species differ in their ability to reduce allocation to non-beneficial arbuscular mycorrhizal fungi. Ecology 93, 711-718.

Grman, E., Robinson, T.M.P., 2013. Resource availability and imbalance affect plant-mycorrhizal interactions: a field test of three hypotheses. Ecology 94, 62–71.

Han, Y., Dong, S., Zhao, Z., Sha, W., Li, S., Shen, H., Xiao, J., Zhang, J., Wu, X., Jiang, X., Zhao, J., Liu, S., Dong, Q., Zhou, H., Jane C, Y., 2019. Response of soil nutrients and stoichiometry to elevated nitrogen deposition in alpine grassland on the Qinghai–Tibetan Plateau. Geoderma 343, 263–268.

Hautier, Y., Niklaus, P.A., Hector, A., 2009. Competition for light causes plant biodiversity loss after eutrophication. Science 324, 636–638.

He, H., Wu, M., Guo, L., Fan, C., Zhang, Z., Su, R., Peng, Q., Pang, J., Lambers, H., 2020. Release of tartrate as a major carboxylate by alfalfa (Medicago sativa L.) under phosphorus deficiency and the effect of soil nitrogen supply. Plant and Soil 449, 169–178.

He, H., Zhang, Z., Peng, Q., Chang, C., Su, R., Cheng, X., Li, Y., Pang, J., Du, S., Lambers, H., 2021. Increasing nitrogen supply to phosphorus-deficient Medicago sativa decreases shoot growth and enhances root exudation of tartrate to discharge surplus carbon dependent on nitrogen form. Plant and Soil 469, 193–211.

Hermans, C., Hammond, J.P., White, P.J., Verbruggen, N., 2006. How do plants respond

to nutrient shortages by biomass allocation? Trends in Plant Science 11, 610–617.

Hopkins, D. W., Sparrow, A. D., Shillam, L. L., English, L. C., Dennis, P. G., Novis, P., Elberling, B., Gregorich, E. G., & Greenfield, L. G. (2008). Enzymatic activities and microbial communities in an Antarctic dry valley soil: Responses to C and N supplementation. Soil Biology and Biochemistry, 40(9), 2130–2136.

Hsieh, L.C., Lin, S., Shih, AC–C., Chen, J., Lin, W., Tseng, C, Li, W, Chiou, T., 2009. Uncovering Small RNA–Mediated Responses to Phosphate Deficiency in Arabidopsis by Deep Sequencing. Plant Physiology 151, 2120–2132.

Jackson, L.E., Burger, M., Cavagnaro, T.R. 2008. Roots nitrogen transformations and ecosystem services. Annual Review of Plant Biology, 341-363.

Jia, Y., Yu, G., He, N., Zhan, X., Fang, H., Sheng, W., Zuo, Y., Zhang, D., Wang, Q., 2014. Spatial and decadal variations in inorganic nitrogen wet deposition in China induced by human activity. Scientific Reports 4, 3763.

Jiang, S., Liu, Y., Luo, J., Qin, M., Johnson, N.C., Opik, M., Vasar, M., Chai, Y., Zhou, X., Mao, L., Du, G., An, L., Feng, H., 2018. Dynamics of arbuscular mycorrhizal fungal community structure and functioning along a nitrogen enrichment gradient in an alpine meadow ecosystem. New Phytologist 220, 1222–1235.

Johnson, N.C., 2010. Resource stoichiometry elucidates the structure and function of arbuscular mycorrhizas across scales. New Phytologist 185, 631–647.

Kidd, D.R., Ryan, M.H., Hahne, D., Haling, R.E., Lambers, H., Sandral, G.A., Simpson, R.J., Cawthray, G.R., 2018. The carboxylate composition of rhizosheath and root exudates from twelve species of grassland and crop legumes with special reference to the occurrence of citramalate. Plant and Soil 424, 389–403.

Koerner, C., 2015. Paradigm shift in plant growth control. Current Opinion in Plant Biology 25, 107–114.

Kourtev, P.S., Ehrenfeld, J.G., Häggblom, M., 2002. Exotic plant species alter the

microbial community structure and function in the soil. Ecology 83, 3152–3166.

Lambers, H., 2022. Phosphorus acquisition and utilization in plants. Annual Review of Plant Biology 73, 17–42.

Lambers, H., Albornoz, F., Lukasz, L., Laliberté, E., Ranathunge, K., Teste, F.P., Zemunik, G., 2018. How belowground interactions contribute to the coexistence of mycorrhizal and non-mycorrhizal species in severely phosphorus-impoverished hyperdiverse ecosystems. Plant and Soil 424, 11–33.

Lambers, H., Shane, M.W., Cramer, M.D., Pearse, S.J., Veneklaas, E.J., 2006. Root structure and functioning for efficient acquisition of phosphorus: matching morphological and physiological traits. Annals of Botany 98, 693–713.

Li, W., Jin, C., Guan, D., Wang, Q., Wang, A., Yuan, F., Wu, J., 2015. The effects of simulated nitrogen deposition on plant root traits: A meta-analysis. Soil Biology and Biochemistry 82, 112–118.

Li, Y., Niu, S., Yu, G., 2016. Aggravated phosphorus limitation on biomass production under increasing nitrogen loading: a meta-analysis. Global Change Biology 22, 934–943.

Li, Y., Li, Y., Yao, X., Wen, Y., Zhou, Z., Lei, W., Zhang, D., Lin, H., 2022. Nitrogen-inducible GLK1 modulates phosphate starvation response via the PHR1-dependent pathway. New Phytologist 236, 1871–1887.

Liu, B., Li, H., Li, H., Zhang, A., Zed, R., 2021. Long-term biochar application promotes rice productivity by regulating root dynamic development and reducing nitrogen leaching. Global Change Biology Bioenergy 13, 257–268.

Liu, H., Mi, Z., Lin, L., Wang, Y., Zhang, Z., Zhang, F., Wang, H., Liu, L., Zhu, B., Cao, G., Zhao, X., Sanders, N.J., Classen, A.T., Reich, P.B., He, J-S., 2018. Shifting plant species composition in response to climate change stabilizes grassland primary production. Proceedings of the National Academy of Sciences 115,

4051–4056.

Liu, Y., Xu, R., Wang, Y., Pan, Y., Piao, S., 2015. Wet deposition of atmospheric inorganic nitrogen at five remote stations on the Tibetan plateau. Atmospheric Chemistry and Physics 15, 17491–17526.

Lu, M., Yang, Y., Luo, Y., Fang, C., Zhou, X., Chen, J., Yang, X., Li, B., 2011. Responses of ecosystem nitrogen cycle to nitrogen addition: a meta-analysis. New Phytologist 189, 1040–1050.

Luo, M., Moorhead, D.L., Ochoa-Hueso, R., Mueller, C.W., Ying, S.C., Chen, J., 2022. Nitrogen loading enhances phosphorus limitation in terrestrial ecosystems with implications for soil carbon cycling. Functional Ecology 36, 2845-2858.

Lü, C., Tian, H., 2007. Spatial and temporal patterns of nitrogen deposition in China: Synthesis of observational data. Journal of Geophysical Research 112, D22S05.

Lü, X., Reed, S., Yu, Q., He, N., Wang, Z., Han, X., 2013. Convergent responses of nitrogen and phosphorus resorption to nitrogen inputs in a semiarid grassland. Global Change Biology 19, 2775–2784.

Lynch, J.P., Ho, M.D., 2005. Rhizoeconomics: Carbon costs of phosphorus acquisition. Plant and Soil 269, 45–56.

McCormack, M.L., Adams, T.S., Smithwick, E.A., Eissenstat, D.M., 2012. Predicting fine root lifespan from plant functional traits in temperate trees. New Phytologist 195, 823–831.

Muller, I., Schmid, B., Weiner, J., 2000. The effect of nutrient availability on biomass allocation patterns in 27 species of herbaceous plants. Perspectives in Plant Ecology Evolution and Systematics 3, 115–127.

Müller, M., Oelmann, Y., Schickhoff, U., Böhner, J., Scholten, T., 2017. Himalayan treeline soil and foliar C: N:P stoichiometry indicate nutrient shortage with elevation. Geoderma 291, 21–32.

Neumann G. 2006. Quantitative determination of acid phosphatase activity in the rhizosphere and on the root surface. In: J Luster, R Finlay, eds. Handbook of methods used in rhizosphere research. Birmensdorf, Switzerland: Swiss Federal Research Institute WSL: 426–427.

Niederberge, J., Todt, B., Boča, A., Nitschke, R., Kohler, M., Kühn, P., Bauhus, J., 2015. Use of near-infrared spectroscopy to assess phosphorus fractions of different plant availability in forest soils. Biogeosciences 12, 3415–3428.

Noë, R., Kiers, E.T., 2018. Mycorrhizal Markets, firms, and co-ops. Trends in Ecology & Evolution 33, 777–789.

Oldroyd, G.E.D., Leyser, O., 2020. A plant's diet, surviving in a variable nutrient environment. Science 368, eaba0196.

Olsson, P.A., Francis, R., Read, D.J., Soderstrom, B., 1998. Growth of arbuscular mycorrhizal mycelium in calcareous dune sand and its interaction with other soil microorganisms as estimated by measurement of specific fatty acids. Plant and Soil 201, 9-16.

Ostonen, I., Helmisaari, H-S., Borken, W., Tedersoo, L., Kukumaegi, M., Bahram, M., Lindroos, A-J., Nojd, P., Uri, V., Merila, P., Asi, E., Lõhmus, K., 2011. Fine root foraging strategies in Norway spruce forests across a European climate gradient. Global Change Biology 17, 3620–3632.

Pan, S., Wang, Y., Qiu, Y., Chen, D., Zhang, L., Ye, C., Guo, H., Zhu, W., Chen, A., Xu, G., Zhang, Y., Bai, Y., Hu, S., 2020. Nitrogen-induced acidification, not N-nutrient, dominates suppressive N effects on arbuscular mycorrhizal fungi. Global Change Biology 26, 6568-6580.

Pang, J., Ryan, M., Siddique, K., & Simpson, R., 2017. Unwrapping the rhizosheath. Plant and Soil 418, 129–139.

Pang, J., Wen, Z., Kidd, D., Ryan, M., Yu, R., Li, L., Cong, W., Siddique, K., and

Lambers, H., 2021. Advances in Understanding Plant Root Uptake of Phosphorus. Gregory, P. (ed.), Understanding and improving crop root function, Burleigh Dodds Science Publishing, Cambridge, UK.

Pang, J., Ryan, M. H., Wen, Z., Lambers, H., Liu, Y., Zhang, Y., Guillaume Tueux, Jenkins, S., Mickan, B., WS Wong, Wan, J., & Siddique, K. H. M. 2023. Enhanced nodulation and phosphorus acquisition from sparingly-soluble iron phosphate upon treatment with arbuscular mycorrhizal fungi in chickpea. Physiologia Plantarum 175(2).

Pätzold, S., Hejcman, M., Barej, J., Schellberg, J., 2013. Soil phosphorus fractions after seven decades of fertilizer application in the Rengen Grassland Experiment. Journal of Plant Nutrition and Soil Science. 176, 910–920.

Pearse, S.J., Veneklaas, E.J., Cawthray, G., Bolland, M.D., Lambers, H., 2007. Carboxylate composition of root exudates does not relate consistently to a crop species' ability to use phosphorus from aluminium, iron or calcium phosphate sources. New Phytologist 173, 181–190.

Phillips, J.M., Hayman, D.S., 1970. Improved procedures for clearing roots and staining parasitic and vesicular–arbuscular mycorrhizal fungi for rapid assessment of infection. Transactions of British Mycological Society 55, 158–161.

Phoenix, G.K., Booth, R.E., Leake, J.R., Read, D.J., Grime, J.P., Lee, J.A., 2004. Simulated pollutant nitrogen deposition increases P demand and enhances root-surface phosphatase activities of three plant functional types in a calcareous grassland. New Phytologist 161: 279–289.

Pregitzer, K.S., Hendrick, R.L., Fogel, R., 1993. The demography of fine roots in response to patches of water and nitrogen. New Phytologist 125, 575–580.

Prescott, C.E., Grayston, S.J., Helmisaari, H-S., Kastovska, E., Körner, C., Lambers, H., Meier, I.C., Millard, P., Ostonen, I., 2020. Surplus carbon drives allocation

and plant–soil interactions. Trends in Ecology & Evolution 35, 1110–1118.

Raven, J.A., Lambers, H., Smith, S.E., Westoby, M., 2018. Costs of acquiring phosphorus by vascular land plants: patterns and implications for plant coexistence. New Phytologist 217, 1420-1427.

Ryan, M.H., Tibbett, M., Edmonds-Tibbett, T., Suriyagoda, L.D., Lambers, H., Cawthray, G.R., Pang, J., 2012. Carbon trading for phosphorus gain: the balance between rhizosphere carboxylates and arbuscular mycorrhizal symbiosis in plant phosphorus acquisition. Plant, Cell & Environment 35, 2170-2180.

Ren, F., Yang, X., Zhou, H., Zhu, W., Zhang, Z., Chen, L., Cao, G., He, J-S., 2017. Contrasting effects of nitrogen and phosphorus addition on soil respiration in an alpine grassland on the Qinghai-Tibetan Plateau. Scientific Reports 6, 34786.

Rui, Y., Wang, S., Xu, Z., Wang, Y., Chen, C., Zhou, X., Kang, X., Lu, S., Hu, Y., Lin, Q., Luo, C., 2011. Warming and grazing affect soil labile carbon and nitrogen pools differently in an alpine meadow of the Qinghai–Tibet Plateau in China. Journal of Soils and Sediments 11, 903–914.

Schleuss, P.M., Widdig, M., Heintz-Buschart, A., Kirkman, K., Spohn, M., 2020. Interactions of nitrogen and phosphorus cycling promote P acquisition and explain synergistic plant-growth responses. Ecology 101, e03003.

Shen, J., Yuan, L., Zhang, J., Li, H., Bai, Z., Chen, X., Zhang, W., Zhang, F., 2011. Phosphorus dynamics: from soil to plant. Plant Physiology 156, 997-1005.

Smilauerova, M., 2001. Plant root response to heterogeneity of soil resources: Effects of nutrient patches, AM symbiosis, and species composition. Folia Geobotanica 36, 337-351.

Song, P., Zhang, R., Zhang, Y., Zhou, Z-C., Feng, Z-P., 2016. Effects of simulated nitrogen deposition on fine root morphology, nitrogen and phosphorus efficiency of Pinus massoniana clone under phosphorus deficiency. Chinese Journal of Plant

Ecology 40, 1136–1144.

Toth, R., Miller, R. J., Jarstfer, A. G., Alexander, T. K., Bennett, E. 1991. The Calculation of Intraradical Fungal Biomass from Percent Colonization in Vesicular-Arbuscular Mycorrhizae. Mycologia, 83, 553–553.

Treseder, K.K., 2004. A meta-analysis of mycorrhizal responses to nitrogen, phosphorus, and atmospheric CO_2 in field studies. New Phytologist 164, 347–355.

Treseder, K.K., 2013. The extent of mycorrhizal colonization of roots and its influence on plant growth and phosphorus content. Plant and Soil 371, 1–13.

Trouvelot, A., Kough, J.L., Gianinazzi-Pearson, V., 1986. Mesure du taux de mycorhizationVA d'un systyeme radiculaire. Recherche de methodes d'estimation ayant une signification fonctionnelle. In: GianinazziPearson V, Gianinazzi S, eds. Physiological and genetical aspects of mycorrhizae. Paris, France: INRA Press, pp. 217–221.

Vance, C.P., Uhde-Stone, C., Allan, D.L., 2003. Phosphorus acquisition and use: critical adaptations by plants for securing a nonrenewable resource. New Phytologist 157, 423–447.

Ven, A., Verlinden, M.S., Verbruggen, E., Vicca, S., 2019. Experimental evidence that phosphorus fertilization and arbuscular mycorrhizal symbiosis can reduce the carbon cost of phosphorus uptake. Functional Ecology 33, 2215–2225.

Wan, L.-Y., Qi, S., Zou, C. B., Dai, Z.-C., Ren Guangqian, Chen, Q., Zhu, B., & Zou, C. B., 2019. Elevated nitrogen deposition may advance invasive weed, Solidago canadensis, in calcareous soils. Journal of Plant Ecology 12(5), 846–856.

Wang, D., He, H., Gao, Q., Zhao, C., Zhao, W., Yin, C., Chen, X., Ma, Z., Li, D., Sun, D., Cheng, X., Liu, Q., 2017. Effects of short-term N addition on plant biomass allocation and C and N pools of the Sibiraea angustata scrub ecosystem. European

Journal of Soil Science 68, 212–220.

Wen, Z., Li, H., Shen, Q., Tang, X., Xiong, C., Li, H., Pang, J., Ryan, M.H., Lambers, H., Shen, J., 2019. Trade-offs among root morphology, exudation and mycorrhizal symbioses for phosphorus-acquisition strategies of 16 crop species. New Phytologist 223, 882–895.

Wen, Z., White, P.J., Shen, J., Lambers, H., 2022. Linking root exudation to belowground economic traits for resource acquisition. New Phytologist 233, 1620–1635.

Williamson, L.C., Ribrioux, S., Fitter, A.H., Leyser, H.M.O., 2001. Phosphate availability regulates root system architecture in Arabidopsis. Plant Physiology 126, 875–882.

Wrb, World Reference Base for Soil Resources, 2014 (update 2015). International soil classification system for naming soils and creating legends for soil maps. FAO/ISRIC/ISSS, Rome.

Wurzburger, N., Wright, S.J., 2015. Fine-root responses to fertilization reveal multiple nutrient limitation in a lowland tropical forest. Ecology 96, 2137–2146.

Xie, L., Wang, L., Pang, X., Liu, Q., Yin, C., 2021. Effects of soil water regime and nitrogen addition on ectomycorrhizal community structure of Picea asperata seedlings. Journal of Plant Nutrition and Soil Science 184, 415–429.

Yan, C., Yuan, Z., Liu, Z., Zhang, J., Liu, K., Shi, X., Lock, T.R., Kallenbach, R.L., 2021. Aridity stimulates responses of root production and turnover to warming but suppresses the responses to nitrogen addition in temperate grasslands of northern China. Science of the Total Environment 753, 10.

You, C., Wu, F., Gan, Y., Yang, W., Hu, Z., Xu, Z., Tan, B., Liu, L., Ni, X., 2017. Grass and forbs respond differently to nitrogen addition: a meta-analysis of global grassland ecosystems. Scientific Reports 7, 1563.

Yu, R., Li, X., Xiao, Z., Lambers, H., Li, L., 2020. Phosphorus facilitation and covariation of root traits in steppe species. New Phytologist 226, 1285–1298.

Zhang, D., Zhang, C., Tang, X., Li, H., Zhang, F., Rengel, Z., Whalley, W. R., Davies, W. J., & Shen, J. (2015). Increased soil phosphorus availability induced by faba bean root exudation stimulates root growth and phosphorus uptake in neighbouring maize. New Phytologist, 209(2), 823–831.

Zhao, Q., Zeng, D.H., 2019. Nitrogen addition effects on tree growth and soil properties mediated by soil phosphorus availability and tree species identity. Forest Ecology and Management 449, 117478.

Zheng, S., Ren, H., Li, W., Lan, Z., 2012. Scale-dependent effects of grazing on plant C: N: P stoichiometry and linkages to ecosystem functioning in the Inner Mongolia grassland. Plos One 7, e51750.

Zheng, Z., Bai, W., & Zhang, W.-H. (2019). Root trait-mediated belowground competition and community composition of a temperate steppe under nitrogen enrichment. Plant and Soil, 437(1-2), 341–354.

Zhou, J., Li, X-L., Peng, F., Li, C., Lai, C., You, Q., Xue, X., Wu, Y., Sun, H., Chen, Y., Zhong, H., Lambers, H., 2021. Mobilization of soil phosphate after 8 years of warming is linked to plant phosphorus-acquisition strategies in an alpine meadow on the Qinghai-Tibetan Plateau. Global Change Biology 27, 6578–6591.

Zhu, Y.G., Cavagnaro, T., Smith, S.E., Dickson, S., 2001. Backseat driving? Accessing phosphate beyond the rhizosphere-depletion zone. Trends in Plant Science 6, 194–195.

Figure Legends

Fig. 1. Root biomass and morphology (root length, diameter, and specific root length) under different nitrogen (N) and phosphorus (P) levels in the field. (**a**) Root biomass, (**b**) root length, (**c**) root diameter, and (**d**) specific root length. All indexes were influenced by the significant interaction between N and P addition ($P < 0.05$, Table S4). Lowercase letters indicate that means vary among fertiliser treatments ($P < 0.05$). Data are presented as the mean (+ SE) of six replicates. P0: without P addition; P+: with P addition; N0: without N addition; N+: with N addition.

Fig. 2. Rhizosheath exudate (acid phosphatase [APase] and carboxylates), colonisation rate by arbuscular mycorrhizal fungi (AMF), and AMF phospholipid fatty acid (PLFA) concentration under different N and P levels in the field experiment. (**a**) APase, (**b**) carboxylates, (**c**) colonisation rate by AMF, and (**d**) total root length colonised by AMF. All indexes (except APase) were influenced by the significant interaction between N and P addition ($P < 0.05$, Table S4). Lowercase letters indicate that means vary among fertiliser treatments ($P < 0.05$). Data are presented as the mean (+ SE) of six replicates. P0: without P addition; P+: with P addition; N0: without N addition; N+: with N addition.

Fig. 3. Changes in root morphology under different nitrogen (N) and phosphorus (P) levels between species in the glasshouse experiment. (**a**) Root biomass without P addition, (**b**) root biomass with P addition, (**c**) root length without P addition, (**d**) root length with P addition, (**e**) root diameter without P addition, (**f**) root diameter with P addition, (**g**) specific root length without P addition, and (**h**) specific root length with P addition. Diagonal stripes indicate N addition. Data are presented as the mean (+ SE) of four replicates.

Fig. 4. Changes in root exudate (acid phosphatase [APase] and carboxylates) concentrations, arbuscular mycorrhizal fungi (AMF) colonisation rate, and the total root length colonised by AMF under different nitrogen (N) and phosphorus (P) levels

between species in the glasshouse experiment. (**a**) Acid phosphatase without P addition, (**b**) acid phosphatase with P addition, (**c**) carboxylates without P addition, (**d**) carboxylates with P addition, (**e**) colonisation rate by AMF without P addition, (**f**) colonisation rate by AMF with P addition, (**g**) total root length colonised without P addition, and (**h**) total root length colonised with P addition. Diagonal stripes indicate N addition. Data are presented as the mean (+ SE) of four replicates.

Fig. 5. Hierarchical cluster analysis between different functional groups (purple: grasses; pink: sedge; grey: forbs) and indicators with nitrogen addition alone. The size of the circle represents the strength of association. Abbreviations: SRL = specific root length.

Fig. 6. Simplified framework of changes in plant phosphorus (P)-acquisition strategies in response to nitrogen (N) addition under different soil P levels. Blue dashed boxes indicate the dominant P effects, grey dashed boxes indicate the dominant N effects, and black thin dashed boxes indicate changes in functional groups. Small arrows represent an increase (red arrows) and a decrease (blue arrows) in the variables with N addition. Abbreviations: AMF = arbuscular mycorrhizal fungi.

Fig. 1.

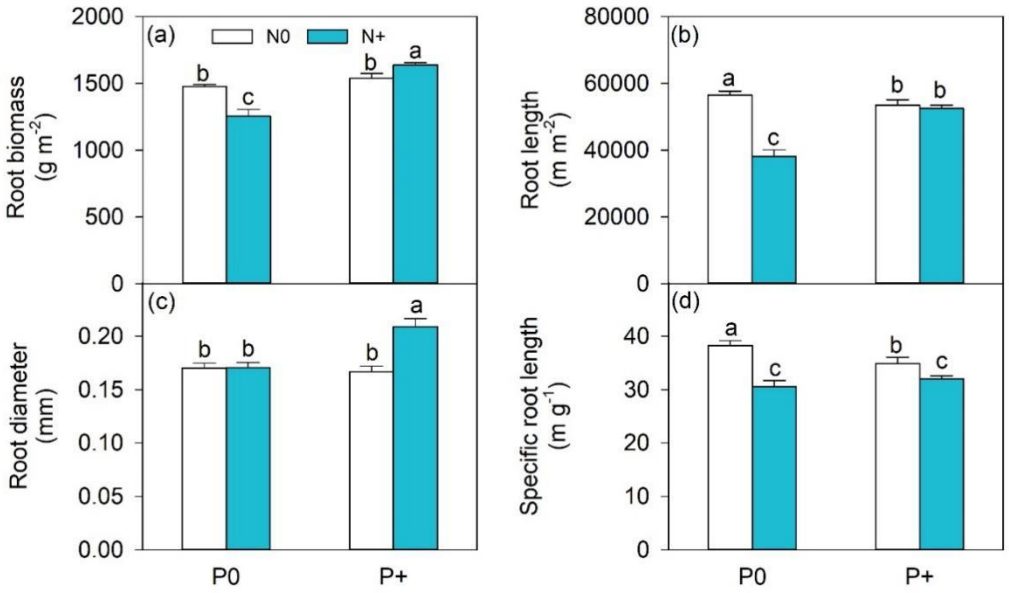
(a)
N0
N+
Root biomass (g m-2)
2000
1500
1000
500
0
b
c
b
a
(b)
Root length (m m-2)
80000
60000
40000
20000
0
a
c
b
b
(c)
Root diameter (mm)
0.20
0.15
0.10
0.05
0.00
b
b
b
a
(d)
Specific root length (m g-1)
40
30
20
10
0
a
c
b
c
P0
P+

Fig. 2.

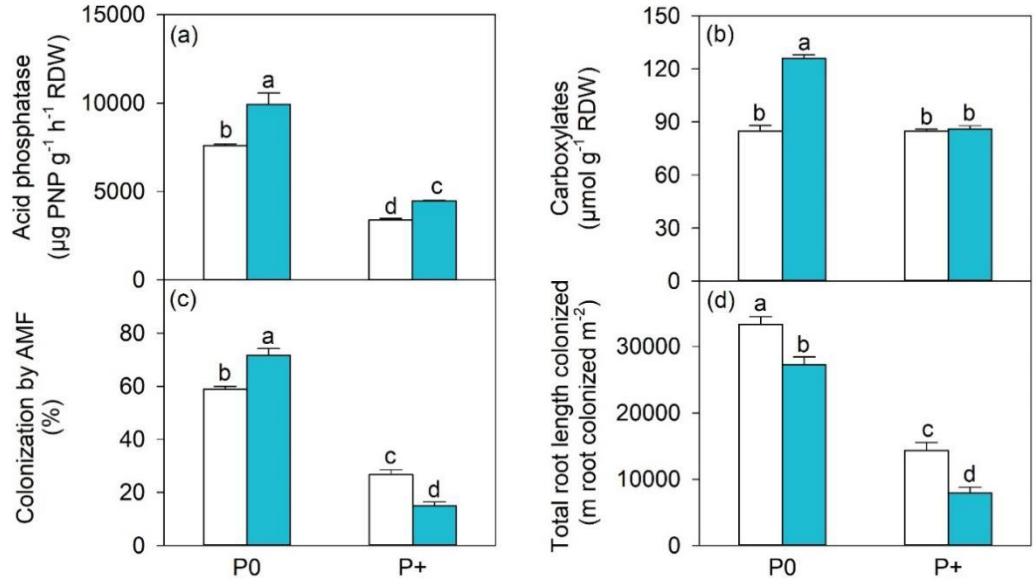
(a)
Acid phosphatase (µg PNP g-1 h-1 RDW)
15000
10000
5000
0
b
a
d
c
(b)
Carboxylates (µmol g-1 RDW)
150
120
90
60
30
0
b
a
b
b
(c)
Colonization by AMF (%)
80
60
40
20
0
b
a
c
d
(d)
Total root length colonized (m root colonized m-2)
30000
20000
10000
0
a
b
c
d
P0
P+

Fig. 3.

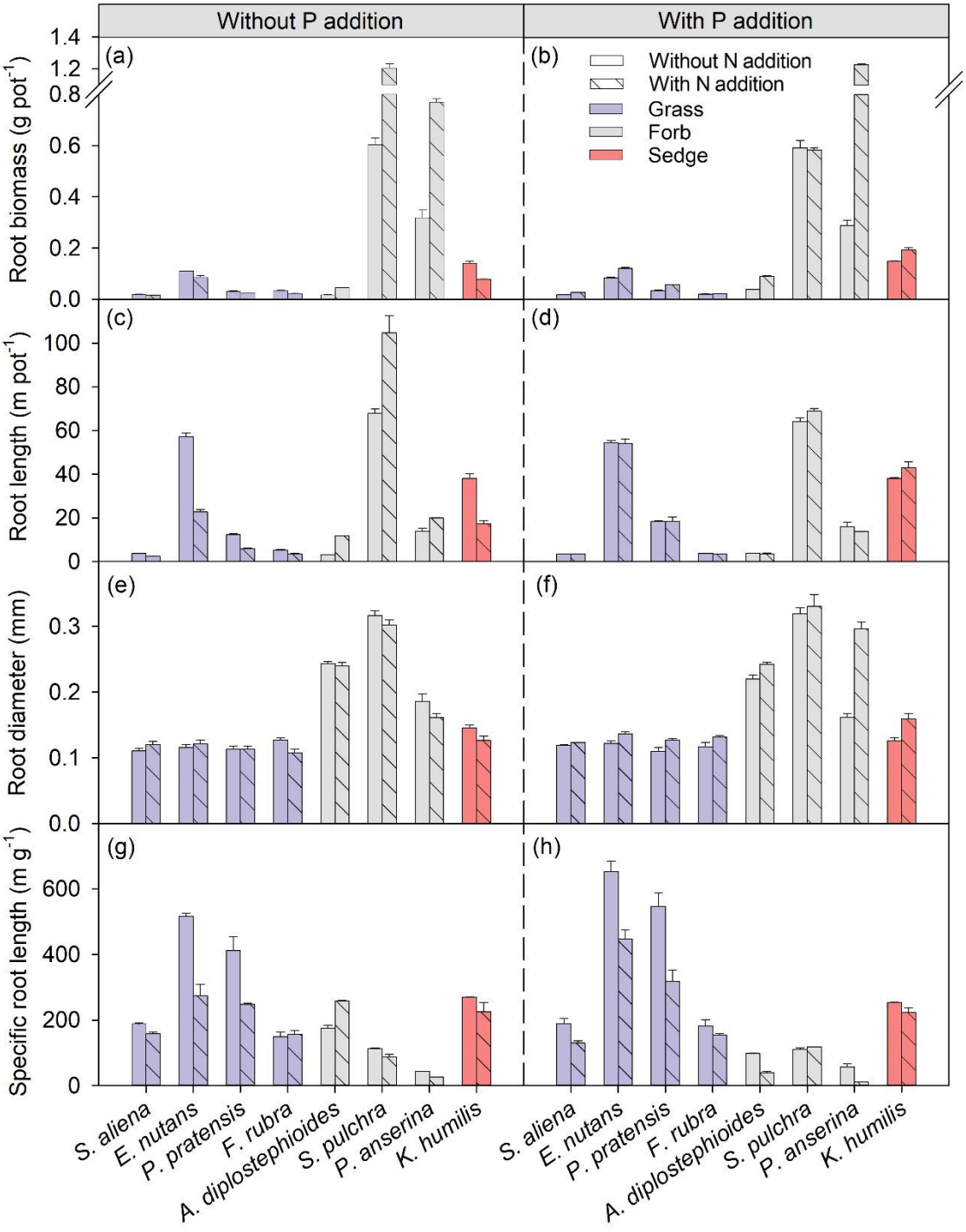
Without P addition
With P addition
(a)
(b)
(c)
(d)
(e)
(f)
(g)
(h)
Without N addition
With N addition
Grass
Forb
Sedge
Root biomass (g pot-1)
Root length (m pot-1)
Root diameter (mm)
Specific root length (m g-1)
S. aliena
E. nutans
P. pratensis
F. rubra
A. diplostephioides
S. pulchra
P. anserina
K. humilis

Fig. 4.

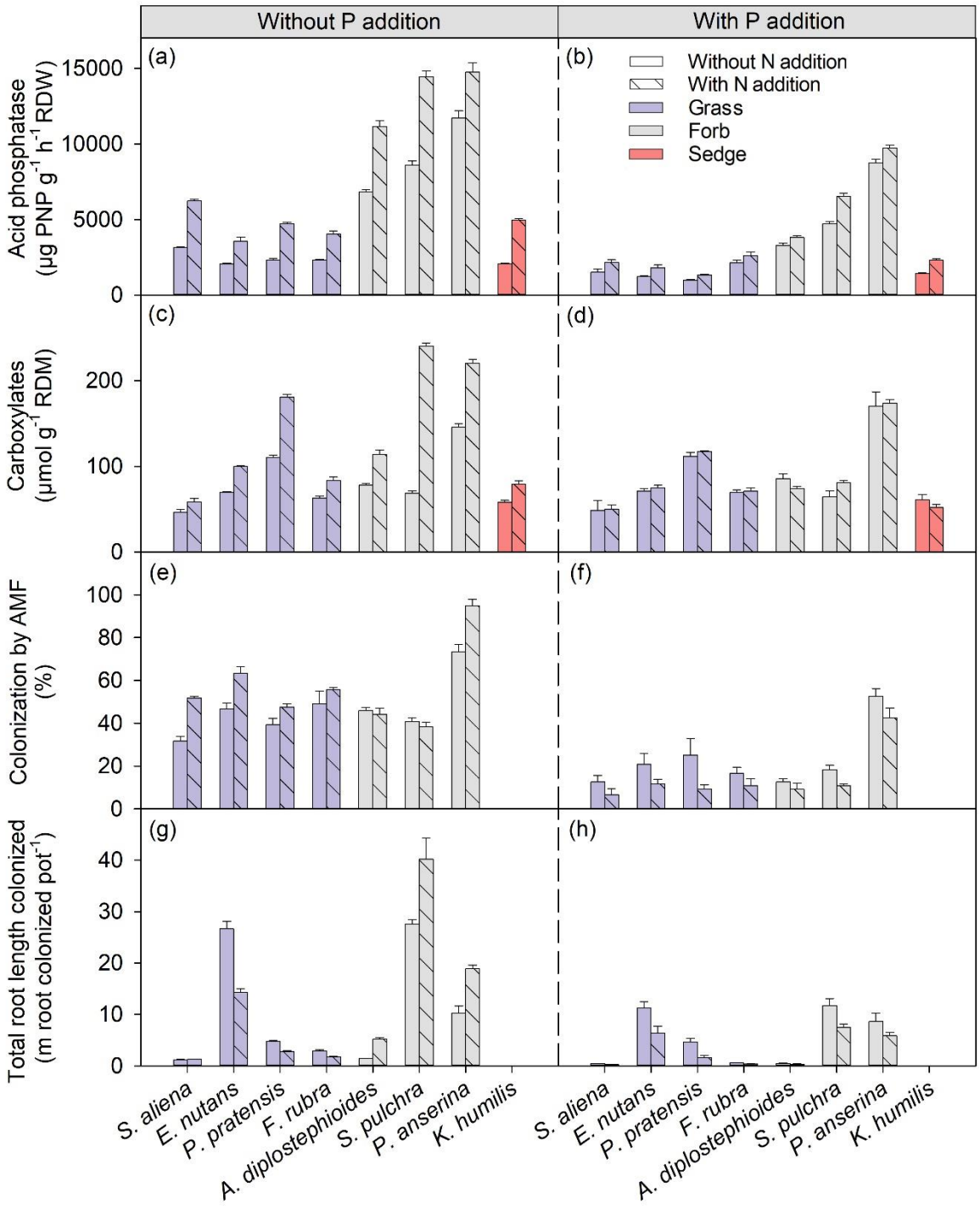
Without P addition
With P addition
(a)
(b)
(c)
(d)
(e)
(f)
(g)
(h)
Without N addition
With N addition
Grass
Forb
Sedge
Acid phosphatase (μg PNP g-1 h-1 RDW)
Carboxylates (μmol g-1 RDM)
Colonization by AMF (%)
Total root length colonized (m root colonized pot-1)
0
5000
10000
15000
100
200
20
40
60
80
10
30
S. aliena
E. nutans
P. pratensis
F. rubra
A. diplostephioides
S. pulchra
P. anserina
K. humilis

Fig. 5.

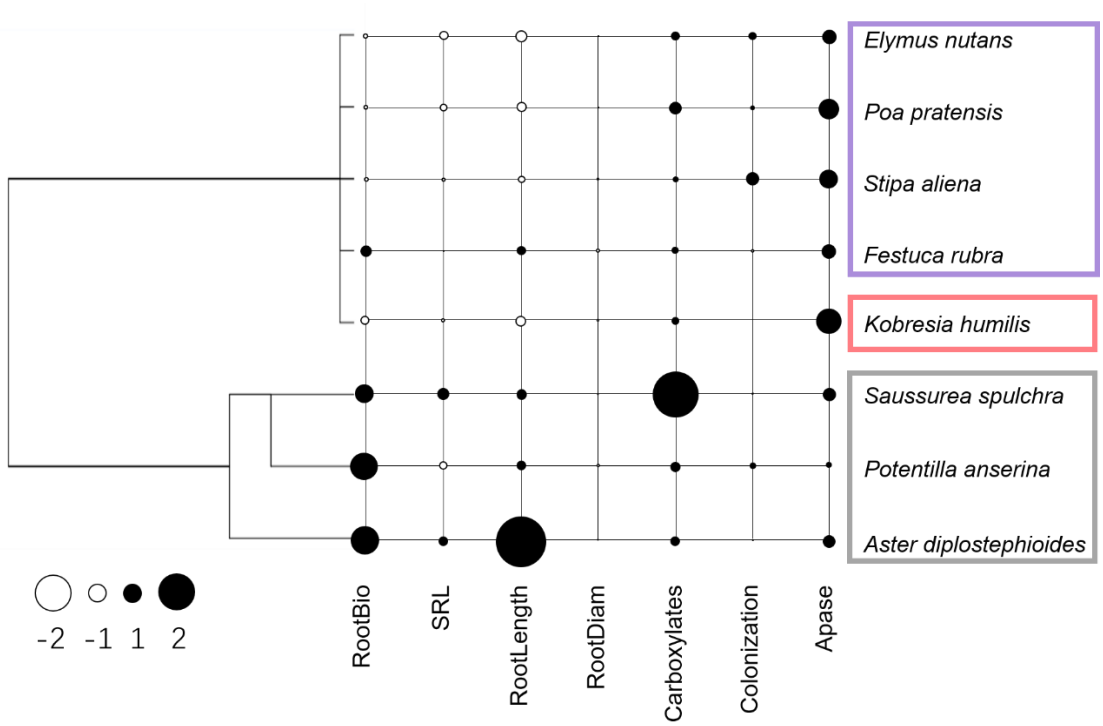
Elymus nutans
Poa pratensis
Stipa aliena
Festuca rubra
Kobresia humilis
Saussurea spulchra
Potentilla anserina
Aster diplostephioides
-2 -1 1 2
RootBio
SRL
RootLength
RootDiam
Carboxylates
Colonization
Apase

Fig. 6.

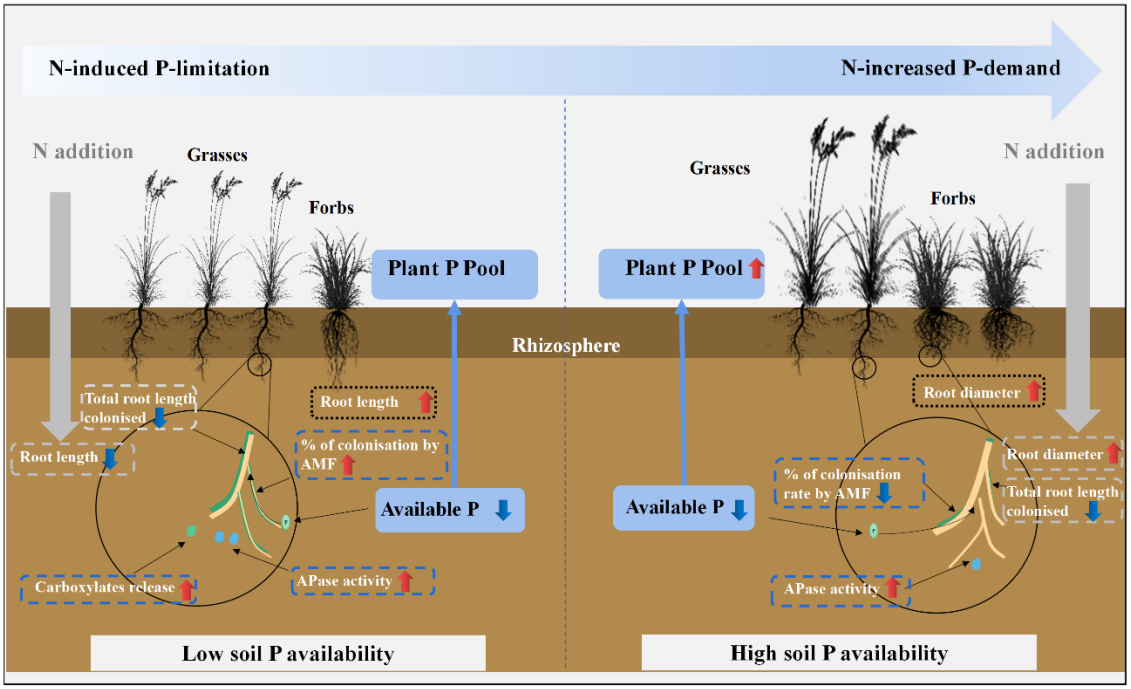
N-induced P-limitation
N-increased P-demand
N addition
Grasses
Forbs
Plant P Pool
Rhizosphere
Total root length colonised
Root length
Root length
% of colonisation by AMF
Available P
Carboxylates release
APase activity
Low soil P availability
Grasses
Forbs
N addition
Plant P Pool
Root diameter
Root diameter
% of colonisation rate by AMF
Total root length colonised
Available P
APase activity
High soil P availability

Table 1. Effects of nitrogen (N) and phosphorus (P) addition on soil properties.

Variable	Control	N addition	P addition	N + P	*P* values, two-way ANOVA		
					N	P	N × P
pH	7.37±0.12	7.61±0.05	7.52±0.14	7.34±0.14	0.859	0.596	0.069
SOC (g kg^{-1})	60.5±1.3	51.7±3.5	52.4±2.0	74.6±4.0	0.038	0.025	<0.001
Total N (g kg^{-1})	8.18±0.50	8.63±0.36	7.57±0.17	8.36±0.39	0.120	0.261	0.655
NO_3^- (mg kg^{-1})	2±0.1	18±3	2±1	9±1	<0.001	0.004	0.001
NH_4^+ (mg kg^{-1})	6±1	12±3	5±1	5±2	0.058	0.022	0.065
Total P (g kg^{-1})	0.70±0.03	0.70±0.02	1.26±0.09	1.16±0.05	0.364	<0.001	0.319
Available P (mg kg^{-1})	64.5±3.2	50.6±4.7	407.3±20.7	273.6±11.5	<0.001	<0.001	<0.001

pH, soil organic carbon (SOC), total nitrogen (total N), soil nitrate and ammonium (NO_3^- and NH_4^+), total phosphorus (total P), and available P concentrations were recorded in 2018. Data are presented as the mean (± SE) of six replicates.

Table 2. Effects of nitrogen (N) and phosphorus (P) addition on plant variables.

Variable	Control	N addition	P addition	N + P	*P* values, two-way ANOVA		
					N	P	N × P
Shoot biomass (g m^{-2})	298±34	472±42	320±25	543±67	<0.001	0.308	0.597
Total biomass (g m^{-2})	1776±39	1726±32	1857±52	2182±65	0.010	<0.001	0.001
Root/shoot biomass ratio	5.23±0.48	2.83±0.42	4.95±0.43	3.22±0.34	<0.001	0.894	0.438
Shoot P concentration (mg g^{-1})	1.21±0.04	1.12±0.07	3.93±0.15	3.58±0.20	0.101	<0.001	0.325
Shoot N concentration (mg g^{-1})	16.8±0.64	23.3±0.71	16.0±0.18	17.9±0.48	<0.001	<0.001	<0.001
Shoot N/P ratio	13.9±0.32	21.3±1.35	4.08±0.14	5.10±0.37	＜0.001	<0.001	<0.001
Root P concentration (mg g^{-1})	0.86±0.02	1.06 ± 0.04	0.91±0.01	2.20±0.05	<0.001	0.001	0.160
Shoot P uptake (mg m^{-2})	362±48	517±42	1262±114	1945±277	0.013	<0.001	0.100
Root P storage (mg m^{-2})	1277±31	1325±59	1391±29	3597±43	<0.001	<0.001	<0.001
Total plant P pool (mg m^{-2})	1639±45	1842±57	2653±118	5542±274	<0.001	<0.001	<0.001

Plant shoot biomass, total biomass, root/shoot biomass ratio, shoot P and N concentrations, shoot N/P ratio, root P concentration, shoot P uptake, root P storage and total plant P pool were recorded in 2018. Data are presented as the mean (± SE) of six replicates.

Manuscript 3

Effects of winter grazing and N addition on soil phosphorus fractions in an alpine grassland on the Qinghai-Tibet Plateau

Agriculture, Ecosystems & Environment, 2023, 357, 108700

Zhen-Huan Guan[1, #], Zuonan Cao[2, 3, #], Xiao Gang Li[1], Peter Kühn[2], Guozheng Hu[3], Thomas Scholten[2], Jianxiao Zhu[1] & Jin-Sheng He[1, 4, *]

[1]State Key Laboratory of Herbage Improvement and Grassland Agro-ecosystems, College of Pastoral Agriculture Science and Technology, and College of Ecology, Lanzhou University, Lanzhou 730000, China

[2]Department of Geosciences, Soil Science and Geomorphology, University of Tübingen, Tübingen 72070, Germany

[3]Institute of Environment and Sustainable Development in Agriculture, Chinese Academy of Agricultural Sciences, Beijing, 100081, China

[4]Institute of Ecology, College of Urban and Environmental Sciences, Peking University, Beijing, 100871, China

[#]These authors contributed equally to the work and should be considered co-first authors

* Corresponding author:

Jin-Sheng He

State Key Laboratory of Herbage Improvement and Grassland Agro-ecosystems, College of Pastoral Agriculture Science and Technology, and College of Ecology, Lanzhou University, Lanzhou 730000, & Institute of Ecology, College of Urban and

Environmental Sciences, Peking University, Beijing, 100871, China

E-mail addresses: jshe@pku.edu.cn

Abstract

Nutrient cycling in alpine grasslands is susceptible to climate change and anthropogenic activities, which can affect soil phosphorus (P) availability. Despite the crucial role of soil P availability in maintaining stability and productivity of grassland ecosystems, limited research has been conducted on the effects of nitrogen (N) addition and winter grazing on P transformation on the Qinghai-Tibet Plateau. In an 8-year experiment, we applied four different N addition rates (0, 25, 50, and 100 kg urea ha^{-1} $year^{-1}$) in combination with winter grazing to investigate the effects of N addition and winter grazing on the soil P fractions. The results reveal that increasing the N addition gradually reduced the resin-Pi and NaOH-Pi contents in the soil by increasing the plant P uptake and promoting the release of carboxylates in the rhizosheath, regardless of grazing. Winter grazing decreased the $NaHCO_3$-Pi and NaOH-Pi contents compared with the no-grazing treatment by increasing the P uptake of the plants. In contrast, neither grazing nor N addition affected the $HCl_{conc.}$-P or residual-P content. In the no-grazing plots, the soil $NaHCO_3$-Po content exhibited a gradual increase in response to N addition, whereas N addition had no discernible effect on the NaOH-Po content. In the grazing plots, the $NaHCO_3$- and NaOH-Po contents gradually decreased with N addition, which was associated with the increased acid phosphatase activity in the rhizosheath and the export of forage. Thus, we conclude that N addition promotes the dissolution of NaOH-Pi to more available inorganic P forms. Under winter grazing conditions only, the transformation of P from inorganic to organic forms gradually decreased with increasing N additions.

Keywords

Alpine grasslands, Nitrogen addition, Soil phosphorus fractions, Winter grazing

1. Introduction

The alpine grasslands on the Qinghai-Tibet Plateau (QTP) play a crucial role in maintaining global ecological stability and providing livelihoods for local pastoral communities (Li et al., 2022). The ecological stability of grasslands is a determining factor in the provisioning of ecosystem services, which are under threat from both climate change and intensive management (Li et al., 2020). To facilitate the sustainable development of grassland productivity, the Chinese government has introduced measures such as alternating winter and summer grazing and erecting fences since the 1990s (Qiu, 2016). Additionally, limited soil phosphorus (P) availability (less than 3% of the total P) poses a significant threat to grassland productivity (Rui et al., 2011; Mou et al., 2020; Zhou et al., 2021). While numerous studies have suggested that nitrogen (N), rather than P, is the primary factor limiting grass productivity in most areas of the plateau (Gao et al., 2018; Han et al., 2019; Wang et al., 2022a), it appears that plant productivity may have shifted from being limited by N to being limited by P due to increasing N accumulation in the last decade (Li et al., 2016; Zhao & Zeng, 2019; He et al., 2020a; Chen et al., 2021). Hence, the availability of soil P is a pivotal factor that impacts both the stability and productivity of grassland ecosystems.

Plants acquire available inorganic P (Pi) from the soil solution, while organic P (Po) is reintroduced into the soil via decomposition of plant residues. These organic materials then undergo mineralization to yield Pi, which constitutes the primary process of the biochemical P cycle (Lambers et al., 2006, 2022). Both Po and Pi can be easily immobilized by soil minerals, resulting in their availability to plants and microbes being partitioned into labile (extracted using resin and $NaHCO_3$), moderately labile (extracted using NaOH and HCl), and stable (extracted using concentrated HCl and H_2SO_4) forms (Hedley et al., 1982; Hou et al., 2018). Even the plant-available P only accounts for a small fraction of the total P in soil (less than 5%) and it could be continuously supplemented with more stable P fractions to meet plant needs (Niederberger et al.,

2019). The mineralization of Po by microorganisms and plant roots that secrete phosphatase to degrade Po provides the primary source of plant-available P (Turner et al., 2013; Shen et al., 2011). In addition, a decrease in the soil pH and biological solubilization via the secretion of carboxylates (e.g., gluconate, citrate, oxalate, and acetate) by plants and microorganisms is an important factor in promoting P mobilization (Bünemann, 2015; Liu et al., 2022). Understanding the different forms of P, particularly the transition from stable to labile P fractions, is essential for regulating soil P dynamics and thus the P availability to plants (Yang and Post, 2011; Fan et al., 2019).

Furthermore, N enrichment, such as N deposition, has been shown to enhance P mobilization by facilitating plant P acquisition from soil P pools (Schluss et al., 2020; Wang et al., 2022a). N also stimulates the production of extracellular phosphatase enzymes, which in turn facilitate the liberation of Pi from organic reservoirs (Lu et al., 2012; Schaap et al., 2021). Moreover, N accumulation in ammonium compounds can indirectly lead to soil acidification, which enhances the dissolution of refractory mineral-bound P into moderately labile and labile P fractions (Fu and Shen, 2017; Fan et al., 2019). Therefore, the enrichment of N, plays a supporting role in all aspects of the P cycle. Despite decades of the N supply being sufficient for plant production, as recent meta-analyses have shown, many ecosystems remain limited by N without a noticeable shift toward P limitation (Chen et al., 2020; Wang et al., 2022a). This observation could be explained by the fact that the amount of P mobilized by the N supply is greater than the amount of immobilized P (Wang et al., 2022a; Xiao et al., 2022). The alpine grasslands on the QTP, which have a low mean annual temperature, have a very low rate of Po mineralization in the soil (Rui et al., 2011; Zhou et al., 2021). Additionally, soils in alpine grasslands that are rich in base cations (Ca^{2+}, Mg^{2+}, and K^{+}) may limit P mobilization by stabilizing the soil pH (Tian & Niu, 2015). Therefore, N enrichment in alpine grasslands is likely to promote P immobilization rather than P mobilization.

Continuous year-round grazing increase P export from the soil through forage and livestock products (Chaneton et al., 1996; Wu et al., 2009), and decreases the P return to the soil by reducing the amount of litter and inhibiting decomposition of aboveground litter (Bardgett & Wardle 2003), resulting in depletion of the soil P pool (Yao et al., 2019). There are also mate-analyses suggesting that grazing can promote rock weathering to increase the soil P pool (He et al., 2020b), but negative effect on soil P mobilization (Yu et al., 2021). Although returning dung and urine to the soil may increase soil P mobilization in the short term, the available P readily accumulates in the topsoil layer due to soil adsorption, and the increase in the soil bulk density caused by trampling causes poor migration to the deeper soil layers (Baron et al., 2001; Wu et al., 2020), which also contributes to the loss of these soil nutrients through run-off, leaching, and transformation by livestock (Vadas et al., 2015). Studies have also shown that grazing negatively affects both the aboveground and belowground biomass (Bai et al., 2012; Bai et al., 2015), alters the structure and composition of the plant community, and reduces the plant's P stock (Li et al., 2010; Bai et al., 2012; Davidson et al., 2017). In contrast to year-round grazing, winter grazing does not interrupt plant growth during the growing season, and has little negative impact on grassland ecosystems (Shi et al., 2017), while avoiding changes in the plant community composition and degradation of dominant plant species caused by the selective foraging behavior of livestock (Johnson & Sandercock, 2010). In addition, the consumption of aboveground litter by livestock provides abundant solar radiation and spatial resources for plant growth the following year, resulting in an increase in the aboveground plant biomass (Chen et al., 2007; Giese et al., 2013; Shi et al., 2022), which in turn may contribute to the transfer of P from the soil to the plants. In winter, especially on the QTP—which is famous for its cold and windy conditions—the grazing duration is short, and the grazing intensity is high, which is not conducive to the return of dung and urine, and the frozen soil can effectively prevent an increase in the capacity caused by trampling. The inference can be drawn that winter grazing may be less favorable for plant P to return to the soil

compared to the year-round grazing.

In alpine grasslands, both N addition and winter grazing may enhance P uptake by plants and increase opportunities for P limitation of plants. Overall, plants may intensify their own P-acquisition strategies in response to P limitation, such as changes in the root morphology, increases in root exudates, and increased levels of symbiosis with arbuscular mycorrhizal fungi (AMF) to mobilize stable P fractions into more available forms (He et al., 2020a; Lambers et al., 2022; Luo et al., 2022). However, the independent effects of gradual N enrichment and winter grazing on the soil P fractions and their interactions are still unclear. As such, it is unclear how alpine grassland plant communities on the QTP adjust their P-acquisition strategies to mobilize and take up P in response to the N supply and winter grazing. To better understand the effects of the N supply and grazing on soil P fractions, we make the following hypotheses:

1) The plant P demand gradually increases as the level of the N supply increases, leading to an adjustment of the plant's P-acquisition strategy and promoting the transformation of occluded P to moderately labile and labile P pools, ultimately resulting in an increase in Po accumulation in the soil.

2) Winter grazing could facilitate P uptake by plants, resulting in more labile Pi in the soil being converted to plant P, less P returning to the soil, and plant P-acquisition strategies adapting to promote P mobilization and uptake.

3) Compared to the no-grazing plots, in the grazing plots, Po accumulation in the soil decreases as the N addition rate increases.

The present study was based on an 8-year field experiment that involved N fertilization and a winter grazing treatment. This experiment was conducted in an alpine grassland on the QTP (Ren et al., 2017). Using a modified Hedley P fractionation procedure (Tiessen & Moir, 2007), in conjunction with analyses of plant and microbial P and plant P-acquisition strategies, our objective was to characterize the P content and P

transformation within the uppermost 30 cm of the soil.

2. Materials and Methods

2.1 Site description and experimental design

The field experiment was carried out at the Haibei National Field Research Station of Alpine Grassland Ecosystem (at 37°37′ N, 101°19′ E) of the Chinese Academy of Sciences, located on the northeast part of the QTP at 3250 m above sea level. This region has a monsoon continental climate, with a mean annual temperature of −1.7°C, a January mean monthly temperature of −14.8°C, a July mean temperature of 9.8°C, and an average annual precipitation of 489.0 mm, with most of the precipitation falling from May to September (Liu et al., 2018). The soil is classified as *Mat-Cryic Cambisol* according to the Chinese Soil Taxonomy Research Group (1995) or *Gelic Cambisol* according to the World Reference Base for Soil Resources classification (2015), and the site is dominated by *Kobresia humilis*, *Stipa aliena*, *Elymus nutans*, and *Festuca ovina*.

Starting in 2011, N fertilizers were applied to 6 × 6 m plots at the soil surface after sunset during the growing season at the beginning of June, July, and August. Four different N-addition rates (control, N25, N50, and N100, corresponding to 25, 50, and 100 kg $(NH_2)_2CO$ ha^{-1} yr^{-1}) were studied. A fully randomized experimental design was adopted with six replicates of each treatment (Fig. S1).

The winter grazing experiment was conducted based on local conditions since 2011. Starting with the fertilized plots mentioned above, the 6 × 6 m plots were divided into two subplots, the first of which was grazed in winter (3 × 6 m) and the second of which was fenced (3× 6 m). Tibetan sheep (*Ovis aries*) grazed in the subplots continuously from December to April each year after plant dieback, and the grazing intensity was two sheep per subplot. Depending on the local conditions, winter grazing completed for the year, when 75% of the surface litter and standing dead material had been eaten. The

no-grazing subplots had no sheep grazing for 8 years.

2.1.1 Soil sampling

Soil samples were collected at depth of 0–10 cm (topsoil, covering the A horizon) and 10–20 and 20–30 cm depths (subsoil). Five soil samples from each subplot and depth were collected at random from six replicate blocks using a soil auger (Ø 50 mm) and were combined into one composite sample. The sampling was conducted in August 2018, and the samples were packed in polyethylene bags and stored in an ice box prior to shipment to the laboratory. The soils were then sieved (< 2 mm), and all of the visible roots, residues, and stones were removed. An aliquot of each soil sample (10 g) was removed aseptically and stored at −80 °C for the purpose of microbial analysis (phospholipid fatty acids [PLFA]). An additional portion was stored at 4 °C for analysis of the soil microbial biomass P (MBP), carbon (MBC), and nitrogen (MBN). The remaining material was air dried at 60°C for further analyses of the soil properties.

2.1.2 Vegetation sampling

The vegetation communities were surveyed in mid-August 2018, the time of the peak biomass. Three species richness surveys, covering 1 m^2 were conducted in each plot. Plants were harvested from a 0.5× 0.5 m square chosen at random within each plot. Shoots (leaves and stems) were cut, and litter was collected with scissors at the base and sorted to measure the aboveground biomass. To measure the plant C, N, and P concentrations, we pooled all the plant species within the square and combined them into a mixed community sample.

2.1.3 Rhizosheath soil and root sampling

The study of root systems was particularly susceptible to under-sampling errors due to the high spatial heterogeneity and non-normal distribution of root diameters in soil (Taylor et al., 2013). Rhizosheath soil and soil cores from root samples (0–10 cm) were collected from each plot using a root auger (Ø 70 mm; Mou et al., 2020). The roots in

the soil were carefully separated from the soil and transferred to a beaker containing 0.2 mM $CaCl_2$ (Pearse et al., 2007). The roots were repeatedly immersed in the solution until all the rhizosheath soil was removed. For the measurements of the activities of the acid phosphatase (ACP) and alkaline phosphatase (ALP), two 0.5 mL aliquots of the soil suspension (sample and control) were transferred to 2 mL centrifuge tubes for analysis (Neumann, 1999). Two drops of concentrated phosphoric acid were added to 7–8 mL subsamples before storage at −20°C until analysis of the carboxylates via high-performance liquid chromatography (Wen et al., 2019). After analysis of the rhizosheath exudates, the soaked roots were harvested and washed with tap water, placed in paper bags, and kept at 4 °C before assessing the C, N, and P contents, the root biomass and morphology, and the colonization by AMF.

2.2 Laboratory measurements

2.2.1 Soil properties and plant nutrients

The soil pH was measured in deionized water in a 1:5 soil: water suspension using air-dried water after shaking for 30 min, and the soil bulk density was determined using the mass per volume method (with 100 cm^3 for the entire core). The soil organic carbon (SOC), total nitrogen (TN), and plant C and N contents were measured using an elemental analyzer (Elementar Vario EL III, Elementar Analysensysteme GmbH, Langenselbold, Germany). The plant P concentrations (shoot, aboveground litter, and roots) were determined colorimetrically after digestion in an $HClO_4$–H_2SO_4 mixture, and the P stocks were calculated by multiplying the biomass by the P concentrations. The amount of soil available N (KCl-extractable ammonium [NH_4^+] and nitrate [NO_3^-]) was determined using a continuous flow analyzer (Skalar San, Breda, Netherlands). The exchangeable cations (Ca^{2+} and Mg^{2+}) were extracted using 1 M NH_4OAc and were measured via atomic absorption spectroscopy (Ngewoh et al., 1989). Consistent with the regular Hedley sequential extraction of P (Hedley et al., 1982), which was later modified by Tiessen and Moir (2007), Pätzold et al. (2013), and Niederberger et al.

(2015), 0.5 g of each soil sample, which was air-dried and sieved, was dissolved. An anion-exchange resin bag containing 0.5 M HCl was used to measure the labile resin-Pi directly from the soil solution, followed by extraction with 0.5 M $NaHCO_3$ (pH 8.5) to obtain the relatively labile plant-available Pi and readily mineralized Po. Furthermore, 0.1 M NaOH was used to extract the soil residue for the moderately labile Pi, which covered the Pi associated with Fe and Al oxides as well as the Po involved in the slow transformation processes. However, in the presence of concentrated HCl, the $HCl_{conc.}$ -P fraction of the highly stable Pi in the primary minerals at 85 °C was applied instead of the fraction extracted using 1 M HCl in the traditional Hedley method, which was found to be negligibly small (Tiessen and Moir, 2007; Alt et al., 2011). For the highly resistant and occluded Pi forms, 0.5 M H_2SO_4 was used to extract the residual P (Table S1). All of the Pi fractions were determined as described above using continuous-flow-analysis (SEAL Auto Analyzer AA3, Analytical GmbH, Norderstedt, Germany), and the total $NaHCO_3$-P and NaOH-P fractions were determined via inductively coupled plasma–optical emission spectrometry (Optima 5300 DV, PerkinElmer, Waltham, MA, USA). The concentrations of the Po fractions were calculated as the difference between the total fractions ($NaHCO_3$- and NaOH-P) and the Pi fractions. The concentrations of different P pools in the soil were calculated on a soil dry weight basis (mg kg^{-1}) and then converted to an area basis (g m^{-2}) based on the bulk densities.

2.2.2 Root morphology

Fresh root samples were washed under running water, spread in water with minimal overlap, and digitized on an Epson Expression 10,000 XL desktop scanner (resolution, 300 dpi). The root images were analyzed using the WinRHIZO software (Regent Instruments, Quebec, QC, Canada) to determine the average diameter and total length of the roots.

2.2.3 Root exudates

The inorganic fractions in all of the extracts were determined after filtration using the

ammonium molybdate spectrophotometric method at 700 nm. These contents were calculated based on the differences in the inorganic fractions extracted from fumigated and non-fumigated samples (Khan & Joergensen, 2012). Analysis of the amount of rhizosheath carboxylates was carried out using a Waters 1525 HPLC equipped with a Waters 2489 detector and a Waters Symmetry C^{18} reverse-phase column (Waters, Milford, MA, USA). The mobile phase was prepared by adjusting 20 M KH_2PO_4 to a pH of 2.5 using concentrated H_3PO_4 at a flow rate of 0.6 mL min^{-1} and 100% methanol at a concentration of 0.01 mL min^{-1}. The following work standards were applied to identify the carboxylates at 210 nm: oxalate, tartrate, formate, malate, malonate, lactate, acetate, citrate, succinate, and propionate were used (Cawthray, 2003). The carboxylates content was given as total content per unit root dry mass (rdm).

The phosphatase activity was determined via colorimetric analysis based on the amount of p-nitrophenol liberated from the soil suspension during incubation with p-nitrophenyl phosphate (PNPP) in a buffer of either pH 6.5 (ACP) or pH 11 (ALP) for 1 h at 37°C (Hopkins et al., 2008). The 0.5 mL aliquots of soil suspension with an oven-dried weight of 1 g were transferred into 2 mL centrifuge tubes, treated with 0.4 mL of Na-Ac buffer and 0.1 mL of substrate solution (PNPP), and incubated. At the end of the incubation, 0.5 mL of 0.5 M NaOH was added to the slurries to halt the enzymatic reactions. The absorbance of the enzyme extracts was monitored at 410 nm (UV-1800, MAPADA, Shanghai, China) immediately after the filtration process was completed. The carboxylate content of the rhizosheath and phosphatase activity was expressed in mmol per unit of dry root weight.

2.2.4 AMF colonization

The root samples were cleaned with a 10% (w/v) solution of KOH in a water bath at 90 °C for 20 min, rinsed with water, and then acidified with 2% (v/v) HCl for 5 min at 18°C (Zhang et al., 2023). Samples were collected from the roots, placed in a water bath, and stained with Trypan blue at 0.05% (w/v) nonvital in a water bath at 90 °C for

30 min (Phillips & Hayman, 1970). The stained root fragments were placed in an acid-glycerol-water lactide solution (v/v/v, 1: 1: 1) overnight to remove the excess stain. For each sample, 30 stained root fragments from first and second order roots with an average length of 1 cm were randomly selected from each sample and were mounted on two slides for visualization under a light microscope (BX63, Olympus Corporation, Tokyo, Japan). The colonization by AMF (%) was evaluated according to the method outlined by Trouvelot et al. (1986).

2.4.5 Microbial biomass nutrients and community structure

The MBP, MBC, and MBN were analyzed using a chloroform fumigation-extraction procedure (Vance et al., 1987; Morel et al., 1996). The soil microbial PLFAs were determined using a modified Bligh–Dyer method (Bligh & Dyer, 1959; Frostegård et al., 1991). The fatty acids were extracted from a 10 g soil sample using a chloroform-methanol-citric acid buffer (Kourtev et al., 2002). The lipid in the concentrated extract was separated on solid-phase extraction cartridges and fractionated into neutral, glycolipid, and polar fractions. After elution with methanol, the polar lipid fraction was dried under nitrogen gas, saponified and methylated. Specific fatty acids were used as a proxy for the biomass of the AMF (Olsson et al., 1998). The individual fatty acid methyl esters were identified and quantified using an MIDI Sherlock Microbial Identification System (MIDI, Newark, DE, USA). The 16:1ω5c content represents the AMF fatty acid fraction. Finally, the contents of the samples were converted to units of nmol per g of soil sample based on the water content.

2.3 Statistical analysis

Two-way analysis of variance (ANOVA) with the least significant difference (LSD) test for post hoc means comparison was used to test the effects of N addition, grazing, and their interactions on the soil parameters, P fractions, plant growth parameters, and P-acquisition strategy indicators in the field experiment. The SPSS 25.0 software (IBM SPSS, Chicago, IL, USA) was used to conduct the above analyses, and differences were

significant at $p < 0.05$.

3. Results

3.1 Soil biochemical properties and plant communities

No significant differences in the soil properties were observed within the depth range of 10–30 cm; thus, the subsequent findings exclusively focus on the 0–10 cm soil depth interval. After 8 years of treatment, the N application increased the NO_3^--N content but reduced the MBC and MBN contents compared with the no N addition treatment, regardless of whether the plots were grazed (Tables 1 and 2). Furthermore, neither N addition nor grazing altered the plant community composition and richness (Table S2).

Table 1. Effects of nitrogen (N) addition rate and grazing (G) on soil biochemical properties in the 0–10 cm depth interval.

Treatment		pH	SOC (g kg^{-1})	TN (g kg^{-1})	MBC (mg kg^{-1})	MBN (mg kg^{-1})	NH_4^+-N (mg kg^{-1})	NO_3^--N (mg kg^{-1})	EX. Mg^{2+} (mg g^{-1})	EX. Ca^{2+} (mg g^{-1})	Soil bulk density (g cm^{-3})
N	Ctrl	7.47±0.08	61.9±5.21	8.80±0.26	1366±3.24	257±4.04	0.63±0.04	2.01±0.42	0.58±0.02	16.82±0.80	0.71±0.02
G	N_{25}	7.40±0.10	61.4±4.92	8.44±0.19	1172±35.8	253±11.7	0.80±0.15	5.16±1.87	0.53±0.03	14.36±1.22	0.71±0.02
	N_{50}	7.46±0.10	66.1±1.36	8.65±0.54	998±12.3	227±1.34	0.97±0.20	2.63±0.52	0.47±0.02	13.46±0.24	0.71±0.02
	N_{10}	7.53±0	67.2±0	8.74±0	925±3.9	172±	0.80±0.	2.88±0	0.41±0	12.03±0	0.70±

	N_{100}	.14	.95	.48	4	3.22	15	.86	.03	.28	0.03
G	Ctrl	7.37±0.12	67.4±0.87	8.18±0.50	1361±8.66	263±8.98	0.67±0.04	1.16±0.14	0.58±0.04	16.15±0.61	0.71±0.01
	N_{25}	7.35±0.05	66.6±0.42	9.01±0.87	1109±83.0	214±4.44	0.74±0.05	4.04±0.94	0.56±0.04	13.80±0.83	0.70±0.04
	N_{50}	7.42±0.02	65.9±0.99	8.26±0.47	1106±22.7	228±17.3	0.79±0.06	3.14±0.39	0.45±0.03	15.10±0.86	0.72±0.03
	N_{100}	7.61±0.05	66.4±1.35	8.63±0.36	939±27.2	168±4.63	0.73±0.04	3.20±0.37	0.36±0.04	11.40±0.89	0.71±0.01

The pH, soil organic carbon (SOC), total nitrogen (TN), microbial biomass carbon (MBC), microbial biomass nitrogen (MBN), soil nitrate and ammonium (NO_3^-_N and NH_4^+_N), soil exchangeable Mg^{2+} and Ca^{2+}, and soil bulk density were recorded. Ctrl indicates the treatment with no N addition, and N addition indicates the treatments with three levels of N fertilizer; G: treatment with grazing; NG: treatment with no grazing. The data are presented as the mean (± SE) of six replicates.

Table 2. Summary of two-way ANOVA results for the effects of N addition and grazing on soil factors

Variable	Two-way ANOVA			Effect of N addition			
	N addition	Grazing	N ×Grazing	Ctrl	N_{25}	N_{50}	N_{100}
pH	n.s	n.s	n.s	a	a	a	a
SOC	n.s	n.s	n.s	a	a	a	a
TN	n.s	n.s	n.s	a	a	a	a
MBC	< 0.001	n.s	n.s	a	b	c	d

MBN	<0.001	n.s	n.s	a	b	b	c
NH_4^-_N	n.s	n.s	n.s	a	a	a	a
NO_3^+_N	0.017	n.s	n.s	b	a	ab	ab
EX. Mg^{2+}	< 0.001	n.s	n.s	a	a	b	b
EX. Ca^{2+}	< 0.001	n.s	n.s	a	b	b	c
Soil bulk density	n.s	n.s	n.s	a	a	a	a

Two-way ANOVA results for the effects of N addition and grazing on soil factors. The pH, soil organic carbon (SOC), total nitrogen (TN), microbial biomass carbon (MBC), microbial biomass nitrogen (MBN), soil nitrate and ammonium (NO_3^-_N and NH_4^+_N), soil exchangeable Mg^{2+} and Ca^{2+}, and soil bulk density were recorded. The different lowercase letters indicate significant differences among the N addition rates ($p < 0.05$). n.s. = no significance (p values).

3.2 Soil phosphorus fractions

The resin-Pi content decreased with increasing N addition, regardless of the grazing condition (Fig. 1a; Tables S3 and S4), and the $NaHCO_3$-Pi content decreased with grazing and was unaffected by N addition (Fig. 1b; Tables S3 and S4). N addition or grazing decreased the NaOH-Pi content (Fig. 1c; Tables S3 and S4). The $NaHCO_3$-Po and NaOH-Po contents decreased with increasing N addition in combination with grazing; whereas, the $NaHCO_3$-Po content increased with N addition without grazing (Figs. 1e, f; Tables S3 and S4). The proportion of the Po content in the total P decreased with increasing N addition in the grazing plots (Fig. 2a; Table S3), and the changes in the Po pool exhibited the same trend (Fig. 2b). Grazing decreased the soil total P content compared with no grazing (Fig. 1h; Table S3). Neither grazing nor N addition affected the contents of HCl_{conc}-P and residual-P and all the P fractions at depths of 10–30 cm (Figs. 1d and g; Table S4).

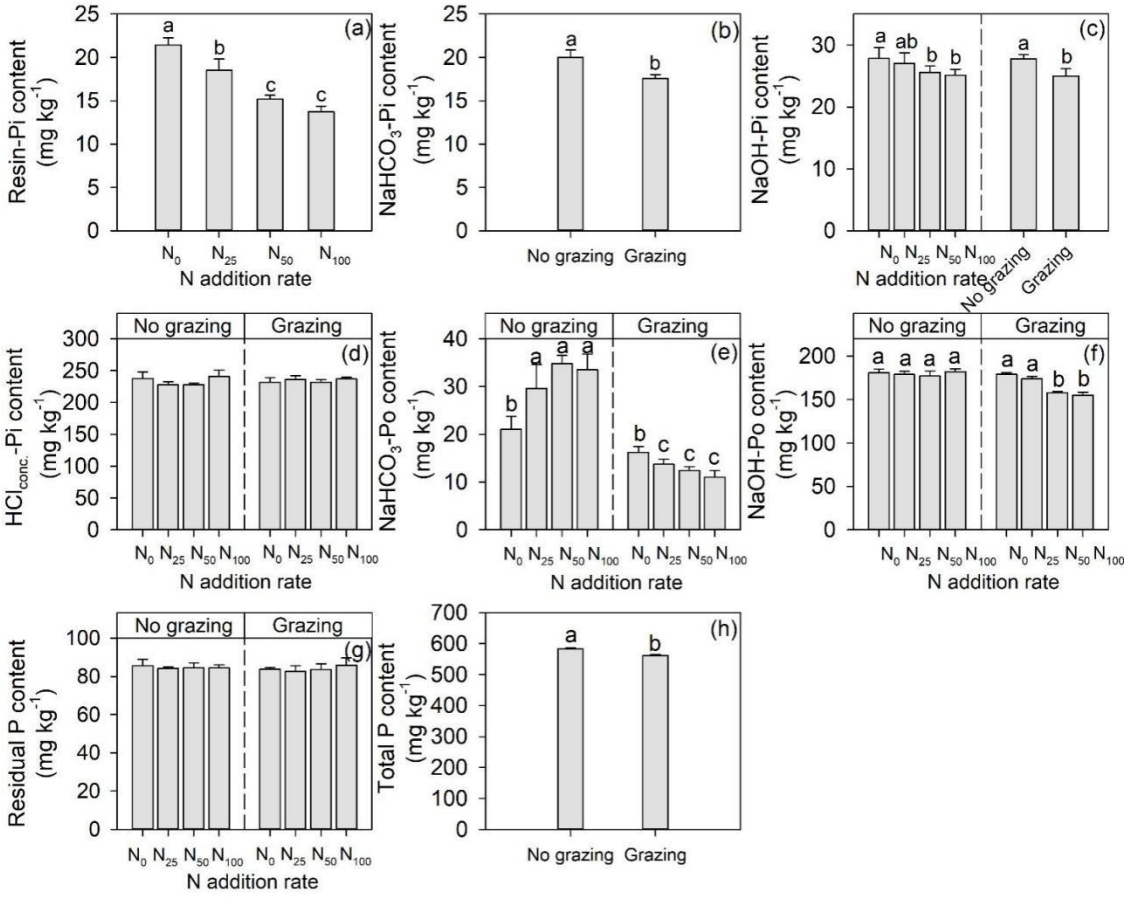

Fig. 1. Dependences of soil P fractions (a−g) and total P (h) contents at depths of 0 to 10 cm on grazing and nitrogen addition rates. The different lowercase letters indicate that the means are different at $p < 0.05$. The N addition rate did not significantly affect the (b) $NaHCO_3$-Pi and (h) total P contents and grazing did not significantly affect the (a) resin-Pi. The values are expressed as the mean ± 95% confidence intervals.

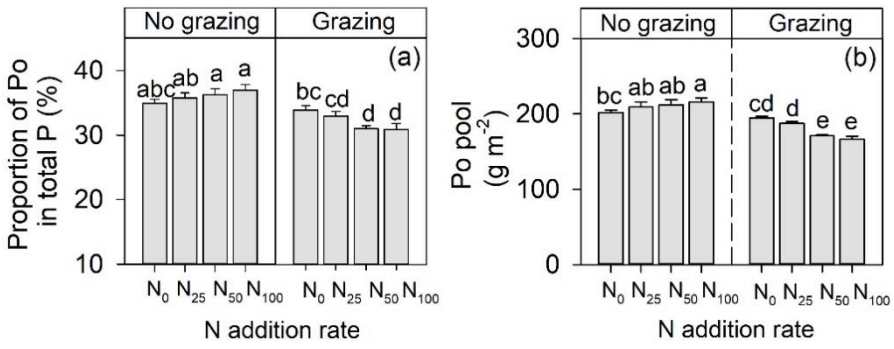

Fig. 2. Plots of the (a) proportions of total organic P (Po, sum of $NaHCO_3$- and NaOH-Po) in the total P and (b) Po pool versus the nitrogen addition rates and grazing in the 0–10 cm soil depths interval. The different lowercase letters indicate that the means are different at $p < 0.05$. The values are expressed as the mean ± 95% confidence intervals.

3.3 Plant and microbial phosphorus content

N addition or grazing increased the shoot P stock ($p < 0.05$; Fig. 3a; Table S3). Grazing reduced the aboveground litter biomass and litter P stock (Fig. 3b; Table S3). The P stock in the plant roots remained stable in all the treatments (Fig. 3c), and N addition elevated the N: P ratio of the shoots compared to the treatment with no N supply (Fig. 3d; Table S3). In addition, in the plots with N addition, a decrease in the MBP pool was observed in the soil regardless of the grazing condition (Fig. 4a; Table S3); whereas, the ALP and ACP activities did not change in the soil (Figs. 4b and c; Table S3).

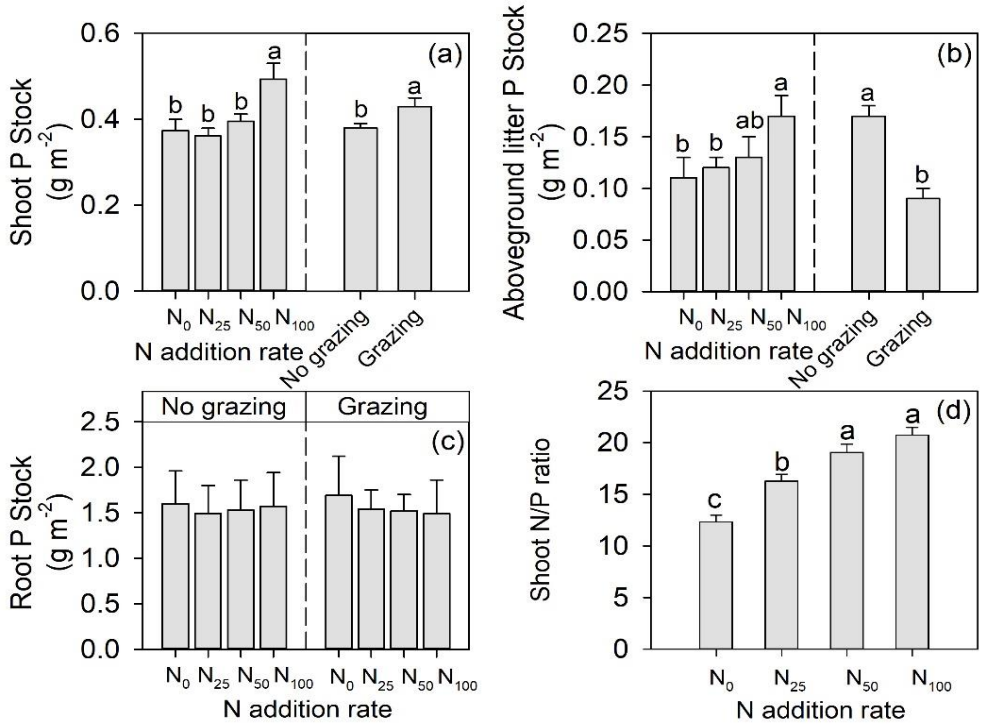

Fig. 3. Dependences of the (a) shoot P stock, (b) aboveground litter P stock, (c) root P stock, and (d) shoot N:P ratio on the nitrogen addition rate and grazing. The different lowercase letters indicate that the means are different at $p < 0.05$. The N addition rate and grazing did not have a significant effect on the (c) root P stock. The values are expressed as the mean ± 95% confidence intervals.

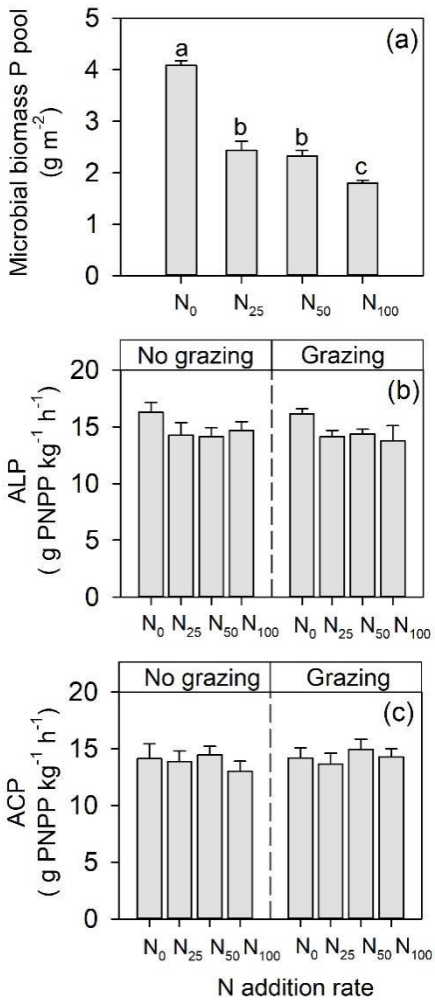

Fig. 4. Dependences of the (a) microbial biomass phosphorus pool, (b) alkaline phosphatase (ALP) in soil, and (c) acid phosphatase (ACP) in soil on nitrogen addition rate and grazing. The different lowercase letters indicate that the means are different at $p < 0.05$. The grazing did not significantly affect these three indicators. The values are expressed as the mean ± 95% confidence intervals.

3.4 Plant P acquisition strategy in the rhizosheath

The ACP activity in the rhizosheath and the carboxylate release increased with increasing N supply (Figs. 5a, b; Table S3). The significant interaction between the N application and grazing affected the ACP activity (Fig. 5a; Table S3). Notably, the AMF colonization decreased with increasing N addition, except in the N100 treatment, where

the AMF colonization was the highest among the treatments (Fig. 5c; Table S3). Neither N addition nor grazing affected the root length density, root diameter, or PLFA content (Table S5).

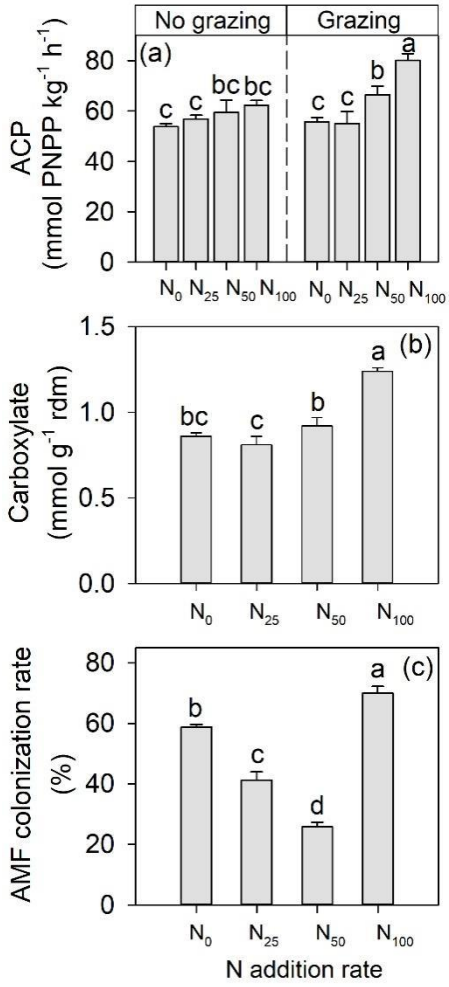

Fig. 5. Dependences of the (a) acid phosphatases (ACP), (b) carboxylate release, and (c) AMF colonization rate in the rhizosheath on grazing and nitrogen addition rate. The different lowercase letters indicate that the means are different at $p < 0.05$. The grazing did not significantly affect the carboxylate release and the AMF colonization rate. The values are expressed as the mean ± 95% confidence intervals.

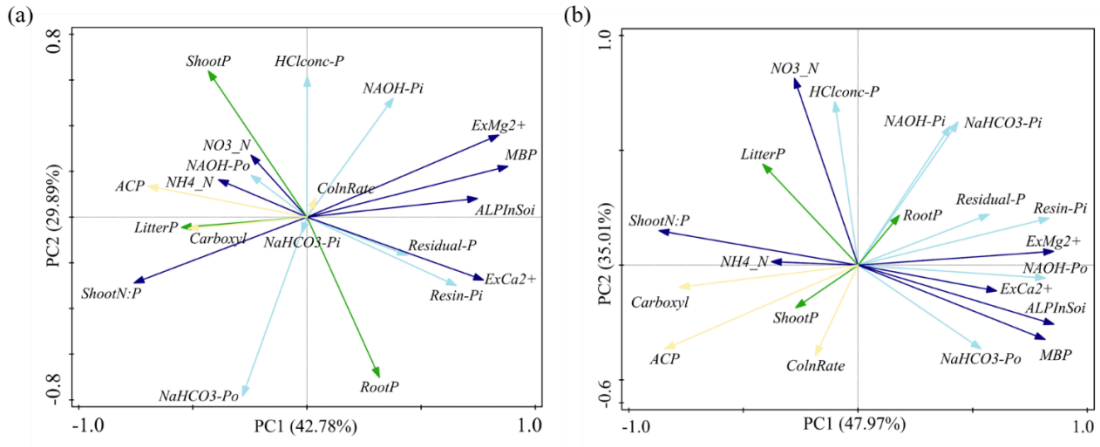

Fig. 6. Principal component analysis (PCA) revealed that the two principal components are a) N addition with no grazing and b) N addition combined with grazing. Green arrows: plant P pools; yellow arrows: plant P-acquisition strategies; cyan arrows: soil P fractions and blue arrows: other soil and microbial factors.

3.5 Relationships between plant and microbial factors and soil phosphorus fractions

Principal component analysis (PCA) revealed that in the no-grazing plots, the two principal components explained 72.73% of the total data variance (Fig. 6a). The resin-Pi and residual-P pools were strongly correlated with PC 1 (42.87%), while the $NaHCO_3$-Po, $HCl_{conc.}$ -P and NaOH-Pi fractions were strongly correlated with PC 2 (29.89%). The plant shoot and litter P pools were positively correlated with the rhizosheath ACP activity and carboxylate release. For the grazing treatments, the components explained 83.07% of the variance (Fig. 6b). Positive correlations were found between the shoot P pool and plant P-acquisition strategies (rhizosheath ACP, carboxylate, and AMF colonization), and the root P pool was positively correlated with the soil Pi pools.

4. Discussion

Winter grazing is a common livestock management practice on the QTP, and N enrichment is a prominent environmental issue, but their effects and the effects of their

interactions on the soil P transformation are poorly understood. Our experiment demonstrated that N addition alone increased plant P uptake by adjusting the P-acquisition strategies (i.e., increased rhizosheath ACP activity, carboxylate release, AMF colonization), leading to the dissolution of NaOH-Pi into more available forms of Pi and an increase in P transformation from inorganic to organic pools in the soil. These results support our first hypothesis that N inputs may result in an increase in Po accumulation in the soil. In agreement with our second hypothesis, winter grazing increased the plant P stock and rhizosheath ACP activity but decreased the $NaHCO_3$-Pi, NaOH-Pi, Po and total P contents of the soil. With increasing N application, there was a greater accumulation of Po in the soil of the no-grazing plots; whereas in the grazing plots, the soil Po pool decreased with increasing N application, which is consistent with our third hypothesis (Fig. 7).

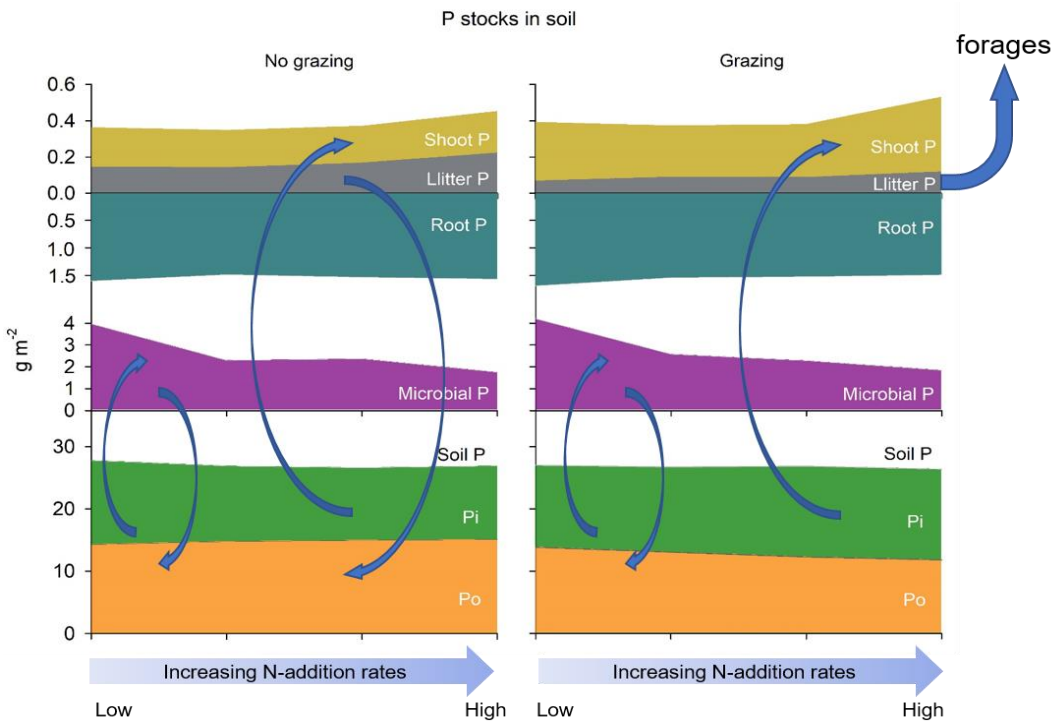

Fig. 7. General trends of the stocks of the P pools in the soil with increasing N addition rate under no grazing (left) and grazing (right) conditions. The arrows show the main pathways of the increased net accumulation and transformation of organic P in alpine grassland soil.

4.1 N addition enhanced the transformation from Pi to Po without grazing

Our results revealed that the resin-Pi and NaOH-Pi contents decreased with increasing N addition. The gradual increases in the N:P ratio of the shoots and the shoot P stock with increasing N addition indicate that the P requirement of the plants increases with increasing N addition. The resin-Pi in the soil is immediately accessible to plants as their P demand increases (Lal & Stewart, 2016). Until the soluble resin-Pi is depleted, the relatively stable Pi fraction can be released through ligand exchange with the bicarbonate ion for only a short period, i.e., one growing season (Hou et al., 2016; Lal & Stewart, 2016). The principal component analysis revealed that there was a strong negative correlation between the carboxylate release and NaOH-Pi content, confirming that the increased release of carboxylates from the rhizosphere with increasing N addition rate is an important physiological strategy for P-mining to mobilize sparingly soluble soil P. This is attributed to the fact that carboxylates exhibit a stronger binding affinity than phosphates (especially moderately labile P) towards binding sites located on the soil surface (Lambers et al. 2006; Kidd et al., 2018).

In alpine grassland soils, phosphate can precipitate with Ca in alkaline soil environments and can be converted to stable forms (Ca-Pi; it was classified as $HCl_{conc.}$-P in this study), which are less available to plants (Lal & Stewart, 2016). N addition promotes carboxylate release in the rhizosphere (Prescott et al., 2020), decreasing the soil pH and increasing the Ca-Pi dissolution (Lal & Stewart, 2016; Wang et al., 2022b). In this study, N addition did not change the soil pH or the $HCl_{conc.}$-P content, which is inconsistent with previous results for the Inner Mongolia grassland (Wang et al., 2022a). This difference is due to the shorter development time of the QTP soils, which leads to less movement of mineral ions in the soil body, combined with the weak biochemical effect and low SOC decomposition under the cold alpine climatic conditions, so the exchangeable Ca^{2+} and Mg^{2+} contents of the QTP soils are much higher than those in other regions (Jiang et al., 2005; Baumann et al., 2009; Wang et al., 2013; Zhang et al., 2015; Huang et al., 2019; Chen et al., 2021; Niu et al., 2022). Additionally, abundant exchangeable Ca^{2+} and Mg^{2+} are an important factor in buffering against N-induced soil acidification (Tian and Niu, 2015). Although the highest N addition rate decreased the soil exchangeable Ca^{2+} and Mg^{2+} contents by 23.4% and 29.8%, respectively (Table 2), in our experimental fields, they were still high enough to maintain a stable soil pH until these cations were depleted (Bowman et al., 2008). Ultimately, N addition promoted

the conversion of the resin-Pi in the soil to plant P, which was subsequently returned to the soil as Po and gradually accumulated.

The soil $NaHCO_3$-P content and total P pool increased with increasing N addition, and the P stock in the plants and litter and shoot N:P ratio increased with increasing N addition, indicating that N addition increased the plant P requirements and the contribution of the plant residual P to the soil Po. In addition to plant synthesis, the weakening of microbial mineralization is another factor contributing to the increase in the proportion of Po in the total P with increasing N input (Bünemann, 2015). This finding contradicts the results of previous studies suggesting that N addition enhances the activities of P-cycling enzymes (Allison et al., 2008;Schleuss et al., 2020). Our results suggest that the accumulation of NO_3^- over the 8-year study period exceeded the N uptake capacity of the plants and microorganisms (Aber et al., 1989; Bell et al., 2010; Jing et al., 2016), which may have contributed to the inconsistency of the results with those of previous studies. Although the ACP activity in the rhizosheath increased with increasing N addition, the ACP activity in the soil did not change. Another factor influencing phosphatase in soil could be that N addition induces plants to allocate fewer photosynthetic products belowground, and decreases microbial biomass and soil ALP activity.

4.2 Winter grazing increases plant P uptake and reduces Po accumulation in soil

Winter grazing promotes the transfer of P from the soil to plants. This is evidenced by the higher plant P stock and lower soil Pi content, especially the $NaHCO_3$-Pi and NaOH-Pi fractions, in the grazing plots compared to the no-grazing plots. The alpine grassland on the QTP has dense plant growth (Luo et al., 2002; Chen et al., 2007), and due to the cold climate all year round, the decomposition of dead material is slow, so under the no-grazing condition, the cover of litter and standing dead matter the reduces photosynthetically active radiation of the plant community (especially the low-growing plants) in the growing season (Klein et al. 2004), which is unfavorable to the growth of the plant community and the absorption of soil nutrients. Winter grazing significantly reduced the amount of aboveground litter through livestock foraging, and the better sunshine radiation condition favored plant growth the next year in the growing season, which in turn promoted plant P uptake compared with the no-grazing plots (Shi et al., 2022).

We also found that grazing reduced the soil $NaHCO_3$-Po and NaOH-Po contents, the total Po pool, and the proportion of Po in the total P. This suggests that winter grazing hinders the transformation of Pi to Po. Winter grazing usually has a high intensity, with Tibetan sheep consuming more than 75% of the litter biomass throughout the grazing season (according to a local survey, data not given). In grazing area, dung decomposition is a key process of returning plant P to the soil (Jin et al., 2022). Alpine grasslands have an extremely cold climate and high wind speeds in winter (Chen et al., 2007). To avoid fat loss from livestock during grazing, grazing periods are short, making it difficult to return dung and urine to the soil in the grazing area. In fact, it has been observed that Tibetan sheep tend to defecate less at grazing sites. Even when livestock excreted small amounts of dung, the P content of dried dung was significantly lower than that of fresh dung (McDowell et al., 2005). Therefore, the high export of litter as forage reduces the recycling of Po. We even found that the phosphatase activity increased more rapidly with increasing N addition in the grazing plots compared to the no-grazing plots, which further accelerated the degradation of the Po.

4.3 Po fractions response to the combined effect of N addition and winter grazing

Our study further revealed that the soil Po pool and its proportion of the total P decreased with increasing N addition in the grazing plots compared to the no-grazing plots, in which the soil Po pool increased with increasing N addition. Under no-grazing condition, plant P uptake increases with the increasing N addition, and except for an amount in the form of litter blown away by the wind or carried away with surface runoff, the remainder plant P returns to the soil where it is stored in the organic form. Under the grazing condition, both N addition and winter grazing promoted P uptake by plants, so that more soil P was converted to plant P than under grazing condition, but little was returned to the soil caused by forage export, so that the proportion of Po pool in the total P in the soil gradually decreased (Fig.7). Notably, N supply and winter grazing had an interactive effect on the inter-root phosphatase activity in plant communities, i.e., rhizosheath ACP activity showed a more pronounced upward trend with increasing N addition under the winter grazing condition compared to the no-grazing condition. This was also responsible for the decline in the Po pool in the grazing plots.

These results emphasize the need for sustainable livestock management and consideration of the effects of grazing and N addition on soil P transformation and nutrient limitation. Further research is needed to understand the mechanisms underlying

these processes and the development of effective livestock management to prevent Po loss in alpine grassland ecosystems.

5. Conclusion

The results of the present study provide valuable insights into the complex interactions of N addition and grazing on the soil P fractions in the alpine grasslands on the QTP. Using a modified Hedley P fractionation method, we observed clear trends in the contents of the various P fractions with increasing N addition in both the grazing and no-grazing plots. In the no-grazing plots, the soil Pi pool decreased while the Po gradually accumulated with increasing N addition. Conversely, in the grazing plots, the Po pools gradually decreased with increasing N addition. In alpine grassland, N addition did not affect the soil pH, but it did reduce the microbial P pool. The results suggest that plants only drive the conversion of Pi to Po in the upper 10 cm of the soil under N addition. Furthermore, plant P-acquisition strategies (release of carboxylate and symbiosis with AMF) resulted in the mobilization of the moderately labile Pi pools in the soil. Therefore, we concluded that grazing may enhance P uptake by plants and remove the litter P pools, resulting in ongoing Po loss from the soil. It should be noted that our results concerned the effects of winter grazing on the soil P fractions, but the soil and plant samples were collected in the period of the peak biomass. The main reason for this was that in alpine grasslands, the P-acquisition strategies of plants have an important influence on the P transformation, and plant growth stops completely in winter and the plant samples cannot be collected whereas the effects of winter grazing on P transformation are long-lasting. Future studies could investigate the responses of the soil P fractions and the dynamics of grazing during different seasons.

Acknowledgments

This work was conducted at the Haibei National Field Research Station of Alpine Grassland Ecosystem, managed by the Northwest Institute of Plateau Biology, Chinese Academy of Sciences. This study was financially supported by the National Natural Science Foundation of China (Grants: 32192461, 32130065, 42007078) and the Top Leading Talents Program of Gansu Province (No. 842016). The authors declare no competing interests.

Author's contributions

Z-H.G. and J-S.H. designed the study; Z-H.G. and Z.C. performed the field and

laboratory work; Z-H.G. and Z.C. analyzed the data; Z-H.G. and Z.C. wrote the manuscript with discussion with X.L. G.H. and P.K., and all authors contributed to the article and approved the submitted version.

Data availability statement

The original contributions presented in the study are included in the article/supplementary material. Further inquiries can be directed to the corresponding author.

References

Aber, J. D., Nadelhoffer, K. J., Steudler, P., & Melillo, J. M. (1989). Nitrogen Saturation in Northern Forest Ecosystems: Excess nitrogen from fossil fuel combustion may stress the biosphere. *BioScience*, *39*(6), 378–386. https://doi.org/10.2307/1311067

Allison, S. D., Czimczik, C. I., & Treseder, K. K. (2008). Microbial activity and soil respiration under nitrogen addition in Alaskan boreal forest. *Global Change Biology*, *14*(5), 1156–1168. https://doi.org/10.1111/j.1365-2486.2008.01549.x

Alt, F., Oelmann, Y., Herold, N., Schrumpf, M., & Wilcke, W. (2011). Phosphorus partitioning in grassland and forest soils of Germany as related to land-use type, management intensity, and land-use-related pH. *Journal of Plant Nutrition and Soil Science*, *174*(2), 195–209. https://doi.org/10.1002/jpln.201000142

Bai, W., Fang, Y., Zhou, M., Xie, T., Li, L., & Zhang, W. (2015). Heavily intensified grazing reduces root production in an Inner Mongolia temperate steppe. *Agriculture Ecosystems & Environment*, *200*, 143–150. https://doi.org/10.1016/j.agee.2014.11.015

Bai, Y., Wu, J., Clark, C. D., Pan, Q., Zhang, L., Chen, S., Wang, Q., & Han, X. (2012). Grazing alters ecosystem functioning and C: N: P stoichiometry of grasslands along a regional precipitation gradient. J*ournal of Applied Ecology*, *49*(6), 1204–1215. https://doi.org/10.1111/j.1365-2664.2012.02205.x

Bardgett, R. D., & Wardle, D. A. (2003). Herbivore-mediated linkages between aboveground and belowground communities. *Ecology*, *84*(9), 2258–2268. e

Baron, V. S., Dick, A. C., Mapfumo, E., Malhi, S. S., Naeth, M. A., & Chanasyk, D. S. (2001). Grazing Impacts on Soil Nitrogen and Phosphorus under Parkland Pastures. *Journal of Range Management*, *54*(6), 704. https://doi.org/10.2307/4003675

Baumann, F., He, J.-S., Schimdt, K., Kühn, P., & Scholten, T. (2009). Pedogenesis, permafrost, and soil moisture as controlling factors for soil nitrogen and carbon contents across the Tibetan Plateau. *Global Change Biology*, *15*(12), 3001–3017. https://doi.org/10.1111/j.1365-2486.2009.01953.x

Bell, T. H., Klironomos, J. N., & Henry, H. A. L. (2010). Seasonal Responses of Extracellular Enzyme Activity and Microbial Biomass to Warming and Nitrogen Addition. *Soil Science Society of America Journal*, *74*(3), 820–828.

https://doi.org/10.2136/sssaj2009.0036

Bligh, E. G., & Dyer, W. J. (1959). A rapid method of total lipid extraction and purification. *Canadian Journal of Biochemistry and Physiology*, *37*(8), 911–917. https://doi.org/10.1139/o59-099

Bowman, W.D., Cleveland, C.C., Halada, L., Hresko, J., & Baron, J.S. (2008). Negative impact of nitrogen deposition on soil buffering capacity. *Nature Geoscience*, *1*(11) , 767–770. https://doi.org/10.1038/ngeo339

Bünemann, E. K. (2015). Assessment of gross and net mineralization rates of soil organic phosphorus – A review. *Soil Biology and Biochemistry*, *89*, 82–98. https://doi.org/10.1016/j.soilbio.2015.06.026

Cawthray, G. R. (2003). An improved reversed-phase liquid chromatographic method for the analysis of low-molecular mass organic acids in plant root exudates. *Journal of Chromatography A*, *1011*(1-2), 233–240. https://doi.org/10.1016/s0021-9673(03)01129-4

Chaneton, E. J., Lemcoff, J. H., & Lavado, R. S. (1996). Nitrogen and Phosphorus Cycling in Grazed and Ungrazed Plots in a Temperate Subhumid Grassland in Argentina. *The Journal of Applied Ecology*, *33*(2), 291–302. https://doi.org/10.2307/2404751

Chen, J., Groenigen, K. J., Hungate, B. A., Terrer, C., Groenigen, J., Maestre, F. T., Ying, S. C., Luo, Y., Jørgensen, U., Sinsabaugh, R. L., Olesen, J. E., & Elsgaard, L. (2020). Long-term nitrogen loading alleviates phosphorus limitation in terrestrial ecosystems. *Global Change Biology*, *26*(9), 5077–5086. https://doi.org/10.1111/gcb.15218

Chen, J., Yamamura, Y., Hori, Y., Masae Shiyomi, Yasuda, T., Zhou, H., Li, Y., & Tang, Y. (2007). Small-scale species richness and its spatial variation in an alpine meadow on the Qinghai-Tibet Plateau. *Ecological Research*, *23*(4), 657–663. https://doi.org/10.1007/s11284-007-0423-7

Chen, Q., Yuan, Y., Hu, Y., Wang, J., Si, G., Xu, R., Zhou, J., Xi, C., Hu, A., & Zhang, G. (2021). Excessive nitrogen addition accelerates N assimilation and P utilization by enhancing organic carbon decomposition in a Tibetan alpine steppe. *Science of the Total Environment*, *764*, 142848. https://doi.org/10.1016/j.scitotenv.2020.142848

Chinese Soil Taxonomy Research Group, 1995. Chinese soil taxonomy. Science Press, Beijing. pp. 58–147.

Davidson, K. E., Fowler, M. S., Skov, M. W., Doerr, S. H., Beaumont, N., & Griffin, J. N. (2017). Livestock grazing alters multiple ecosystem properties and services in salt marshes: a meta-analysis. *Journal of Applied Ecology, 54*(5), 1395–1405. https://doi.org/10.1111/1365-2664.12892

Fan, Y., Zhong, X., Lin, F., Liu, C., Yang, L., Wang, M., Chen, G., Chen, Y., & Yang, Y. (2019). Responses of soil phosphorus fractions after nitrogen addition in a subtropical forest ecosystem: Insights from decreased Fe and Al oxides and increased plant roots. *Geoderma*, *337*, 246–255. https://doi.org/10.1016/j.geoderma.2018.09.028

Frostegård, Å., Tunlid, A., & Bååth, E. (1991). Microbial biomass measured as total lipid phosphate in soils of different organic content. *Journal of Microbiological Methods*, *14*(3), 151–163. https://doi.org/10.1016/0167-7012(91)90018-l

Fu, G., & Shen, Z.-X. (2017). Response of alpine soils to nitrogen addition on the Tibetan Plateau: A meta-analysis. *Applied Soil Ecology*, *114*, 99–104. https://doi.org/10.1016/j.apsoil.2017.03.008

Gao, Y., Cooper, D. J., & Zeng, X. (2018). Nitrogen, not phosphorus, enrichment controls biomass production in alpine wetlands on the Tibetan Plateau, China. *Ecological Engineering*, *116*, 31–34. https://doi.org/10.1016/j.ecoleng.2018.02.016

Giese, M. A., Brueck, H., Gao, Y., Lin, S., Steffens, M., Kögel-Knabner, I., T. Glindemann, Susenbeth, A., Taube, F., Klaus Butterbach-Bahl, X. Long Zheng, Hoffmann, C., Bai, Y., & Han, X. (2013). N balance and cycling of Inner Mongolia typical steppe: a comprehensive case study of grazing effects. *Ecological Monographs*, *83*(2), 195–219. https://doi.org/10.1890/12-0114.1

Han, Y., Dong, S., Zhao, Z., Sha, W., Li, S., Shen, H., Xiao, J., Zhang, J., Wu, X., Jiang, X., Zhao, J., Liu, S., Dong, Q., Zhou, H., & Yeomans, J. C. (2019). Response of soil nutrients and stoichiometry to elevated nitrogen deposition in alpine grassland on the Qinghai-Tibetan Plateau. *Geoderma*, *343*, 263–268. https://doi.org/10.1016/j.geoderma.2018.12.050

He, H., Wu, M., Guo, L., Fan, C., Zhang, Z., Su, R., Peng, Q., Pang, J., & Lambers,

H. (2020a). Release of tartrate as a major carboxylate by alfalfa (*Medicago sativa L.*) under phosphorus deficiency and the effect of soil nitrogen supply. *Plant and Soil*, *449*(1-2), 169–178. https://doi.org/10.1007/s11104-020-04481-9

He, M., Zhou, G., Yuan, T., Groenigen, K. J., Shao, J., & Zhou, X. (2020b). Grazing intensity significantly changes the C: N: P stoichiometry in grassland ecosystems. *e*, *29*(2), 355–369. https://doi.org/10.1111/geb.13028

Hedley, M. J., Stewart, J. W. B., & Chauhan, B. S. (1982). Changes in Inorganic and Organic Soil Phosphorus Fractions Induced by Cultivation Practices and by Laboratory Incubations. *Soil Science Society of America Journal*, *46*(5), 970–976. https://doi.org/10.2136/sssaj1982.03615995004600050017x

Hopkins, D. W., Sparrow, A. D., Shillam, L. L., English, L. C., Dennis, P. G., Novis, P., Elberling, B., Gregorich, E. G., & Greenfield, L. G. (2008). Enzymatic activities and microbial communities in an Antarctic dry valley soil: Responses to C and N supplementation. *Soil Biology and Biochemistry*, *40*(9), 2130–2136. https://doi.org/10.1016/j.soilbio.2008.03.022

Hou, E., Chen, C., Luo, Y., Zhou, G., Kuang, Y., Zhang, Y., Heenan, M., Lu, X., & Wen, D. (2018). Effects of climate on soil phosphorus cycle and availability in natural terrestrial ecosystems. *Global Change Biology*, *24*(8), 3344–3356. https://doi.org/10.1111/gcb.14093

Hou, E., Chen, C., Kuang, Y., Zhang, Y., Heenan, M., & Wen, D. (2016). A structural equation model analysis of phosphorus transformations in global unfertilized and uncultivated soils. *Global Biogeochemical Cycles*, *30*(9), 1300–1309. https://doi.org/10.1002/2016GB005371

Huang, X., Jia, Z., Guo, J., Li, T., Sun, D., Meng, H., Yu, G., He, X., Ran, W., Zhang, S., Hong, J., & Shen, Q. (2019). Ten-year long-term organic fertilization enhances carbon sequestration and calcium-mediated stabilization of aggregate-associated organic carbon in a reclaimed Cambisol. *Geoderma*, *355*, 113880. https://doi.org/10.1016/j.geoderma.2019.113880

Jiang, R., Zhang, Y-G., & Li, Q. (2005). Pedogenic and anthropogenic influence on calcium and magnesium behaviors in stagnic anthrosols. *Pedosphere*, *15*(3), 341–346.

Jin, Y., Gao, L., Yan, C., Gao, P., Chang, S., Du, W., Zhang, Y., Wang, Z., Hou, F.

(2022). Decomposition and C, N and P release of Tibetan sheep dung from an alpine meadow with different stocking rates. *Ecological Indicators*, 144. https://doi.org/10.1016/j.ecolind.2022.109561

Jing, X., Yang, X., Ren, F., Zhou, H., Zhu, B., & He, J.-S. (2016). Neutral effect of nitrogen addition and negative effect of phosphorus addition on topsoil extracellular enzymatic activities in an alpine grassland ecosystem. *Applied Soil Ecology*, *107*, 205–213. https://doi.org/10.1016/j.apsoil.2016.06.004

Johnson, T. N., & Sandercock, B. K. (2010). Restoring tallgrass prairie and grassland bird populations in tall fescue pastures with winter grazing. *Rangeland Ecology & Management*, **63**(6), 679–688. https://doi.org/10.2111/rem-d-09-00076.1

Khan, K. S., & Joergensen, R. G. (2012). Relationships between P fractions and the microbial biomass in soils under different land use management. *Geoderma*, *173-174*, 274–281. https://doi.org/10.1016/j.geoderma.2011.12.022

Kidd D. R., Ryan M. H., Hahne D., Haling R. E., Lambers, H., Sandral, G. A., Simpson, R. J., Cawthray, G. R. (2018). The carboxylate composition of rhizosheath and root exudates from twelve species of grassland and crop legumes with special reference to the occurrence of citramalate. *Plant and Soil*, *424*(1-2), 389–403. https://doi.org/10.1007/s11104-017-3534-0

Klein, J. A., Harte, J., Zhao, X. (2004). Experimental warming causes large and rapid species loss, dampened by simulated grazing, on the Tibetan Plateau. *Ecology Letters*, *7*, 1170–1179. https://doi.org/10.1111/j.1461-0248.2004.00677.x

Kourtev, P.S., Ehrenfeld, J.G., Häggblom, M. (2002). Exotic plant species alter the microbial community structure and function in the soil. *Ecology*, *83*, 3152–3166. https://doi.org/10.1890/0012-9658(2002)083[3152:EPSATM]2.0.CO;2

Lambers, H., de Britto Costa, P., Cawthray, G. R., Denton, M. D., Finnegan, P. M., Hayes, P. E., Oliveira, R. S., Power, S. C., Ranathunge, K., Shen, Q., Wang, X., & Zhong, H. (2022). Strategies to acquire and use phosphorus in phosphorus-impoverished and fire-prone environments. *Plant and Soil*, *476*(1-2), 133–160. https://doi.org/10.1007/s11104-022-05464-8

Lambers, H., Shane, M.W., Cramer, M.D., Pearse, S.J., Veneklaas, E.J. (2006). Root structure and functioning for efficient acquisition of phosphorus: matching

morphological and physiological traits. *Annals of Botany*, *98*, 693–713.

Lambers, H. (2022). Phosphorus acquisition and utilization in plants. *Annual Review of Plant Biology*, *73*, 17–42. https://doi.org/10.1146/annurev-arplant-102720-125738

Lal, R., & Stewart, B. A. (2016). *Soil Phosphorus*. CRC Press. https://doi.org/10.1201/9781315372327

Li, C., Hao, X., Willms, W. D., Zhao, M., & Han, G. (2010). Effect of long-term cattle grazing on seasonal nitrogen and phosphorus concentrations in range forage species in the fescue grassland of southwestern Alberta. *Journal of Plant Nutrition and Soil Science, 173*(6), 946–951. https://doi.org/10.1002/jpln.200900243

Li, M., Zhang, X., He, Y., Niu, B., & Wu, J. (2020). Assessment of the vulnerability of alpine grasslands on the Qinghai-Tibetan Plateau. *PeerJ*, *8*, e8513. https://doi.org/10.7717/peerj.8513

Li, T., Cai, S., Singh, R. K., Cui, L., Fava, F., Tang, L., Xu, Z., Li, C., Cui, X., Du, J., Hao, Y., Liu, Y., & Wang, Y. (2022). Livelihood resilience in pastoral communities: Methodological and field insights from Qinghai-Tibetan Plateau. *Science of the Total Environment*, *838*, 155960. https://doi.org/10.1016/j.scitotenv.2022.155960

Li, Y., Niu, S., & Yu, G. (2016). Aggravated phosphorus limitation on biomass production under increasing nitrogen loading: a meta-analysis. *Global Change Biology*, *22*(2), 934–943. https://doi.org/10.1111/gcb.13125

Liu, H., Mi, Z., Lin, L., Wang, Y., Zhang, Z., Zhang, F., Wang, H., Liu, L., Zhu, B., Cao, G., Zhao, X., Sanders, N. J., Classen, A. T., Reich, P. B., & He, J.-S. (2018). Shifting plant species composition in response to climate change stabilizes grassland primary production. *Proceedings of the National Academy of Sciences*, *115*(16), 4051–4056. https://doi.org/10.1073/pnas.1700299114

Liu, X., Han, R., Cao, Y., Turner, B. L., & Ma, L. Q. (2022). Enhancing Phytate Availability in Soils and Phytate-P Acquisition by Plants: A Review. *Environmental Science & Technology*, *56*(13), 9196–9219. https://doi.org/10.1021/acs.est.2c00099

Lu, X., Mo, J., Gilliam, F. S., Fang, H., Zhu, F., Fang, Y., Zhang, W., & Huang, J. (2012). Nitrogen Addition Shapes Soil Phosphorus Availability in Two Reforested Tropical Forests in Southern China. *Biotropica*, *44*(3), 302–311. https://doi.org/10.1111/j.1744-7429.2011.00831.x

Luo, M., Moorhead, D. L., Ochoa-Hueso, R., Mueller, C. W., Ying, S. C., & Chen, J. (2022). Nitrogen loading enhances phosphorus limitation in terrestrial ecosystems with implications for soil carbon cycling. *Functional Ecology*, *36*(11), 2845–2858. https://doi.org/10.1111/1365-2435.14178

Luo T., Li W., Zhu H. (2002). Estimated biomass and productivity of natural vegetation on the tibetan plateau. *Ecological Applications 12*(4), 980–997. https://doi.org/10.1890/1051-0761(2002)012[0980:EBAPON]2.0.CO;2

McDowell, R. W. & Stewart, I. (2005). Phosphorus in fresh and dry dung of grazing dairy cattle, deer, and sheep. *Journal of Environmental Quality*, *34*, 598–607. https://doi.org/10.2134/jeq2005.0598

Morel, C., Tiessen, H., & Stewart, J. W. B. (1996). Correction for P-sorption in the measurement of soil microbial biomass P by $CHCl_3$ fumigation. *Soil Biology and Biochemistry*, *28*(12), 1699–1706. https://doi.org/10.1016/s0038-0717(96)00245-3

Mou, X., Wu, Y., Niu, Z., Jia, B., Guan, Z-H., Chen, J., Li, H., Cui, H., Kuzyakov, Y., Li, X. (2020). Soil phosphorus accumulation changes with decreasing temperature along a 2300 m altitude gradient. *Agriculture Ecosystems & Environment 301*. https://doi.org/10.1016/j.agee.2020.107050

Neumann, G., & Römheld, V. (1999). Root excretion of carboxylic acids and protons in phosphorus-deficient plants. *Plant and Soil*, *211*(1), 121–130. https://doi.org/10.1023/a:1004380832118

Ngewoh, Z. S., Taylor, R. W., & Shuford, J. W. (1989). Exchangeable cations and CEC determinations of some highly weathered soils. *Communications in Soil Science and Plant Analysis*, *20*(17-18), 1833–1855. https://doi.org/10.1080/00103628909368187

Niederberger, J., Kohler, M., & Bauhus, J. (2019). Distribution of phosphorus fractions with different plant availability in German forest soils and their relationship with common soil properties and foliar P contents. *SOIL*, *5*(2), 189–204. https://doi.org/10.5194/soil-5-189-2019

Niederberger, J., Todt, B., Boča, A., Nitschke, R., Kohler, M., Kühn, P., & Bauhus, J. (2015). Use of near-infrared spectroscopy to assess phosphorus fractions of different plant availability in forest soils. *Biogeosciences*, *12*(11), 3415–3428.

https://doi.org/10.5194/bg-12-3415-2015

Niu, G., Wang, Y., Wang, R., Ning, Q., Guan, H., Yang, J., Lu, X., Han, X., & Huang, J. (2022). Intensity and Duration of Nitrogen Addition Jointly Alter Soil Nutrient Availability in a Temperate Grassland. *Journal of Geophysical Research: Biogeosciences*, *127*(3). https://doi.org/10.1029/2021jg006698

Olsson, P.A., Francis, R., Read, D.J., Soderstrom, B. (1998). Growth of arbuscular mycorrhizal mycelium in calcareous dune sand and its interaction with other soil microorganisms as estimated by measurement of specific fatty acids. *Plant and Soil*, *201*, 9-16. https://doi.org/10.1023/A:1004379404220

Pätzold, S., Hejcman, M., Barej, J., & Schellberg, J. (2013). Soil phosphorus fractions after seven decades of fertilizer application in the Rengen Grassland Experiment. *Journal of Plant Nutrition and Soil Science*, *176*(6), 910–920. https://doi.org/10.1002/jpln.201300152

Pearse, S. J., Veneklaas, E. J., Cawthray, G., Bolland, M. D. A., & Lambers, H. (2007). Carboxylate composition of root exudates does not relate consistently to a crop species' ability to use phosphorus from aluminium, iron or calcium phosphate sources. *New Phytologist*, *173*(1), 181–190. https://doi.org/10.1111/j.1469-8137.2006.01897.x

Phillips, J. M., & Hayman, D. S. (1970). Improved procedures for clearing roots and staining parasitic and vesicular-arbuscular mycorrhizal fungi for rapid assessment of infection. *Transactions of the British Mycological Society*, *55*(1), 158–161. IN16–IN18. https://doi.org/10.1016/s0007-1536(70)80110-3

Prescott, C. E., Grayston, S. J., Helmisaari, H.-S., Kaštovská, E., Körner, C., Lambers, H., Meier, I. C., Millard, P., & Ostonen, I. (2020). Surplus Carbon Drives Allocation and Plant–Soil Interactions. *Trends in Ecology & Evolution*, *35*(12), 1110–1118. https://doi.org/10.1016/j.tree.2020.08.007

Qiu, J. (2016). Trouble in Tibet. *Nature*, *529*, 142–145. https://doi.org/10.1038/529142a

Ren, F., Yang, X., Zhou, H., Zhu, W., Zhang, Z., Chen, L., Cao, G., He, J-S. (2017). Contrasting effects of nitrogen and phosphorus addition on soil respiration in an alpine grassland on the Qinghai-Tibetan Plateau. *Scientific Reports 6*, 34786.

https://doi.org/10.1038/srep34786

Rui, Y., Wang, S., Xu, Z., Wang, Y., Chen, C., Zhou, X., Kang, X., Lu, S., Hu, Y., Lin, Q., & Luo, C. (2011). Warming and grazing affect soil labile carbon and nitrogen pools differently in an alpine meadow of the Qinghai–Tibet Plateau in China. *Journal of Soils and Sediments*, *11*(6), 903–914. https://doi.org/10.1007/s11368-011-0388-6

Schaap, K. J., Fuchslueger, L., Hoosbeek, M. R., Hofhansl, F., Martins, N. P., Valverde-Barrantes, O. J., Hartley, I. P., Lugli, L. F., & Quesada, C. A. (2021). Litter inputs and phosphatase activity affect the temporal variability of organic phosphorus in a tropical forest soil in the Central Amazon. *Plant and Soil*, *469*(1-2), 423–441. https://doi.org/10.1007/s11104-021-05146-x

Schleuss, P. M., Widdig, M., Heintz-Buschart, A., Kirkman, K., & Spohn, M. (2020). Interactions of nitrogen and phosphorus cycling promote P acquisition and explain synergistic plant-growth responses. *Ecology*, *101*(5). https://doi.org/10.1002/ecy.3003

Shen, J., Yuan, L., Zhang, J., Li, H., Bai, Z., Chen, X., Zhang, W., & Zhang, F. (2011). Phosphorus Dynamics: From Soil to Plant. *Plant Physiology*, *156*(3), 997–1005. https://doi.org/10.1104/pp.111.175232

Shi, G., Yao, B., Liu, Y., Jiang, S., Wang, W., Pan, J., Zhao, X., Feng, H., & Zhou, H. (2017). The phylogenetic structure of AMF communities shifts in response to gradient warming with and without winter grazing on the Qinghai–Tibet Plateau. *Applied Soil Ecology*, *121*, 31–40. https://doi.org/10.1016/j.apsoil.2017.09.010

Shi, C., Li, Y., Bai, Z., Wu, L., Wang, H., Zhang, T., Chang, Q., & Li, F. Y. (2022). Grazing season regulates plant community structure and production by altering plant litter mass in a typical steppe. *Applied Vegetation Science, 25*(4). https://doi.org/10.1111/avsc.12703

Taylor, B. N, Beidler, K. V., Cooper, E. R., Strand, A. E., Pritchard, S. G. (2013). Sampling volume in root studies: the pitfalls of under-sampling exposed using accumulation curves. *Ecology Letters 16*(7): 862–869. https://doi.org/10.1111/ele.12119

Tian, D., & Niu, S. (2015). A global analysis of soil acidification caused by nitrogen addition. *Environmental Research Letters*, *10*(2), 024019. https://doi.org/10.1088/1748-9326/10/2/024019

Tissen, H., & Moir, J. O. (2007). *Characterization of available P by sequential extraction. In: Carter MR (ed) Soil sampling and methods of analysis.* (pp. 293–306). Lewis Publishers.

Trouvelot, A., Kough, J. L., & Gianinazzi-Pearson, V. (1986). *Mesure du taux de mycorhization VA d'un système radiculaire. Recherche de méthode d'estimation ayant une signification fonctionnelle*. 217–222. http://pascal-francis.inist.fr/vibad/index.php?action=getRecordDetail&idt=8758731

Turner, B. L., Lambers, H., Condron, L. M., Cramer, M. D., Leake, J. R., Richardson, A. E., Smith, S. E. (2013). Soil microbial biomass and the fate of phosphorus during long-term ecosystem development. *Plant and Soil 367*(1-2), 225–234.

Vadas, P. A., Busch, D. L., Powell, J. Mark., & Brink, G. E. (2015). Monitoring runoff from cattle-grazed pastures for a phosphorus loss quantification tool. *Agriculture, Ecosystems & Environment*, *199*, 124–131. https://doi.org/10.1016/j.agee.2014.08.026

Vance, E. D., Brookes, P. C., & Jenkinson, D. S. (1987). An extraction method for measuring soil microbial biomass C. *Soil Biology and Biochemistry*, *19*(6), 703–707. https://doi.org/10.1016/0038-0717(87)90052-6

Wang, A. G., Wang, W., Hu, C. C., Li, Q., & He, Z. J. (2013). Distribution of Exchangeable Ca and Mg in the Soil Environment of Yunnan Plateau. *Advanced Materials Research*, *726-731*, 85–89. https://doi.org/10.4028/www.scientific.net/amr.726-731.85

Wang, R., Yang, J., Liu, H., Sardans, J., Zhang, Y., Wang, X., Wei, C., Lü, X., Dijkstra, F. A., Jiang, Y., Han, X., & Peñuelas, J. (2022a). Nitrogen enrichment buffers phosphorus limitation by mobilizing mineral-bound soil phosphorus in grasslands. *Ecology*, *103*(3). https://doi.org/10.1002/ecy.3616

Wang, W., Zhao, J., & Xing, Z. (2022b). Spatial patterns of leaf nitrogen and phosphorus stoichiometry across southeast to central Tibet. *Journal of Mountain Science*, 19(9), 2651–2663. https://doi.org/10.1007/s11629-021-7194-4

Wen, Z., Li, H., Shen, Q., Tang, X., Xiong, C., Li, H., Pang, J., Ryan, M. H., Lambers, H., & Shen, J. (2019). Tradeoffs among root morphology, exudation and mycorrhizal symbioses for phosphorus-acquisition strategies of 16 crop species. *New Phytologist*, *223*(2), 882–895. https://doi.org/10.1111/nph.15833

Wu, G.-L., Du, G.-Z., Liu, Z.-H., & Thirgood, S. (2009). Effect of fencing and grazing on a Kobresia-dominated meadow in the Qinghai-Tibetan Plateau. *Plant and Soil*, 319(1-2), 115–126. https://doi.org/10.1007/s11104-008-9854-3

Wu, L., Li, X., Zhao, M., & Bai, Y. (2020). Grazing regulation of phosphorus cycling in grassland ecosystems: Advances and prospects. *Chinese Science Bulletin*, 65(23), 2469–2482. https://doi.org/10.1360/tb-2020-0321

World Reference Base for Soil Resources (WRB). (2015). International soil classification system for naming soils and creating legends for soil maps. FAO/ISRIC/ISSS, Rome.

Xiao, J., Dong, S., Shen, H., Li, S., Wessell, K., Liu, S., Li, W., Zhi, Y., Mu, Z., & Li, H. (2022). N Addition Overwhelmed the Effects of P Addition on the Soil C, N, and P Cycling Genes in Alpine Meadow of the Qinghai-Tibetan Plateau. *Frontiers in Plant Science*, *13*. https://doi.org/10.3389/fpls.2022.860590

Yang, X., & Post, W. M. (2011). Phosphorus transformations as a function of pedogenesis: A synthesis of soil phosphorus data using Hedley fractionation method. *Biogeosciences*, *8*(10), 2907–2916. https://doi.org/10.5194/bg-8-2907-2011

Yao, X., Wu, J., Gong, X., Lang, X., Wang, C., Song, S., & Ali Ahmad, A. (2019). Effects of long term fencing on biomass, coverage, density, biodiversity and nutritional values of vegetation community in an alpine meadow of the Qinghai-Tibet Plateau. *Ecological Engineering*, *130*, 80–93. https://doi.org/10.1016/j.ecoleng.2019.01.016

Yu, R., Zhang, W., Fornara, D. A., & Li, L. (2021). Contrasting responses of nitrogen: Phosphorus stoichiometry in plants and soils under grazing: A global meta-analysis. *Journal of Applied Ecology*, *58*(5), 964–975. https://doi.org/10.1111/1365-2664.13808

Zhang, A., Wang, X.-X., Zhang, D., Dong, Z., Ji, H., & Li, H. (2023). Localized nutrient supply promotes maize growth and nutrient acquisition by shaping root morphology and physiology and mycorrhizal symbiosis. *Soil and Tillage Research*, *225*, 105550. https://doi.org/10.1016/j.still.2022.105550

Zhang, Y., Yang, S., Fu, M., Cai, J., Zhang, Y., Wang, R., Xu, Z., Bai, Y., & Jiang, Y. (2015). Sheep manure application increases soil exchangeable base cations in a semi-arid steppe of Inner Mongolia. *Journal of Arid Land*, *7*(3), 361–369.

https://doi.org/10.1007/s40333-015-0004-5

Zhao, Q., & Zeng, D.-H. (2019). Nitrogen addition effects on tree growth and soil properties mediated by soil phosphorus availability and tree species identity. *Forest Ecology and Management*, *449*, 117478. https://doi.org/10.1016/j.foreco.2019.117478

Zhou, J., Li, X., Peng, F., Li, C., Lai, C., You, Q., Xue, X., Wu, Y., Sun, H., Chen, Y., Zhong, H., & Lambers, H. (2021). Mobilization of soil phosphate after 8 years of warming is linked to plant phosphorus-acquisition strategies in an alpine meadow on the Qinghai-Tibetan Plateau. *Global Change Biology*, *27*(24), 6578–6591. https://doi.org/10.1111/gcb.1591